**UNIVERSIDADE DE LISBOA**

**FACULDADE DE CIÊNCIAS**

**DEPARTAMENTO DE BIOLOGIA ANIMAL**

# Metabolic switch in uterine cervix cancer – *in vitro* study of adenocarcinoma (HeLa) and squamous cell carcinoma (SiHa) cell lines

**Lídia Jorge Santos Silva**

**Mestrado em Biologia Humana e Ambiente**

**2012**

**UNIVERSIDADE DE LISBOA**

**FACULDADE DE CIÊNCIAS**

**DEPARTAMENTO DE BIOLOGIA ANIMAL**

# Metabolic switch in uterine cervix cancer – *in vitro* study of adenocarcinoma (HeLa) and squamous cell carcinoma (SiHa) cell lines

**Lídia Jorge Santos Silva**

**Mestrado em Biologia Humana e Ambiente**

Dissertação orientada por:
**Prof. Doutora Jacinta Serpa (orientação externa)**
UIPM (IPO Lisboa)/CEDOC – Faculdade de Ciência Médicas da Universidade Nova de Lisboa
**Prof. Doutora Ana Crespo (orientação interna)**
CBA – Faculdade de Ciência da Universidade de Lisboa

**2012**

## Agradecimentos

Em primeiro lugar, agradeço à Prof. Doutora Jacinta Serpa, minha orientadora, pela oportunidade de participar neste projecto, que me iniciou no mundo da investigação científica. Pela sua disponibilidade, ajuda e todos os conhecimentos transmitidos. Agradeço ainda o apoio na revisão desta dissertação, a confiança e o incentivo ao pensamento crítico e autonomia.

O meu agradecimento à Prof. Doutora Ana Crespo pela disponibilidade de aceitar co-orientar este meu trabalho, pela simpatia, dedicação e por me ter cativado ainda mais pelo "mundo do metabolismo".

Ao Doutor Sérgio Dias por ter aceite receber-me no seu laboratório e me ter concedido a oportunidade de participar neste projecto. Um especial agradecimento ao seu olhar crítico, à sua acessibilidade e disponibilidade. Agradeço também o apoio na revisão desta dissertação.

Ao grupo da Angiogénese que tão bem me acolheu. Obrigada a todos pela ajuda, disponibilidade, simpatia e também pelas vossas sugestões e críticas.

Aos restantes colegas do UIPM que, de alguma forma, contribuíram para a realização desta dissertação.

À Lara pela sua imprescindível ajuda na realização do FISH.

À Fernanda por me ter apresentado o admirável mundo da imunohistoquímica, pela sua simpatia e disponibilidade.

À Sofia Fragoso pela boa disposição, pela ternura com que preparou os lanches que partilhámos e por todas as palavras de incentivo.

Dirijo um agradecimento muito especial à Sofia Gouveia, pela ajuda, o apoio, a paciência, o incentivo e a enorme disponibilidade com que sempre que ensinou e iniciou na aventura da investigação. Obrigada por acreditares no meu trabalho e por teres tornado simples todas as técnicas com que, no âmbito desta dissertação, me cruzei. Agradeço ainda a excelente companhia e a simpatia com que me recebeu.

Finalmente agradeço ao Duarte pelo apoio incansável, pela dedicação, pela paciência e por ter sempre acreditado em mim e no meu trabalho. Um obrigado especial!

Um enorme obrigado aos meus pais pelo apoio, pela confiança e incentivo. Por todas as palavras de carinho e força. Por me terem ensinado a ser quem sou!

## Resumo

O cancro é uma doença complexa que envolve numerosas alterações na fisiologia da célula que conduzem, em última instância, a tumores malignos. Os processos biológicos através dos quais as células normais são transformadas em células cancerígenas malignas têm sido alvo de vasta investigação durante várias décadas (Seyfried & Shelton, 2010). Existem seis alterações essenciais na fisiologia celular que estão na base do crescimento celular maligno e são a auto-suficiência em termos de sinais de crescimento, a insensibilidade a sinais inibidores de crescimento, a evasão à morte celular programada (apoptose), um potencial replicativo ilimitado, a angiogénese sustentada e a invasão tecidular e metastização (Hanahan & Weinberg, 2000). Contudo, recentemente, têm sido propostos outros atributos distintos às células cancerígenas funcionalmente importantes para o desenvolvimento de cancro, que incluem a reprogramação do metabolismo energético celular, por forma a suportar o crescimento celular e a proliferação contínua, e a evasão ao controlo imunitário (Hanahan & Weinberg, 2011). Ao longo da última década, os tumores têm sido identificados como órgãos cuja complexidade pode exceder a dos tecidos saudáveis normais, contrastando com a anterior visão reducionista dos tumores como um conjunto relativamente homogéneo de células cancerígenas. Desta forma, a biologia de um tumor só pode ser entendida analisando os tipos celulares especializados que o constituem bem como a microambiente tumoral criado durante o processo de tumorigénese (Seyfried & Shelton, 2010) .

Em termos de incidência global, estima-se que 12.7 milhões de novos casos de cancro e 7.6 milhões de mortes causadas por cancro ocorram por ano (Ferlay et al., 2010).

O cancro do colo do útero é o terceiro cancro mais comum entre as mulheres, e o sétimo globalmente (Ferlay et al., 2010; Yugawa & Kiyono, 2009), sendo a quarta causa de morte por cancro entre as mulheres, mundialmente (Jemal et al., 2011; Ferlay et al., 2010). Apesar de a incidência deste tipo de tumor ter diminuído nos países desenvolvidos, a incidência mundial estimada ronda os 500 000 novos casos por ano (Jemal et al., 2011; Yugawa & Kiyono, 2009). Em Portugal, o cancro do colo do útero surge como o quarto mais frequente entre as mulheres (Globocan, 2008).

Em termos histológicos, existem duas variantes de cancro do colo do útero com significado clínico, os adenocarcinomas (AC) (que compreendem 10 a 25 % dos casos) e os carcinomas pavimento celulares (SCC) (que compreendem cerca de 85 a 90% dos casos) (Chan et al., 2003; Smith et al., 2000). Sabe-se que em algumas doentes, o tumor apresenta um crescimento endofítico, invadindo o endométrio, enquanto noutros casos, o tumor cresce exofíticamente para o canal da vagina (Nguyen & Averette, 1999). Além disso, neste tipo de tumor, a composição da flora vaginal, concretamente, a presença de *Doderlein bacilli*, bacilo que possui a capacidade de converter o glicogénio presente na mucosa vaginal em ácido láctico, contribui para a criação e manutenção de um microambiente rico em ácido láctico que pode desempenhar um papel na selecção das células cancerígenas e na progressão tumoral (Gupta, 2011; Redondo-Lopez et al., 1990).

O virus do papiloma humano (HPV) é o agente etiológico do cancro do colo do útero, contudo, a infecção por HPV não é o único factor envolvido na carcinogénese do carcinoma do colo do útero (Yeasmin et al., 2011). Alterações genómicas em oncogenes e genes supressores de tumor nas células do colo uterino são também essenciais ao desenvolvimento de carcinoma do colo do útero (Yeasmin et al., 2011). A amplificação genética em certas regiões cromossómicas é um dos mecanismos de activação de vários oncogenes e outros genes relacionados com o desenvolvimento e progressão tumoral (Schwab, 1999). Estudos em carcinoma do colo do útero, revelaram que os receptores do factor de crescimento epidérmico (EGF) e o proto-oncogene c-Myc estão frequentemente activados por amplificação e estão claramente associados ao fenótipo maligno (Hale et al., 1993; Pfeiffer et al., 1989).

As células tumorais reprogramam o seu metabolismo energético de forma a sustentar as elevadas taxas proliferativas (Tennant et al., 2009; DeBerardinis et al., 2008). Além disso, esta reprogramação permite-lhes resistir a alguns sinais de morte celular, particularmente aqueles mediados por danos oxidativos (King & Gottlieb, 2009). Para se dividir uma célula necessita de aumentar em tamanho mas também de replicar o seu DNA – processos que são altamente exigentes do ponto de vista metabólico e que requerem grandes quantidade de proteínas, lípidos e nucleótidos, tal como energia no forma de ATP, o que implica um aumento no consumo de glucose e aminoácidos (Tennant et al., 2010). O fenótipo metabólico melhor caracterizado que se observa nas células tumorais é o efeito de Warburg, que consiste no cancelamento do ciclo de Krebs e cadeia transportadora de electrões e aumento da taxa de glicólise na presença de concentrações normal de oxigénio (Vander Heiden et al., 2009; Warburg, 1956). Consequentemente, ao contrário da maioria das células normais, muitas células tumorais produzem quantidades substanciais da sua energia através da glicólise aeróbia, convertendo a maior parte da glucose a lactato ao invés de a metabolizarem mediante fosforilação oxidativa (Semenza, 2008; Warburg, 1956).

Em suma, as células tumorais apesentam maior consumo de nutrientes e também maior produção de subprodutos do que os tecidos normais, resultando numa acumulação de metabolitos no interior da célula e na criação de um ambiente mais hostil no exterior da mesma.

As alterações metabólicas e as adaptações desenvolvidas pelas células tumorais, extensivamente estudadas durante o último século, criam um fenótipo que é essencial ao crescimento tumoral e à sobrevivência da célula tumoral, alterando o fluxo ao longo de vias metabólicas chave, tais como a glicólise e a glutaminólise (Tennant et al., 2009). Estas alterações incluem a alteração da expressão (Semenza et al., 1996), mutação e inactivação pós-traducional de uma enzima (Kim et al., 2006) ou a substituição de uma enzima por uma isoforma diferente (Atsumi et al., 2002). Por outro lado, embora os factores chave envolvidos na criação do fenótipo metabólico das células tumorais estejam por elucidar, a literatura actual indica que o c-Myc, p53 o HIF-1 são cruciais neste processo e que existe uma acção combinada desta tríade de factores de transcrição na regulação do metabolismo tumoral (Yeung et al., 2008).

Assim, as observações referidas anteriormente colocam a glicólise como contribuinte chave para o fenótipo maligno e suportam a procura de novos tratamentos para o cancro que têm como alvo esta via metabólica essencial. Na verdade, a maioria das adaptações metabólicas desenvolvidas pelas células tumorais são únicas e exclusivas relativamente aos tecidos saudáveis(Porporato et al., 2011). De forma a estabelecer novos alvos terapêuticos os transportadores de compostos carboxilatos, principalmente de glucose, lactato e piruvato devem ser estudados bem como as enzimas que catalisam passos chave em vias metabólicas centrais, como é o caso da lactato e da piruvato desidrogenase.

A reacção reversível de redução do piruvato a lactato é catalisada pela família de enzimas lactato desidrogenases (LDH), formadas pelo rearranjo de até quatro cópias de duas subunidades diferentes: a subunidade LDH-H codificada no gene *LDHB* e a subunidade LDH-M codificada no gene *LDHA* para formar tetrâmeros activos que conduzem à formação de cinco enzimas, LDH1 a LDH5. A LDH5/LDH-4M (LDHA) catalisa preferencialmente a redução de piruvato a lactato e a LDH1/LDH-4H (LDHB) a conversão de lactato em piruvato (Porporato et al., 2011). A família de genes LDH também o gene *LDHC,* expresso nos testículos e espermatozóides, que codifica uma terceira isoenzima, a LDHC (Holmes & Goldberg, 2009).

A reacção catalisada pela LDH5/LDH-4M produz concentrações equimolares de lactato e protões, então, de forma a evitar a acidificação intracelular e a morte, as células glicolíticas exportam protões através de sistemas adaptados ao transporte dos mesmos, em que se incluem os transportadores de monocarboxilatos (MCT), entre os quais o MCT1, MCT2, MCT3 e MCT4 efectuam o simporte passivo de lactato e protões (Halestrap & Meredith, 2004).

Tem sido reportada a sobre-expressão e activação do gene *LDHA* no tecido tumoral comparativamente com o tecido normal (Walenta & Mueller-Klieser, 2004; Lewis et al., 2000; Shim et al., 1997). Estudos anteriores revelaram transactivação do promotor deste gene pelo factor de transcrição c-Myc (Shim et al., 1997), aumentando directamente a sua expressão. Em relação ao *LDHB* não foi ainda estabelecida uma relação definitiva entre a expressão deste gene e o cancro, com alguns autores a reportarem o aumento (Chen et al., 2006) da mesma no tumor e outros, o seu silenciamento transcricional no tumor (Leiblich et al., 2006; Maekawa et al., 2003). Recentemente, tem sido também identificada expressão do gene *LDHC* num largo espectro de tumores (Koslowski et al., 2002).

Sabe-se que o MCT4 transporta preferencialmente o lactato para o exterior da célula e o MCT1 regula preferencialmente a entrada do mesmo em células tumorais (mas também o efluxo) e células endoteliais tumorais (Draoui & Feron, 2011). Existem estudos que demonstram a sobre-expressão de *MCT1* em carcinoma da mama (Pinheiro et al., 2010) e outros em que se verificou a sobre-expressão de *MCT1* e *MCT4* em neuroblastoma, cancro do colo do útero e colorectal (Pinheiro et al., 2009; Pinheiro et al., 2008; Sonveaux et al., 2008; Fang et al., 2006).

Com base no trabalho científico que vem sendo realizado na área do metabolismo tumoral, foi definido como objectivo desta tese a caracterização do perfil metabólico de duas linhas celulares de cancro de colo do útero de dois tipos histológicos diferentes, adenocarcinoma (HeLa) e carcinoma pavimento celular (SiHa), determinando a relevância das enzimas LDHA, LDHB e LDHC e dos transportadores MCT1 e MCT4. Especificamente, compreender o papel do factor de crescimento EGF e do lactato de sódio (NaLac) na regulação da expressão de *LDHA*, *LDHB, LDHC, MCT1* e *MCT4* nas linhas celulares HeLa e SiHa.

Os resultados revelaram que em células HeLa, a presença de NaLac promove a sobre-expressão de *LDHA* através da interacção do factor de transcrição c-Myc com o promotor do gene. Nesta linha celular foi também identificada amplificação genética de c-Myc. Em células SiHa a presença de NaLac promove igualmente um aumento na expressão de *LDHA*, a nível do mRNA, contudo não por intermédio da acção de c-Myc. Nesta linha celular, observou-se também um aumento no número de cópias de c-Myc, porém em resultado de aneuploidia, uma vez que estas células apresentaram mais de dois cromossomas 8, onde se localiza o c-Myc.

Relativamente ao gene *LDHB*, verificou-se que, em ambas as linhas celulares, a presença de NaLac promove a sobre-expressão do mesmo. Em relação às células SiHa observou-se ainda que a estimulação com EGF promove a expressão de *LDHB* sendo este efeito activador potenciado pela presença de NaLac. Em termos de regulação da expressão de *LDHB* propõe-se que esta seja mediada pelo factor de transcrição STAT3.

No que concerne à expressão dos transportadores de monocarboxilatos, verificou-se que a expressão de *MCT1* em células HeLa na presença de NaLac é regulada pelo factor de transcrição c-Myc que actuará, neste cenário, como repressor. Já no que diz respeito às células SiHa os dados apontam para a existência de repressão da expressão do gene pelo c-Myc, em condições controlo, e para a sua activação na presença de NaLac. Em termos de perspectivas futuras, a elucidação do papel do c-Myc como activador ou repressor da expressão de *MCT1* dependerá do estudo dos seus parceiros nos diferentes contextos.

Em relação ao MCT4, este encontra-se sobre-expresso em ambas as linhas celulares quando expostas a NaLac.

Os resultados obtidos na análise de casos de AC e SCC do colo do útero evidenciaram o papel crucial do microambiente tumoral na selecção de células tumorais. No contexto oxidativo em que os tumores pavimentosos se desenvolvem, a sobre-expressão de MCT1 pode conferir vantagens às células tumorais,

dada a sua importância na importação de lactato. Além disso, esta sobre-expressão pode estar na base do switch do consumo de glucose para o de lactato neste tipo de tumor, tal como foi descrito em células SiHa.
Nos casos de AC, as baixas concentrações de lactato que caracterizam o microambiente tumoral dos AC, parecem promover a diminuição da expressão de MCT1. Por outro lado, se considerarmos o papel do microambiente tumoral como agente de selecção, os menores níveis de lactato podem selecionar as células tumorais que expressam menos MCT1 dada a sua menor necessidade de importar lactato, comparativamente com as células tumorais de carcinomas pavimentosos.

O estudo da migração e proliferação *in vitro* revelou que a estimulação com EGF e a presença de NaLac promove a migração e proliferação das células SiHa. Propomos que o factor de transcrição c-Myc possa estar implicado neste fenótipo via regulação da expressão de MCT1, cuja função permite fornecer à célula tumoral fontes de energia alternativas de modo a sustentar a sua avidez energética. Assim sendo, o factor de transcrição c-Myc pode estar implicado na regulação de vários genes alvo regulando processos não só relacionados com o metabolismo mas também com o controlo do ciclo celular.

O estabelecimento de modelos *in vivo*, nomeadamente para estudo das consequências da inibição de MCT1 a nível do crescimento e progressão tumoral surge como futura abordagem.

**Palavras-chave:** Lactato, EGF, cancro do colo do útero, c-Myc, microambiente tumoral, LDHs, MCTs

## Abstract

Emerging evidence indicates that impaired cellular energy metabolism is the defining characteristic of nearly all cancers regardless their cellular or tissue origin. Tumor cells have a remarkably different metabolism from that of the tissues from which they are derived. Although lactate is generally considered a waste product, several studies show that it is a prominent substrate that fuels the oxidative metabolism of oxygenated tumor cells. The study of the enzymes involved in lactate production (LDHA) and consumption (LDHB), as well as its transporters (MCTs), will help to define new therapeutic targets.

The main objective of this thesis is to characterize the metabolic profile of two uterine cervix cancer cell lines from two different histological types, adenocarcinoma (HeLa) and squamous cell carcinoma (SiHa), namely *LDHs* and *MCTs* expression regulation by sodium lactate (NaLac) and Epidermal Growth Factor (EGF).

Our findings suggested c-Myc activation of *LDHA* expression in HeLa cells grown in the presence of NaLac. Regarding SiHa cells, it was observed *LDHA* upregulation, at mRNA levels, by NaLac, however not c-Myc mediated. NaLac promotes *LDHB* expression in both cell lines. In SiHa cells, EGF promotes *LDHB* expression too, being this activator effect increased by NaLac. We proposed NaLac-mediated c-Myc repression of *MCT1* expression in HeLa cells. In SiHa cells, NaLac activates *MCT1* expression, decreasing c-Myc interaction with *MCT1* promoter or promoting an alternative role of c-Myc as an activator. NaLac also promotes *MCT4* expression.

In the oxidative context where SCC cancer cells develop, the upregulation of MCT1 confer crucial advantages to these cells, given its importance in lactate uptake and could be in the basis of a switch from glucose to lactate consumption in SCC tumors, as described in SiHa cells. We suggested that c-Myc could also be involved in cell migration and proliferation *in vitro*, via MCT1.

**Keywords:** Lactate, EGF, uterine cervix cancer, c-Myc, tumor microenvironment, LDHs, MCTs

# Table of contents


Agradecimentos ..... i
Resumo ..... iii
Abstract ..... vii
Index of figures ..... xiii
Index of tables ..... xv
List of abbreviations ..... xvii
1. Introduction ..... 1
1.1 Cancer ..... 1
1.2 Uterine cervix: Histology and microenvironment ..... 1
1.3 Uterine cervix cancer ..... 2
1.3.1 Worldwide incidence ..... 2
1.3.2 Histological types ..... 3
1.3.3 Human Papillomavirus (HPV) ..... 3
1.3.3.1 HPV genome ..... 4
1.3.3.2 HPV and uterine cervix cancer in Portugal ..... 6
1.3.4 Signaling pathways altered in uterine cervix cancer ..... 6
1.3.4.1 Epidermal growth factor receptor (EGFR) and uterine cervix cancer ..... 6
1.3.4.2 c-Myc and uterine cervix cancer ..... 7
1.4 Metabolic alterations in cancer ..... 8
1.4.1 Advantages of aerobic glycolysis ..... 9
1.4.2 Lactate as a signaling molecule ..... 10
1.5 Lactate dehydrogenases (LDHs) ..... 11
1.5.1 LDHs and cancer ..... 12
1.5.2 Regulation of LDHs ..... 13
1.6 Monocarboxylate transporters (MCTs) ..... 13
1.6.1 MCTs and cancer ..... 14
1.6.2 Regulation of MCTs ..... 15
1.7 Metabolic symbiosis in tumor microenvironment ..... 15
1.8 LDHs and MCTs as therapeutic targets ..... 16

2. Objectives ..... 17
3. Materials and methods ..... 19
3.1 Role of EGF growth factor in the regulation of *LDH*s (*LDHA, LDHB*, *LDHC*) and *MCT*s (*MCT1* and *MCT4*) expression in the presence and absence of Sodium Lactate (NaLac) ..... 19
3.1.1 Cell culture ..... 19
3.1.2 Gene expression ..... 19
3.1.2.1 Reverse transcription–Polymerase Chain Reaction ..... 19
3.1.2.2 Quantitative Real-Time PCR ..... 20
3.1.3 Protein levels ..... 21
3.1.3.1 Western blot ..... 21
3.1.3.2 Immunofluorescence ..... 22
3.1.4 Epigenetic regulation *and LDHA, LDHB and MCT1* promoters ..... 23
3.1.4.1 Methylation pattern ..... 23
3.1.4.1.1 Bisulfite DNA conversion ..... 23
3.1.4.1.2 Automate sequencing of *LDHA*, *LDHB* and *MCT1* promoters' CpG islands ..... 24
3.1.5 Activity of *LDHA*, *LDHB* and *MCT1* promoters ..... 25
3.1.5.1 Amplification of *LDHA*, *LDHB* and *MCT1* promoter sequences ..... 25
3.1.5.2 DNA automate sequencing of *LDHA*, *LDHB* and *MCT1* promoter sequences ..... 25
3.1.5.3 Plasmids generation and cloning ..... 26
3.1.5.4 Transient transfection of promoters' deletion constructs into HeLa and SiHa cell lines ..... 28
3.1.5.4.1 Luciferase activity of *LDHA* and *LDHB* and *MCT1* promoters' deletion constructs ..... 29
3.1.6 c-Myc-antibody chromatin Immunoprecipitation (ChIP) ..... 29
3.2 Detection of c-Myc copy number by Fluorescent in situ hybridization (FISH) ..... 30
3.3 Histological analysis ..... 31
3.3.1 Tissue microarray ..... 31
3.3.2 Immunohistochemistry for MCT1 ..... 32
3.3.3 Detection of c-Myc copy number by FISH ..... 32
3.4 Role of NaLac and EGF in cell migration, cell cycle regulation and proliferation i*n vitro* ..... 33
3.4.1 Cell migration - *In vitro* wound healing assay ..... 33
3.4.2 Cell cycle analysis by Flow Cytometry ..... 33
3.4.3 Cell proliferation *in vitro* ..... 34
3.5 Statistical analysis ..... 36
4. Results ..... 37

4.1 Role of EGF and NaLac in the regulation of *LDH*s (*LDHA*, *LDHB*, *LDHC*) and *MCT*s (*MCT1, MCT4*) expression ..... 37
4.1.1 *LDHs* and *MCTs* relative gene expression and protein levels in HeLa and SiHa cell lines ..... 37
4.1.2 Epigenetic regulation of *LDHA*, *LDHB* and *MCT1* promoters ..... 47
4.1.2.1 Methylation pattern of *LDHA, LDHB* and *MCT1* promoters ..... 47
4.1.3 Activity of *LDHA*, *LDHB* and *MCT1* promoters ..... 49
4.1.4 Role of c-Myc transcription factor in the regulation of *LDHA* and *MCT1* expression ..... 51
4.2 Detection of c-Myc copy number by Fluorescent in situ hybridization (FISH) ..... 53
4.3 Histological analysis ..... 54
4.4 Role of NaLac and EGF in cell migration, cell cycle regulation and proliferation i*n vitro* ..... 58
4.4.1 Cell migration ..... 58
4.4.2 Cell cycle regulation and proliferation *in vitro* ..... 60
4.4.2.1 Cell cycle analysis ..... 60
4.4.2.2 Proliferation curve ..... 61
5. Discussion ..... 63
6. Future perspectives ..... 73
7. Conclusions ..... 75
8. Bibliographic references ..... 79
Appendix I ..... 93
Appendix II ..... 95

## Index of figures

Figure 1 - Uterine cervix cancer metaplasia ..... 2
Figure 2 - HPV genome. ..... 4
Figure 3 - HPV-mediated progression to uterine cervix cancer ..... 5
Figure 4 - pGL3-Basic Vector ..... 26
Figure 5 - pGL3-Control Vector ..... 27
Figure 6 - LSI MYC Dual color, Break Apart Rearrangement Probe (a) and LSI IGH/MYC, CEP8 Tri-color, Dual Fusion Translocation Probe (b) ideograms ..... 31
Figure 7 - Relative gene expression of lactate dehydrogenases (LDHs) in HeLa cells (a) and SiHa cells (b) ..... 38
Figure 8 - LDHs protein levels in HeLa (LDHA and LDHB) and SiHa (LDHA, LDHB and LDHC) cells assessed by western-blot ..... 39
Figure 9 - Immunofluorescence for LDHA and LDHB in HeLa cells ..... 40
Figure 10 - Immunofluorescence for LDHA, LDHB and LDHC in SiHa cells ..... 41
Figure 11 - Relative gene expression of monocarboxylate transporters (MCTs) in HeLa cells (a) and SiHa cells (b) ..... 42
Figure 12 - Immunofluorescence for MCT1 and MCT4 in HeLa cells ..... 43
Figure 13 - Immunofluorescence for MCT1 and MCT4 in SiHa cells ..... 44
Figure 14 - MCT4 protein levels in SiHa cells assessed by western-blot ..... 45
Figure 15 - Relative gene expression of EGF receptor (*EGFR*) in HeLa cells (a) and SiHa cells (b) ..... 46
Figure 16 - Relative gene expression in SiHa cells chronically exposed to NaLac (long term (LT) exposition) with and without EGF stimulation of these cells ..... 47
Figure 17 - Schematic representation of the methylation pattern of two *LDHA* promoter CpG islands in HeLa and SiHa cells ..... 48
Figure 18 - Schematic representation of the methylation pattern of three *LDHB* promoter CpG islands in HeLa and SiHa cells ..... 48
Figure 19 - Schematic representation of the methylation pattern of one *MCT1* promoter CpG island in HeLa and SiHa cells ..... 48
Figure 20 - Luciferase activity of *LDHA (*f1, f2, f3) and *LDHB (*f1, f2) deletion constructs in transfected HeLa and SiHa cells ..... 50
Figure 21 - Luciferase activity of *MCT1 (*f1 and f2) deletion constructs in transfected HeLa and SiHa cells ..... 51
Figure 22 - Relative occupancy of c-Myc factor at *LDHA* and *MCT1* promoters (relative to IgG) in HeLa cells. 52
Figure 23 - Relative occupancy of c-Myc factor at *LDHA* and *MCT1* promoters (relative to IgG) in SiHa cells. 52
Figure 24 - Copy number analysis of c-Myc through Fluorescent in situ hybridization (FISH) ..... 54
Figure 25 - Percentage of MCT1 positive (+) and negative (-) AC cases with disomy or aneusomy for chromosome 8 and c-Myc ..... 54
Figure 26 - Percentage of MCT1 positive (from +/- to +++) and negative (-) SCC cases with disomy, trisomy, aneusomy or aneusomy and amplification for chromosome 8 and c-Myc ..... 55
Figure 27 - Percentage of MCT1 positive (+) and negative (-) SCC cases with disomy, trisomy, aneusomy or aneusomy and amplification for chromosome 8 and c-Myc ..... 55
Figure 28 - MCT1 immunodetection in SCC, CIN and normal ectocervix ..... 56
Figure 29 - MCT1 immunodetection in AC and normal endocervix ..... 57
Figure 30 - *In vitro* Wound Healing assay in SiHa cells ..... 58
Figure 31 - Quantification of wound closure in SiHa cells ..... 59

Figure 32 - Proliferation curve of SiHa cells after treatment with anti-proliferative agent Mitomycin (5µg/mL). 59
Figure 33 - Flow cytometric analysis showing the cell cycle distribution of SiHa cells (PI staining)..... 60
Figure 34 - Proliferation curve for SiHa cells..... 61
Figure 35 – Schematic representation of *LDHA*, *LDHB*, *MCT1* and *MCT4* gene expression regulation in HeLa cells..... 76
Figure 36 – Schematic representation of *LDHA*, *LDHB*, *MCT1* and *MCT4* gene expression regulation in SiHa cells..... 77

Figure A1 - Negative controls of immunofluorescence for SiHa and HeLa cells..... 95
Figure A2 - Copy number analysis of c-Myc with Fluorescent in situ hybridization (FISH)..... 95

## Index of tables

Table 1 - Predicted expression levels of the most relevant enzymes and metabolite transporters to metabolic symbiosis ..... 16
Table 2 - Program used for cDNA synthesis ..... 20
Table 3 - PCR program for cDNA amplification using quantitative Real Time-PCR primers ..... 20
Table 4 - Quantitative Real-Time PCR program ..... 21
Table 5 - PCR program for amplification of bisulfite treated DNA ..... 23
Table 6 - PCR program for amplification of bisulfite treated DNA ..... 24
Table 7 - Automate sequencing program ..... 24
Table 8 - PCR program used for amplification of *LDHA, LDHB* and *MCT1* promoter sequences ..... 25
Table 9 - Automate sequencing program ..... 26
Table 10 - PCR program for plasmid constructs amplification ..... 27
Table 11 - Automate sequencing program ..... 28
Table 12 - IP'd DNA quantitative Real-Time PCR program ..... 30
Table 13 - Primers used during the experimental work ..... 35
Table 14 - Frequency (in percentage) of c-Myc copy number detected in SiHa and HeLa cells using FISH ..... 53

Table A1 - Frequency (in percentage) of c-Myc copy number detected in SiHa and HeLa cells assessed by FISH, using 8q24 LSI MYC probe ..... 95

## List of abbreviations

AC – Adenocarcinoma
ATCC - American Type Culture Collection
ATP - Adenosine Triphosphate
bp - base pair
BSA – Bovine serum albumine
cDNA - complementary DNA
ChIP - Chromatin immunoprecipitation
CIN - Cervical Intraepithelial Neoplasia
CIS - Carcinoma in situ
CXCL8 - C-X-C chemokine 8
DAPI - 4'-6-diamidino-2-phenylindole
dd$H_2O$ - sterile bidestilled water
ddNTPs - dideoxynucleotides
DMEM - Dulbecco's modified essential medium
DNA - Deoxyribonucleic acid
dNTPs - deoxynucleotides
DTT - Dithiothreitol
EGF - Epidermal growth factor
EGFR - Epidermal growth factor receptor
ER – Estrogen receptor
FBS - Fetal bovine serum
FDG-PET - Fluorodeoxyglucose positron emission tomography
FH - Fumarate hydratase
FISH - Fluorescent in situ hybridization
Glut-1 - Glucose transporter 1
HER - Human epithelial growth factor response
HGCIN - High-grade cervical intraepithelial neoplasia
HIF-1 - Hypoxia Inducible Factor-1
HIF-1α - Hypoxia-Inducible Factor 1α
HK - Hexokinase
HPV - Human papillomavirus
HR- High-risk
HRP - Horse raddish peroxidase
HSIL - High-grade squamous intraepithelial lesions
ICC - Invasive cervical cancer
Ig - Immunoglobulin
IL-8 - Interleukine-8
IP'd - Immunoprecipitated
iPFK-2 - 6-phosphofructo-2 kinase
LCR - Long control region
LDH - Lactate dehydrogenase
LDH-M - Lactate dehydrogenase subunit M
LDH-H – Lactate dehydrogenase subunit H
LSI - Locus Specific Identifier
LSIL - Low-grade squamous intraepithelial lesions
MCT - Monocarboxylate transporter
mRNA - Messenger Ribonucleic acid
MSSCC - Maxillary sinus squamous cell carcinoma
NaLac – sodium lactate

NF-kB - Nuclear factor-kB
NHE-1 - $Na^+/H^+$ exchanger 1
NSCLC - Non-small cell lung cancer
ON - Overnight
ORFs - Open reading frames
PBS – Phosphate buffered saline
PCR - Polymerase chain reaction
PDH - Pyruvate dehydrogenase
PDK - Pyruvate dehydrogenase kinase
PGE2 – Prostaglandin E2
$pH_e$ - Extracellular pH
$pH_i$ – Intracellular pH
PI - Propidium iodide
$pO_2$ - Oxygen tension
qRT-PCR - Quantitative Real-time PCR
RIPA - Radio-Immunoprecipitation Assay
RNAi - RNA interference
ROS - Reactive Oxygen Species
RPTC - Renal Proximal Tubular cells
RT - Room Temperature
RT-PCR - Reverse transcription polymerase chain reaction
SC - Squamocolumnar
SCC - Squamous cell carcinoma
SDH - Succinate dehydrogenase
SILs - Squamous intraepithelial lesions
SLC16 - Solute carrier family 16
STAT3 - Signal transducer and activator of transcription 3
TBE - Tris-borate-EDTA
TBS - Tris Buffered Saline
TCA- Tricarboxylic acid
TGS - Tris-Glycine-SDS
Tm – Melting temperature
TMA - Tissue microarray
URR - Upstream regulatory region
VEGF - Vascular endothelial growth factor
WHO - World Health Organization

# 1. Introduction

## 1.1 Cancer

Cancer is a complex disease involving numerous tempospatial changes in cell physiology, which ultimately lead to malignant tumors. Tumor cell invasion of surrounding tissues and distant organs is the primary cause of morbidity and mortality for most cancer patients. The biological process by which normal cells are transformed into malignant cancer cells has been the subject of a large research effort in the biomedical sciences for many decades (Seyfried & Shelton, 2010).

Hanahan & Weinberg, 2000 suggested that six essential alterations in cell physiology could underlie malignant cell growth. These six alterations were described as the hallmarks of nearly all cancers and included, 1) self-sufficiency in growth signals, 2) insensitivity to growth inhibitory (antigrowth) signals, 3) evasion of programmed cell death (apoptosis), 4) limitless replicative potential, 5) sustained vascularity (angiogenesis), and 6) tissue invasion and metastasis (Hanahan & Weinberg, 2000). Genome instability, leading to increased mutability, was considered the essential enabling characteristic for manifesting the six hallmarks ( Seyfried & Shelton, 2010; Hanahan & Weinberg, 2000).

Overall, an estimated 12.7 million new cancer cases and 7.6 million cancer deaths occur in 2008, with 56% of new cancer cases and 63% of the cancer deaths occurring in the less developed regions of the world. The most commonly diagnosed cancers worldwide are lung (1.61 million, 12.7% of the total), breast (1.38 million, 10.9%) and colorectal cancers (1.23 million, 9.7%). The most common causes of cancer death are lung cancer (1.38 million, 18.2% of the total), stomach cancer (738 000 deaths, 9.7%) and liver cancer (696 000 deaths, 9.2%) (Ferlay et al., 2010).

## 1.2 Uterine cervix: Histology and microenvironment

The uterine cervix protrudes into vagina (exocervix or ectocervix) and contains an endocervical canal that links the vagina with the uterus. The endocervical canal is lined by cells similar to the uterus – a single layer of tall, columnar, mucus-secreting cells. In areas where the cervix is exposed to the hostile microenvironment of the vagina, the cervix is lined by thick stratified squamous epithelia. The presence of *Doderlein bacilli* - gram-positive and rod-shaped bacilli which grows anaerobically on acid media - in the vaginal mucosa contributes to this hostile microenvironment. It is known that its presence is dependent on estrogen and that its function is to convert the glycogen present in the vaginal mucosa into lactic acid contributing to the acidification of vagina microenvironment (Gupta, 2011; Redondo-Lopez et al., 1990).

At the point where the endocervical canal opens, the junction between the two types of epithelium exists (Brezinski, 2006). The stratified squamous cells in the ectocervix transition into mucinous columnar epithelium in the endocervix with the interface between the two tissues designated as the squamocolumnar (SC) junction (Havens & Sullivan, 2002).

The natural history of the endocervical columnar epithelium is to undergo metaplastic transformation to a mature squamous epithelium, i.e. squamous metaplasia, this change being especially active during adolescence and pregnancy (Havens & Sullivan, 2002) (Figure 1). The area involved with this metaplastic change is designated the transformation zone and it's dynamic throughout a woman's reproductive life, migrating and changing location in the cervix in response to stimuli, including hormones and pH (Braun & Anderson, 2007). High estrogen levels, as experienced in the luteal phase of the menstrual cycle and during pregnancy, promote the gradual transition of squamous epithelium to columnar epithelium. Low estrogen

levels, as occur in menopause, cause the SC junction to recede into the endocervical canal. The adaptations that these cell types undergo are examples of metaplasia – the cellular response of changing from one type of epithelium to another in the face of an environmental stessor. Although the metaplastic changes of the cervix are not pathological, the squamous epithelia cell component of the transformation zone (Figure 1) is vulnerable to stressors, which may cause cell injury or damage (Braun & Anderson, 2007), being the tissue at risk of being influenced by oncogenic factors, principally Human Papillomavirus, to initiate neoplastic change (Brezinski, 2006; Havens & Sullivan, 2002). Accordingly to Burghardt & Ostör, 1983 a substantial majority (~87%) of uterine cervix squamous intraepithelial lesions (SILs) and cancers develop within the specific microenvironment of the cervix at the transformation zone (Burghardt & Ostör, 1983). In addition, recent data suggests that carcinogenic Human Papillomavirus-related cervical intraepithelial neoplasia (CIN) and uterine cervix cancers are linked to a small, discrete cell population that localizes to the SC junction of the cervix that expresses a unique gene expression signature (Herfs et al., 2012).

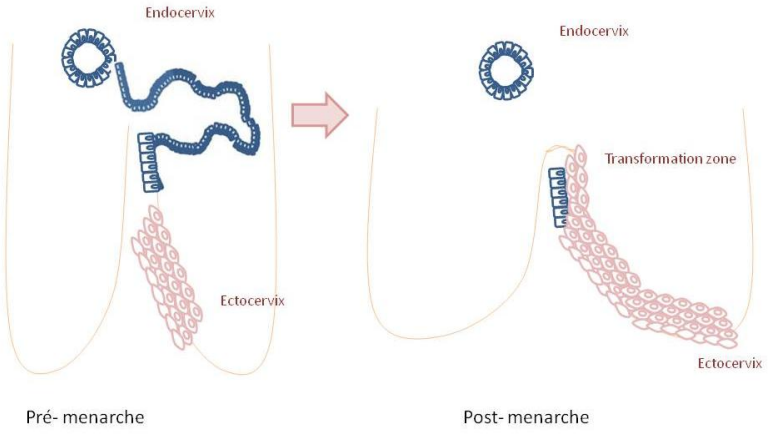


**Figure 1 - Uterine cervix cancer metaplasia.** The endocervical columnar epithelium undergoes metaplastic transformation to a mature squamous epithelium during adolescence.

## 1.3 Uterine cervix cancer

### 1.3.1 Worldwide incidence

Uterine cervix cancer is a major health problem worldwide; it is the third most common cancer in women, and the seventh overall (Ferlay et al., 2010; Yugawa & Kiyono, 2009), and is the fourth leading cause of cancer death in females worldwide, accounting for 9% (529 800) of the total new cancer cases and 8% (275 100) of the total cancer deaths among females in 2008 (Jemal et al., 2011; Ferlay et al., 2010).

Although the incidence of this cancer has declined in developed countries (Yeasmin et al., 2011) there is an estimated 500 000 new cases of uterine cervix cancer (the latest statistics are from 2008) per year worldwide with mortality of approximately one-third of these cases (Jemal et al., 2011; Yugawa & Kiyono, 2009).

### 1.3.2 Histological types

As previously referred, most uterine cervix cancers develop from the transformational zone where columnar epithelium undergoes physiological metaplasia to become squamous epithelium. This area is most vulnerable to neoplastic transformation. The neoplastic or dysplastic process may involve the entire thickness of squamous epithelium (CIS, carcinoma in situ) before penetrating the basement membrane (Nguyen & Averette, 1999).

Uterine cervix cancer is characterized by a well-defined pre-malignant phase that can be suspected on cytological examination of exfoliated cervical cells and confirmed on histological examination of cervical material. There are different classification systems of precursor lesions of cervical squamous-cell carcinoma, World Health Organization (WHO) and Bethesda (Lax, 2011). Cervical intraepithelial neoplasia is categorized into 3 grades (CIN1-3). These pre-malignant changes represent a spectrum of histological abnormalities, designated as dysplasias, epithelial abnormalities in which the cells becomes disorganized, which are characterized by developmental changes in cell growth, shape and organization, ranging from CIN1 (mild dysplasia) to CIN2 (moderate dysplasia) to CIN3 (severe dysplasia/carcinoma in situ) (Woodman et al., 2007). Accordingly to Bethesda classification for cervical cytology this could be low- or high-grade squamous intraepithelial lesions (LSIL and HSIL, respectively) (Lax, 2011).

Cytological and histological examinations cannot reliably distinguish the few women with abnormal smears who will progress to invasive cancer from the vast majority of those whose abnormalities will spontaneously regress (Woodman et al., 2007).

There are two clinically significant variants of uterine cervix cancer. Squamous cell carcinomas that comprise around 85% to 90%, and adenocarcinomas/adenosquamous carcinomas that comprise 10% to 25% of uterine cervix cancer cases (Chan et al., 2003; Smith et al., 2000).

Adenocarcinomas/adenosquamous carcinomas are often larger at the time of diagnosis than squamous carcinomas and frequently exhibit early lymphatic and hematogeneous metastasis, features that make them difficult to cure by conventional therapeutic measures. Moreover, the genetic alterations associated with cervical adenocarcinomas/adenosquamous carcinomas are unknown (Yeasmin et al., 2011).

Squamous cell carcinoma typically presents as an ulcerated and exophytic lesion, while adenocarcinoma presents as an enlarged, barrel-shaped cervix with normal ectocervix (Nguyen & Averette, 1999). Besides that, locally advanced squamous cell carcinomas of the uterine cervix show a physiological microenvironment characterized by low oxygen tension ($pO_2$), regions with hypoxic tissue ($pO_2 < 10$ mmHg), elevated interstitial fluid pressure, high lactate concentration, low extracellular pH ($pH_e$), and energy deprivation (Milosevic et al., 2004; Schwickert et al., 1995; Höckel et al., 1991).

### 1.3.3 Human Papillomavirus (HPV)

Human papillomavirus (HPV) is the etiologic agent of uterine cervix cancer; however, HPV infection is not the only factor in the carcinogenesis of cervix carcinoma (Yeasmin et al., 2011). In addition, the genomic alteration of oncogenes and tumor suppressor genes in uterine cervical cells is essential for uterine cervix carcinogenesis (Yeasmin et al., 2011).

HPVs are small, non-enveloped viruses that contain circular double-stranded DNA genomes of approximately 8000 base pairs (Figure 2) (Hebner & Laimins, 2006) that can cause most benign and malignant lesions in epithelial tissues (skin and mucosa) (de Villiers et al., 2004). HPV genomes replicate episomally, that is in an autonomous manner, in host cells, however HPV DNA is frequently found to be integrated into chromosomes in uterine cervical cancer cells (Yugawa & Kiyono, 2009).

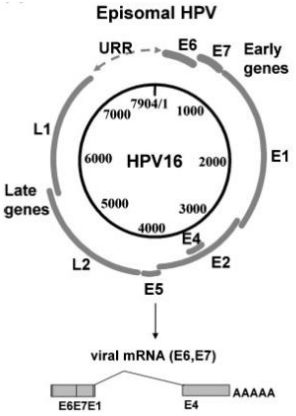


**Figure 2 - HPV genome.** The HPV genome is a circular double-stranded DNA of approximately 8000 base pairs. The genome contains an upstream regulatory region (URR) and eight open reading frames (ORFs) of six early genes (E1, E2, E4, E5, E6, E7) and two late genes (L1, L2). Early genes have roles in viral replication and late genes encode viral capsid proteins. E1 is a viral helicase and recruited to the viral replication origin located in URR by E2, where it forms the DNA replication machinery with cellular proteins. HPV genomes replicate episomally in their life cycle. Adapted from Yugawa & Kiyono, 2009.

#### 1.3.3.1 HPV genome

HPV DNA has eight open reading frames (ORFs), namely E1, E2, E4, E5, E6, E7 (expressed in the early phase of infection), L1 and L2 (expressed in the late phase of infection) and control region designated as the long control region (LCR) or upstream regulatory region (URR) (zur Hausen, 2002; Yugawa & Kiyono, 2009). Early genes have roles in viral replication and late genes encode viral capsid proteins (Yugawa & Kiyono, 2009). E6 and E7 ORFs are oncoproteins involved in proliferation-stimulating and transforming activities through the loss of E1 and E2 ORFs, allowing the integration of E6 and E7 ORFs within the host DNA. Once integrated, HPV DNA can immortalize human keratinocytes due to the interactions between the E6 and E7 oncogenes with p53 and pRb tumor suppressor proteins, respectively, thus inhibiting the process of apoptosis. Moreover LCR regulates the transcription of the E6 and E7 viral oncogenes through the transcription factors of the virus and the host cells (zur Hausen, 2002).

Over 100 different genotypes of HPVs have been identified of which about 40 are known to infect the genital tract (Yugawa & Kiyono, 2009). Epidemiological studies to date suggest that at least 15 (16,18,45,31,33,52,58,35,59,56,51,39,68,73,82) of these, called oncogenic or high-risk (HR) types, (Roden & Wu, 2006) are significantly associated with progression to invasive cervical cancer (ICC) (Bosch et al.,1995). Most of these HR types are phylogenetically related to either HPV16 (31, 33, 35, 52 and 58) or HPV18 (39, 45, 59 and 68) (Chan et al., 1995).

Previous data revealed that high-risk HPVs are associated with more than 90% of uterine cervical cancers (Walboomers et al., 1999). Infection with these HPVs is considered to be the primary cause of uterine cervical dysplasia or low-grade CIN, and uterine cervical cancers are widely thought to arise from these lesions after long periods of time (Woodman et al., 2007; zur Hausen, 2002). Recent data suggest that high-risk HPV types 16 and 18 are responsible for > 70% of cases of uterine cervix cancer (Boulet et al., 2008). Whereas HPV18 is the type most strongly associated with adenocarcinoma of the cervix, HPV16, followed by HPV18, are the types most frequently detected when squamous cell carcinoma is diagnosed (Clifford et al., 2003; Muñoz et al., 2003).

Accordingly to Woodman et al., 2007 the frequency with which HPV16 is found in integrated forms increases with the severity of uterine cervical neoplasia, although in some women with invasive disease only

episomal forms are detected. By contrast, HPV18 is almost always found in only integrated forms in women with high-grade cervical intraepithelial neoplasia (HGCIN) and invasive disease (Figure 3) (Woodman et al., 2007). The timing of viral integration appears to correspond to the development of high-grade CIN as a consequence of high-level expression of E6 and E7 (Figure 3) (von Knebel Doeberitz, 2002). In fact, E6 and E7 are invariably expressed in HPV-positive uterine cervix cancer cells, and play important roles in carcinogenesis as well as maintenance of the transformed phenotype. Deregulated expression of E6 and E7 can bring about substantial biological consequences, such as suppression of immunoresponse, immortalization, transformation and inhibition of differentiation, in addition to the previously referred inactivation of the major tumor suppressors, including p53 and pRB, inducing genomic instability that increases the risk of accumulation of cellular genetic and epigenetic changes (Yugawa & Kiyono, 2009). So, these two viral proteins do not merely immortalize normal human epithelial cells but confer some tumorigenic properties of transformed cells (Yugawa & Kiyono, 2009).

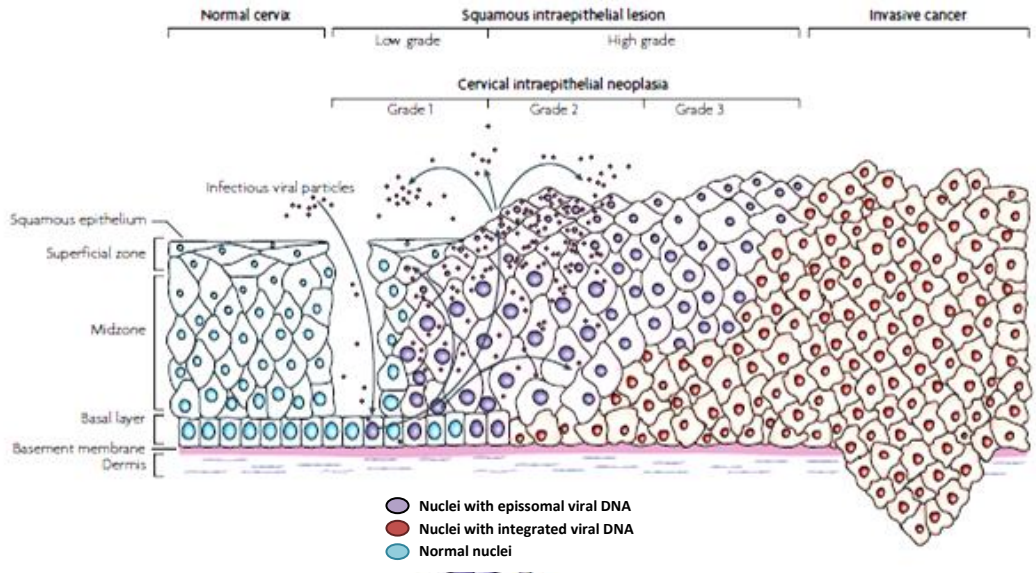


**Figure 3 - HPV-mediated progression to uterine cervix cancer**. Basal cells in the cervical epithelium rest on the basement membrane, which is supported by the dermis. Human papillomavirus (HPV) is thought to access the basal cells through micro-abrasions in the cervical epithelium. Following infection, the early HPV genes E1, E2, E4, E5, E6 and E7 are expressed and the viral DNA replicates from episomal DNA (purple nuclei). In the upper layers of epithelium (the midzone and superficial zone) the viral genome is replicated further, and the late genes L1 and L2, and E4 are expressed. L1 and L2 encapsidate the viral genomes to form progeny virions in the nucleus. The shed virus can then initiate a new infection. Low-grade intraepithelial lesions support productive viral replication. An unknown number of high-risk HPV infections progress to high-grade cervical intraepithelial neoplasia (HGCIN). The progression of untreated lesions to microinvasive and invasive cancer is associated with the integration of the HPV genome into the host chromosomes (red nuclei), with associated loss or disruption of E2, and subsequent upregulation of E6 and E7 oncogene expression. LCR, long control region. Adapted from Woodman et al., 2007.

#### 1.3.3.2 HPV and uterine cervix cancer in Portugal

Accordingly to Pista et al., 2011 the most frequent HPV genotype in Portugal is HPV16 (25.5%), followed by HPV 31, 53, 66, 58, and 51 (Pista et al., 2011). Data from Nobre et al., 2010 also indicate that the most prevalent type in Portuguese women is HPV16 (detected in 33.8% of women infected with HPV), but followed by HPV 58 (9.2%), HPV 33 (7.0%), HPV 18 (6.3%), HPV 53 (5.6%), HPV 31 and 56 (4.9% each), HPV 6 (3.5%), and HPV 66 and 81 (2.8% each). In addition, of 44 uterine cervix carcinoma samples, 71% were associated with HPV 16 (60%) and HPV 18 (11.1%), followed by the high-risk types 33 (11.1%), 35 (4.4%), 45 (4.4%), and 56 (2.2%), the probable high-risk type 53 (4.4%) and the unknown-risk type 67 (2.2%) (Nobre et al., 2010).

Accordingly to Globocan 2008 statistics, the estimated incidence of uterine cervix cancer in Portugal is 949, i.e. 4.9%. In addition, in Portugal, uterine cervix cancer is the fourth most frequent among female (ranking defined by total number of cases).

### 1.3.4 Signaling pathways altered in uterine cervix cancer

Chromosomal instability at a numerical or structural level is a hallmark of malignant tumors. Deletion, duplication and amplification of various genomic regions have been demonstrated to be present in many types of cancers (Duensing & Munger, 2004), including uterine cervix cancer .

Amplification of proto-oncogenes and inactivation of tumor suppressor genes play an important role in the pathogenesis of many different tumors (Kersemaekers et al., 1999).

The genomic alteration of oncogenes and tumor suppressor genes in uterine cervical cells is essential for uterine cervix carcinogenesis. Amplification of DNA in certain chromosomal regions is one of the mechanisms by which genes that are critical for the development and progression of human cancers are activated. Numerous oncogenes and other cancer-related genes have been identified in these amplified regions (Schwab, 1999).

Studies in uterine cervix carcinomas have shown that the receptors for the epidermal growth factor and c-Myc are important for the prognosis of patients with advanced tumors (stages II–IV) (Kersemaekers et al., 1999). Particularly in squamous cell carcinomas proto-oncogenes such as epidermal growth factor receptor (EGFR) and c-Myc are often activated by amplification and are clearly associated with malignant phenotypes (Hale et al., 1993; Pfeiffer et al., 1989).

#### 1.3.4.1 Epidermal growth factor receptor (EGFR) and uterine cervix cancer

The EGFR is a receptor belonging to the human epithelial growth factor response (HER) family of receptor tyrosine kinases. Receptor activation upon ligand binding leads to downstream activation of the PI3K/AKT, RAS/RAF/MEK/ERK and PLCγ/PKC pathways that influence cell proliferation, survival and the metastatic potential of tumor cells. This HER family comprises four structurally related transmembrane receptors: HER1 (EGFR or erbB1), HER2 (HER2neu or c-erb-B2), HER3 (c-erb-B3), and HER4 (c- erb-B4) (Lee et al., 2005).

The oncogenic pathway of some cells is thought to be initiated as a result of HER family receptor mutation, overexpression, structural rearrangements, and/or relief of normal regulatory or inhibitory pathways (Anido et al., 2003; Witton et al., 2003; Woodburn, 1999) .

EGFR plays an important role in the differentiation and morphogenesis of many organs and proliferation and survival in mammalian cells (Lynch et al., 2004). Increased activation by gene amplification,

protein overexpression or mutations of the EGFR has been identified as an etiological factor in a number of human epithelial cancers (Brand et al., 2011; Sarkis et al., 2010). Particularly, overexpression of EGFR has been reported to be frequent in uterine cervix cancer, ranging from approximately 50–70% (Shen et al., 2008; Kersemaekers et al., 1999; Hale et al., 1993).

In certain studies, the expression of EGFR proved to be an independent predictor of poor prognosis for the uterine cervix cancer decreasing local tumor control after radiotherapy (Kersemaekers et al., 1999; Kristensen et al., 1996) while other studies did not confirm this result (Nagai et al., 2000). Lee et al., 2005 have reported that increased expression of HER2 and decreased expression of EGFR membranous staining correlate with improved overall survival in patients with carcinoma of the cervix (Lee et al., 2005). In addition, that overexpression of HER2 was correlated with adenocarcinoma, and overexpression of EGFR correlated significantly with squamous cell histology and is less frequent in adenocarcinomas (Lee et al., 2004; Hale et al., 1993) . Recently, it has been proposed that inhibiting EGFR during radiotherapy may be a promising therapeutic strategy in certain squamous cell carcinomas (Nagy et al., 2011).

Epidermal growth factor (EGF) is single-chain polypeptide (6 kDa) that a wide spectrum of activities including mitogenic, angiogenic and chemotactic effects on normal and tumor cells (Price et al., 1996; Khazaie et al., 1993). EGF plays an important role in the regulation of cell growth, proliferation, and differentiation by binding to its receptor EGFR (Carpenter & Cohen, 1990). Besides that EGF family ligands promote tumor cell motility, adhesion and invasion (Lu et al., 2001; Price et al., 1996; Rosen & Goldberg, 1989). EGF is one of the potent stimulators for uterine cervix cancer cell invasiveness (Shen et al., 2006). Data from Chiang et al., 2008 revealed that $Na^+/H^+$ exchanger 1 (NHE-1) activity is necessary for this EGF-mediated uterine cervix cancer cell migration (Chiang et al., 2008) .

Additionally, EGF has also documented effects on metabolism, through stimulation of various intracellular responses *in vitro*, including $Na^+/K^+$ antiport activity, $Na^+$-dependent phosphate transport, glycolysis, and glucose and amino acid uptake in a variety of cultured epithelial cells (Nowak & Schnellmann, 1995). Accordingly to Nowak & Schnellmann, 1995 an increase in glucose consumption was accompanied by a rapid change in lactate metabolism in Renal Proximal Tubular cells (RPTC) treated with EGF. EGF treatment of these cells resulted in net lactate production that reached a maximum when net glucose consumption was the highest, while in not treated cells there as a net consumption of lactate. So, the authors proposed that EGF shifts glucose metabolism from gluconeogenesis to glycolysis and rapidly stimulates the pentose cycle (Nowak & Schnellmann, 1995).

#### 1.3.4.2 c-Myc and uterine cervix cancer

The c-Myc proto-oncogene is closely associated with cellular proliferation. The gene is located at chromosome 8q24 and encodes two nuclear phosphoproteins with Mr 62,000 and 66,000 (Kersemaekers et al., 1999). c-Myc is a transcription factor normally involved in the regulation of cell metabolism and in the induction of cell proliferation (Grandori et al., 2000).

Amplification or increased expression of c-Myc has been found in many tumors, most notably in lymphoid tumors and carcinomas, including uterine cervix carcinomas (Kersemaekers et al., 1999).

Regarding uterine cervix carcinomas, amplification and/or overexpression of the c-Myc gene were frequently observed in advanced-stage uterine cervix cancers and were shown to be associated with tumor progression (Riou et al., 1990). Accordingly to Bourhis et al., 1990 overexpression of c-Myc (i.e., levels at least three times the mean observed in normal tissues) was present in 33% of invasive carcinomas of the cervix (Bourhis et al., 1990).

Accordingly to Brychtová et al., 2004 expression of c-Myc protein is increased not only in uterine cervix cancer but also in the premalignant lesions since that they found significantly higher levels of c-Myc protein in keratinocytes of high-grade dysplasias in comparison to low-grade dysplasias and control cases. However, the authors did not observe differences between low-grade CIN and a control group of patients. The same significant changes between above mentioned groups were seen in surrounding stromal cells (fibrocytes, fibroblasts, some endothelial cells and lymphocytes) (Brychtová et al., 2004). Other authors had also revealed that c-Myc amplification is frequently detected in precancerous cervical lesions with HPV infection (Chen et al., 2012).

Recent data indicated that c-Myc positivity rates (that is c-Myc gain) in normal subjects, CIN1, CIN2, CIN3 were 5%, 26%, 96%, 100%, respectively, and increased in association with the severity of the histological diagnosis. In squamous cell carcinoma (SCC) c-Myc positivity rate was 100% (Policht et al., 2010). The mean of signals for specimens diagnosed as normal was approximately 2, for CIN1 was close to 2, CIN2 revealed a probe signals means of 2.63, in CIN3 2.95. In cancer cases (SCC) it was verified and increase in mean c-Myc copy number to approximately 4 (Policht et al., 2010).

### 1.4 Metabolic alterations in cancer

Research into tumor cell metabolism has recently entered a new age (Cairns et al., 2011). Although this field was actively explored in the pre-genomics era, the discovery of tumor suppressor genes and oncogenes dampened interest in metabolism as a potential source of cancer cell specificities and related therapeutic targets. However, although the study of tumor-associated genes has led to the identification of oncoproteins as new therapeutic targets, a cure for cancer is still far away. Scientists in the cancer field are therefore reconsidering earlier metabolic discoveries using the molecular tools that are now available. This has led to cancer metabolism's comeback to business (Draoui & Feron, 2011).

In addition to the six recognized hallmarks of cancer (previously cited), aerobic glycolysis or the Warburg effect is also a robust metabolic hallmark of most tumors (Hanahan & Weinberg, 2011; Seyfried & Shelton, 2010).

The view of cancer as a metabolic disease was gradually displaced with the view of cancer as a genetic disease. While there is renewed interest in the energy metabolism of cancer cells, it is widely thought that the Warburg effect and the metabolic defects expressed in cancer cells arise primarily from genomic mutability selected during tumor progression (Seyfried & Shelton, 2010; Hsu & Sabatini, 2008; Kim & Dang, 2006; Shaw, 2006). But accordingly to Seyfried & Shelton, 2010 damage to cellular respiration precedes and underlies the genome instability that accompanies tumor development. Once established, genome instability contributes to further respiratory impairment, genome mutability, and tumor progression. In other words, effects become causes. This hypothesis is based on evidence that nuclear genome integrity is largely dependent on mitochondrial energy homeostasis and that all cells require a constant level of useable energy to maintain viability (Seyfried & Shelton, 2010). So, emerging evidence indicates that impaired cellular energy metabolism is the defining characteristic of nearly all cancers regardless of cellular or tissue origin (Seyfried & Shelton, 2010).

Tumor cells have a remarkably different metabolism from that of the tissues from which they are derived. They exhibit an altered metabolism that allows them to sustain higher proliferative rates (Tennant et al., 2009; DeBerardinis et al., 2008) and resist some cell death signals, particularly those mediated by increased oxidative damage (King & Gottlieb, 2009). However, this means that they are more nutrient hungry and excrete more waste products than normal tissues, resulting in a build-up of metabolites inside the cell and the formation of a more hostile environment outside the cell. In order to divide, a cell needs to both increase its

size and replicate its DNA - processes that are hugely metabolically demanding and which require large quantities of proteins, lipids and nucleotides, as well as energy in the form of ATP. This anabolic drive requires cells to increase their uptake of the building blocks for this process, major factors being amino acids and glucose (Tennant et al., 2010).

So tumor cells reprogramme their metabolic pathways to meet these needs during the process of tumor progression. The best characterized metabolic phenotype observed in tumor cells is the Warburg effect consisting in the abrogation of Krebs cycle and electron transport chain and increase rate of glycolysis even under normal oxygen concentrations (Vander Heiden et al., 2009; Warburg, 1956). As a result, unlike most normal cells, many cancer cells produce substantial amount of their energy from aerobic glycolysis, converting most of the incoming glucose to lactate rather than metabolizing it through oxidative phosphorylation (Semenza, 2008; Warburg, 1956). The evidence that most tumors seem to use glucose at similar or even higher rates than normal organs came from images recorded using [18F]-fluorodeoxyglucose positron emission tomography (FDG-PET), in which tumors often appear as PET-positive as some of the most metabolically active organs (such as the brain and heart) (Gambhir, 2002).

In sum, although cancer cells retain their ability to increase glucose uptake under anaerobic conditions (the Pasteur effect) they show an increased glucose uptake in the presence of oxygen (aerobic glycolysis). However, in contrast to normal tissues, a substantial amount of pyruvate is reduced to lactate instead of being directed into the mitochondrion, a phenotype first described by Otto Warburg (Warburg, 1956).

The metabolic alterations and adaptations of cancer cells have been extensively studied over the past century (Tennant et al., 2010). They create a phenotype that is essential for tumor cell growth and survival, altering the flux along key metabolic pathways, such as glycolysis and glutaminolysis (Tennant et al., 2009). Some of the mechanisms used by tumors to bring about these changes include the altered expression (metabolic adaptation to hypoxia through activation of glycolytic gene transcription (such as *Lactate dehydrogenase A (LDHA)* gene regulation by Hypoxia Inducible Factor-1 (HIF-1)) (Semenza et al., 1996), mutation (of the tricarboxylic acid cycle (TCA) cycle tumor suppressors, succinate dehydrogenase (SDH) and fumarate hydratase (FH)) and post-translational inactivation of an enzyme (Pyruvate dehydrogenase kinase (PDK1) phosphorylates and inactivates the mitochondrial pyruvate dehydrogenase (PDH) complex) (Kim et al., 2006) or the substitution of a different enzyme isoform (high expression of inducible isozyme of 6-phosphofructo-2 kinase (iPFK-2) in proliferating cancer cells) (Atsumi et al., 2002). On the basis of these observations, the development of treatments that target tumor metabolism is receiving renewed attention (Tennant et al., 2010) .

Although the key factors behind the cancer metabolic phenotype still remain to be elucidated, the current literature shows that c-Myc, p53, and HIF-1 are crucial for the tumor cells' aberrant metabolic behavior and that exists an interplay of this triad of transcription factors in the regulation of cancer cell metabolism (Yeung et al., 2008). Focusing on c-Myc, recent data pointed out that c-Myc overexpression is found in 10–20% of all tumors and has been shown to increase glycolysis (Cairns et al., 2011). Besides that, it has been shown that this c-Myc overexpression also increases the cellular capacity to perform both glycolysis and oxidative phosphorylation, and thus provides the cell with metabolic flexibility (Graves et al., 2010).

### 1.4.1 Advantages of aerobic glycolysis

There is some debate about the selective advantages that glycolytic metabolism provides to proliferating tumor cells. Initial work pointed that tumor cells develop defects in mitochondrial function and that aerobic glycolysis is a necessary adaptation to the lack of ATP production through oxidative phosphorylation

(Cairns et al., 2011). However, it was later appreciated that mitochondrial defects are rare (Frezza & Gottlieb, 2009) and that tumors retain the capacity for oxidative phosphorylation and consume oxygen at rates similar to those observed in normal tissues (Moreno-Sánchez et al., 2007; Fantin et al., 2006; Weinhouse, 1976). Other explanations include the concept that glycolysis has the capacity to generate ATP at a higher rate than oxidative phosphorylation and so would be advantageous as long as glucose supplies are not limited. Alternatively, it has been proposed that glycolytic metabolism arises as an adaptation to hypoxic conditions during the early avascular phase of tumor development, as it allows for ATP production in the absence of oxygen. Adaptation to the resulting acidic microenvironment that is caused by excess lactate production may further drive the evolution of the glycolytic phenotype (Gillies et al., 2008; Gatenby & Gillies, 2004). Finally, most recently, it has been proposed that aerobic glycolysis provides a biosynthetic advantage for tumor cells, and that a high flux of substrate through glycolysis allows for effective shunting of carbon to key subsidiary biosynthetic pathways (Vander Heiden et al., 2009).

The aforementioned observations position glycolysis as a key contributor to the malignant phenotype and support the quest for new anticancer treatments targeting glycolysis. Indeed, most of the molecular adaptations supporting high-rate glycolysis are unique to cancer in an otherwise healthy tissue (Porporato et al., 2011). In order to find these new anticancer therapies metabolic studies must consider all the intervenients in metabolomic plateau. The transporters of carboxylate compounds, namely glucose, lactate and pyruvate should be studied as well as the enzymes that catalyse key steps in metabolic pathways, namely lactate and pyruvate dehydrogenases and cytochrome c oxidase.

### 1.4.2 Lactate as a signaling molecule

Traditionally thought of as a glycolytic waste product, lactate may be one such signal. It has been found that inhibition of lactate dehydrogenase (LDH) can block tumor growth, most likely by multiple mechanisms. Much of the evidence for lactate as a multifunctional metabolite comes from work in exercise physiology and muscle metabolism (Philp et al., 2005). Transported by several monocarboxylate transporters (MCTs), lactate may be shared and metabolized among cells, although the idea is still controversial (Hashimoto et al., 2006). The interconversion of lactate and pyruvate might alter the $NAD^+$/NADH ratio in cells, and lactate exchange may serve to coordinate the metabolism of a group of cells (Hsu & Sabatini, 2008).

Recently, lactate has also been pointed out as a signaling molecule, since it stimulates the overexpression of mitochondrial monocarboxylate transporter 1 (MCT1) (increase both at mRNA and protein levels) and cytochrome c oxidase, components of mitochondrial lactate oxidation complex (Hashimoto & Brooks, 2008; Hashimoto et al., 2007). Besides that, accordingly to Hashimoto et al., 2007, in L6 muscle cells, lactate signaling cascade involves Reactive Oxygen Species (ROS) production and converges on transcription factors affecting mitochondrial biogenesis (Hashimoto et al., 2007).

Data from Sonveaux et al., 2008 evidence oxidative preference of some tumor cells for lactate over glucose. Lactate, released as the end-product of glycolysis in the hypoxic tumor cell compartment, prominently fuels the oxidative metabolism of the oxygenated tumor cell subpopulation, thereby sparing glucose for glycolytic cells (evidence of metabolic symbiosis in cancer, described later) (Sonveaux et al., 2008). This mechanism involves a competition between lactate and glucose metabolism for the intracellular $NAD^+$ pool. Existence of this feedback could provide several advantages to oxidative tumor cells. First, oxidation of lactate to pyruvate by LDH involves the sustained production of reducing equivalents that could buffer tumor oxidative stress and activate prosurvival pathways (specifically Akt pathway) (Pelicano et al., 2006). Second, lactate

oxidation does not require the initial energy input that drives ATP production from glucose. Third, respiration of lactate yields 18 ATP per lactate molecule and spares energy normally intended for housekeeping glycolytic enzymes. Lactate oxidation is thus more concise and more effective than glucose in the tumor cell energy metabolism under aerobic conditions (Sonveaux et al., 2008). Finally, because ROS are natural by-products of mitochondrial respiration, it has been proposed that glucose to lactate conversion may protect cancer cells from oxidative stress, as previously referred, and considered an advantage of aerobic glycolysis (Brand & Hermfisse, 1997).

Lactate release from tumor cells is a common endpoint of several metabolic alterations, raising the hypothesis of an association with tumor progression (Walenta et al., 2004). Some evidences support this hypothesis: low interstitial pH is associated with the upregulation of various angiogenic molecules, such as vascular endothelial growth factor (VEGF), which support tumor growth, invasion, and metastasis) (Pinheiro et al., 2008; Fukumura et al., 2001). In this line of evidence lactate accumulation in human tumors has been associated with metastasis, tumor recurrence and poor survival, particularly in squamous cell carcinomas of the uterine cervix cancer (Walenta et al., 2000; Schwickert et al., 1995). So, and like numerous recent reports show, there are various biological activities of lactate that can enhance the malignant behavior of cancer cells. These mechanisms include, beyond the upregulation of VEGF, the activation of hyaluronan synthesis by tumor-associated fibroblasts, upregulation of hypoxia-inducible factor 1α (HIF-1α), and direct enhancement of cellular motility that generates favorable conditions for metastatic spread. Thus, lactate accumulation not only mirrors but also actively enhances the degree of tumor malignancy (Walenta & Mueller-Klieser, 2004).

### 1.5 Lactate dehydrogenases (LDHs)

The reversible pyruvate reduction into lactate reaction is catalyzed by the LDH family of tetrameric enzymes and it also allows glycolytic cells to maintain the levels of pyruvate low enough to avoid cell death (Thangaraju et al., 2009; Thangaraju et al., 2006). LDHs are formed by the arrangement of up to four copies of two different subunits: subunit LDH-H is encoded by the *LDHB* gene and is ubiquitously expressed in healthy tissues, whereas subunit LDH-M is encoded by the HIF-1-target gene *LDHA* and is therefore induced by hypoxia (Porporato et al., 2011). *LDHA* expression is also induced by a variety of oncogenes, including c-Myc (Shim et al., 1997) and may therefore participate in the rapid consumption of pyruvate even when oxygen is available in the tumor cell environment (Feron, 2009).

Compared to LDH-H, LDH-M has a higher $K_m$ for pyruvate and a higher $V_{max}$ for pyruvate reduction (Markert et al., 1975). Consequently, LDH5/LDH-4M preferentially catalyzes the reduction of pyruvate into lactate and plays key roles in the maintenance of a high glycolytic flux and in resistance to apoptosis. Elevated LDH5 expression is of unfavorable prognostic significance to many human tumors (Koukourakis et al., 2005; Koukourakis et al., 2003). Conversely, LDH1/LDH-4H is most commonly silenced in glycolytic cancer cells, a process involving hypermethylation of the *LDHB* gene promoter (Thangaraju et al., 2009; Leiblich et al., 2006).

The LDH5 reaction yields equimolar concentrations of lactate (from pyruvate) and protons (from NADH). So, in order to avoid intracellular acidification and death, glycolytic cells must export protons. Several systems are adapted for the transport of protons among which MCT1, MCT2, MCT3, and MCT4 are passive lactate–proton symporters (Halestrap & Meredith, 2004).

In addition to *LDHA* and *LDHB,* the *LDH* gene family includes *LDHC* gene (also known as *LDHX*) that encodes a third isoenzyme, the LDHC. While *LDHA* and *LDHB* are expressed in somatic tissues, *LDHC* is reportedly expressed in testis and sperm (Holmes & Goldberg, 2009).

### 1.5.1 LDHs and cancer

Previous reports indicate that lactate dehydrogenase is the only glycolytic enzyme whose inhibition should allow a blocking of the aerobic glycolysis of tumor cells without damaging the normal cells which, in conditions of normal functional activity and sufficient oxygen supply, do not need this enzyme. Therefore, this enzyme it is a potential target for cancer therapy once that the inhibition of LDH could result in a selective depletion of ATP in tumor cells (Papaconstantinou & Colowick, 1961).

In previous experiments, oxamic acid, a competitive inhibitor of LDH, was shown to hinder the growth of HeLa cultured *in vitro* (Papaconstantinou & Colowick, 1961). Recent studies show that aerobic glycolysis can be hindered by blocking LDH which causes a failing in the regeneration of NAD, reduced during the conversion of glyceraldehyde 3-phosphate to 1,3-diphosphoglycerate, and necessary to maintain the glycolytic flow (Fiume et al., 2011).

It has been reported that *LDHA* is elevated and activated in many cancers compared with surrounding normal tissue (Walenta & Mueller-Klieser, 2004; Lewis et al., 2000; Shim et al., 1997). In addition, *LDHA* is upregulated in solid tumors in response to hypoxia in a HIF-1α-dependent manner (Draoui & Feron, 2011).

Recent studies demonstrate that LDHA plays a key role in tumor maintenance of *neu*-transformed mouse mammary epithelial cells (Fantin et al., 2006) and that the reduction in LDHA activity resulted in stimulation of mitochondrial respiration and decrease of mitochondrial membrane potential. It also compromised the ability of tumor cells to proliferate under hypoxia. So, accordingly to them, the tumorigenicity of the LDHA-deficient cells was severely diminished, and this phenotype was reversed by complementation with the human ortholog *LDHA* gene (Fantin et al., 2006) .

A definitive relationship between *LDHB* and cancer has not yet been established (Kinoshita et al., 2011). Chen et al., 2006 concluded that in non-small cell lung cancer (NSCLC) the levels of LDHB were significantly elevated in NSCLC sera (Chen et al., 2006). Furthermore, the serum levels of LDHB correlated with the clinical stage of NSCLC and LDHB protein expression was a predictor of very poor prognosis in medulloblastoma patients (Haas et al., 2008).

Recent results from Kinoshita et al., 2011 indicated that mRNA levels of *LDHB* were elevated in cancer tissues. They concluded that the reduction of *miR-375* and the increased expression of *LDHB* are frequent events in maxillary sinus squamous cell carcinoma (MSSCC) cancer cells and that by this way *miR-375* acts as a tumor suppressor and direct regulator of *LDHB* in MSSCC (Kinoshita et al., 2011).

Transcriptional silencing of *LDHB* expression caused by aberrant methylation of the gene promoter region has been reported in gastric and prostate cancers (Leiblich et al., 2006; Maekawa et al., 2003), suggesting that tumors preferentially express LDH isoenzymes with a high *LDHA* gene product content (LDH 5>LDH4>LDH3). In colorectal cancer, suppression of LDHB transcript in a more invasive phenotype was even proposed to account for a large part of the Warburg metabolic switch (i.e. independently of hypoxia-induced changes in *LDHA* expression) (Thorn et al., 2009).

Recent reports suggest that LDHB suppression plays an important role in triggering or maintaining the mitochondrial defects and then contributes to cancer cell invasiveness by inducing claudin-1 protein (Kim et al., 2011). These results suggest the novel idea that glycolytic activation may itself cause mitochondrial defects and may actively promote cancer development. This idea differs from the prevailing theory that activated glycolysis is the consequence of cellular adaptation to overcome mitochondrial defects due to hypoxic condition during cancer development. Further, this idea suggests that mitochondrial dysfunction and glycolytic activation can result in a vicious cycle, that is independent of initiating events for those two

phenomena, and that oncogenic activation of aerobic glycolysis may be sufficient to trigger mitochondrial dysfunction without hypoxic stimulus in tumorigenesis (Kim et al., 2011).

Elevated expression of LDHB in tumor cells could indicate the occurrence of oxidative metabolism, while LDHA expression is likely to correlate with glycolytic metabolism (Nakajima & Van Houten, 2012).

Recently, the germ cell–specific *LDHC* gene, was shown to express in a broad spectrum of tumors, with high frequency in lung cancer (47%), melanoma (44%), and breast cancer (35%) (Koslowski et al., 2002) but the mechanism for ectopic activation of this gene is unknown (Tang & Goldberg, 2009).

### 1.5.2 Regulation of LDHs

Previous data identified *LDHA* as a c-Myc responsive gene (Shim et al., 1997). Accordingly to these authors c-Myc is able to transactivate the *LDHA* promoter and directly increase *LDHA* expression (Shim et al., 1997). It has also been described that HIF-1 increases the expression of genes involved in the enzymatic breakdown of glucose to pyruvate and the enzymes involved in the clearance of pyruvate. So, *LDHA* has been identified as a HIF-1 target (Denko, 2008). Additionally, it has been shown that highly expressed oncogenic c-Myc collaborate with HIF in the activation of several glucose transporters and glycolytic enzymes, as well as LDHA (Dang et al., 2008).

Concerning *LDHB* expression, recent data revealed transactivation of *LDHB* gene expression by a signal transducer and activator of transcription 3 (STAT3), a key tumorigenic driver in many cancer that acts as a downstream mTOR effector in human cancer cells (Zha et al., 2011).

For LDHC expression in cancer cells, it has been demonstrated that it was regulated by transcription factors Sp1 and CREB (Tang & Goldberg, 2009).

## 1.6 Monocarboxylate transporters (MCTs)

Monocarboxylates, such as lactate and pyruvate, play a central role in cellular metabolism and metabolic communication between tissues (Halestrap & Price, 1999). In cancer cells, a steady source of metabolic energy is required to continue the uncontrolled growth and proliferation of these cells (Airley & Mobasheri, 2007).

As previously referred, most cancer cells rely on a high rate of aerobic glycolysis to obtain sufficient ATP in a hypoxic microenvironment (Vander Heiden et al., 2009). As a result lactate is abundantly synthesized from pyruvate (Feron, 2009), what contribute to the acidification of the microenvironment through lactic acid, inducing cellular acidosis, which triggers apoptosis. So, in order to avoid apoptosis, cancer cells must transport the lactate out of the cell (Izumi et al., 2011). By this way only the interstitial pH of tumors is low, while the intracellular pH of tumors is either normal or higher than that of normal tissues (Helmlinger et al., 2002; Dang & Semenza, 1999). Able to adapt to and even benefit from an acidic environment, cancer cells increase proton efflux through pH regulators such as proton pumps, sodium-proton exchangers, bicarbonate transporters, and $H^+$-linked monocarboxylate transporters, which are described to be upregulated in tumor cells (Izumi et al., 2003). Inhibition of these adaptive mechanisms can lead to decreased viability of cancer cells and increased sensitivity to chemotherapeutic agents (Fais et al., 2007; Fang et al., 2006).

On the other hand, lactate is not just a waste product: it was recently identified as a major energy fuel in tumors (Feron, 2009). Lactate is transported by monocarboxylate anion transporters (MCT; also called the solute carrier family 16 (SLC16)) (Halestrap & Price, 1999). In tumor cells take up or export lactate according to the oxygen availability, lactate concentration and expression of the MCT subtype at the plasma membrane ( Semenza, 2008; Brooks, 2000).

It is known that MCT4 (SLC16A3) preferentially transports lactate out of the cell and MCT1 (SLC16A1) regulates preferentially the entry of lactate into both tumor cells and tumor endothelial cells. In addition, MCT4 isoform is largely involved in hypoxia-driven lactate release (Draoui & Feron, 2011).

MCT4 ($K_m$ lactate =22mM) has the lowest affinity for lactate, is encoded by a HIF-1α-target gene (Ullah et al., 2006), and is therefore adapted for the export of lactic acid from glycolytic tumor cells (Dimmer et al., 2000). It plays an important contribution to the regulation of intracellular pH ($pH_i$): although it has only a low affinity for lactate, its high turnover rate ensures efficient proton export (Chiche et al., 2012).

MCT1 ($K_m$ lactate =3.5–10mM) has an intermediate affinity for lactate and is ubiquitously expressed in healthy and cancer tissues. In cancer, it facilitates lactate uptake by oxidative tumor cells in a newly described metabolic pathway involving lactate oxidation into pyruvate to fuel the TCA cycle (Sonveaux et al., 2008).

MCT2 ($K_m$ lactate =0.5mM) and MCT3 ($K_m$ lactate =5mM) have the highest affinity for lactate and are specialized in the import of lactate in very specific tissues such as liver (Cori cycle), kidney, and retina (Philp et al., 2001; Garcia et al., 1995).

Recent data suggest that MCT1 can transport lactate into and out of tumor cells. Whereas most oxidative cancer cells import lactate through MCT1 to fuel mitochondrial respiration, the role of MCT1 in glycolysis-derived lactate efflux remains less clear (Boidot et al., 2012).

### 1.6.1 MCTs and cancer

Pinheiro et al., 2010 showed that *MCT1* is upregulated in breast carcinomas, which does not corroborate a previous report in breast cancer, pointing to a possible silencing of *MCT1* expression by gene promoter hypermethylation (Asada et al., 2003). The identification of genes that have their promoter region hypermethylated (which results in gene silencing) or hypomethylated (which results in increased transcription) might lead to the discovery of new factors that are important for tumor initiation and progression (Baylin & Ohm, 2006). Multiple studies (Bachman et al., 2003; Fahrner et al., 2002; Koizume et al., 2002) have shown that the promoters of silenced genes, when compared with actively transcribed copies of the same genes, contain localized regions of transcriptional-silencing marks that include (in addition to DNA CpG-island methylation) the deacetylation and methylation of key H3 amino acids. Regarding these chromatin events, DNA methylation seems to be the dominant factor in gene silencing (Baylin & Ohm, 2006) .

MCT1 seems to have an important role in tumor progression since it was shown that inhibition of *MCT1*, either pharmacologically or using RNA interference (RNAi), results in the inhibition of xenograft tumor growth and resensitization of tumor cells to radiation (Tennant et al., 2010; Sonveaux et al., 2008).

Sonveaux et al., 2008 found that oxidative SiHa tumor cells, like oxidative muscle fibers, constitutively expressed *MCT1* mRNA at a higher relative level compared with glycolytic WiDr cells. In SiHa cells, *MCT1* was more actively transcribed than *MCT4*, whereas *MCT4* was preferentially expressed in WiDr cells. The plasma membrane expression of *MCT1* in SiHa cells contrasted with the scattered cytosolic, almost undetectable expression of *MCT4*, suggesting that lactate uptake by these cells primarily depends on MCT1. To confirm MCT involvement in lactate uptake, the authors measured changes in intracellular pH in response to acute lactate exposure. A small but significant decrease in intracellular pH was observed in SiHa cells exposed to exogenous lactate, indicating activation of a lactate-proton symporter. In contrast, intracellular pH remained unchanged in WiDr cells after lactate treatment (Sonveaux et al., 2008).

Other studies have shown that *MCT1* and *MCT4* are overexpressed in human neuroblastoma, cervix and colorectal cancers, providing evidence for bad prognosis of cancer (Pinheiro et al., 2009; Pinheiro et al., 2008; Sonveaux et al., 2008; Fang et al., 2006). It was also recently shown that high expression of both *MCT1*

and *MCT4* correlates with the invasiveness of lung cancer cells (Izumi et al., 2011). So, targeting MCT activity would not only induce apoptosis due to cellular acidosis, but would also lead to reduction in tumor angiogenesis, invasion, and metastasis. Thus, these transporters can constitute an attractive target for cancer therapy by preventing cancer maintenance and metastasis (Pinheiro et al., 2008).

### 1.6.2 Regulation of MCTs

Vegrán et al., 2011 identified a lactate/nuclear factor-kB (NF-kB) signaling pathway in endothelial cells, the existence of a lactate-driven, feed-forward Interleukine-8 (IL-8) (also known as C-X-C chemokine 8 – CXCL8) autocrine loop driving angiogenesis in tumors and that MCT1 and MCT4 play key roles in lactate-based dialog between cancer cells and endothelial cells. Accordingly to these authors lactate can also enter tumor endothelial cells through MCT1 (Végran et al., 2011). This study not only showed that lactate can favor the survival of serum-starved endothelial cells but also that lactate can directly initiate pro-angiogenic signaling through stimulation of this autocrine pathway which drives endothelial cell migration and tube formation. The authors had shown that IL-8-specific blocking antibodies and IL-8-targeted siRNA both prevented lactate-induced angiogenesis (Végran et al., 2011).

Recently, it was identified a direct link between p53 function and MCT1 expression. Under hypoxic conditions, p53 loss promoted MCT1 expression and lactate export produced by elevated glycolytic flux, both *in vitro* and *in vivo*. p53 interacted directly with the *MCT1* gene promoter and altered MCT1 mRNA stabilization. In hypoxic $p53^{-/-}$ tumor cells, NF-κB further supported expression of MCT1 to elevate its levels. Following glucose deprivation, upregulated MCT1 in $p53^{-/-}$ cells promoted lactate import and favored cell proliferation by fuelling mitochondrial respiration (Boidot et al., 2012).

Additionally, protein expression of uptake transporters such as MCT1 appeared to be upregulated by c-Myc overexpression (Kang et al., 2009).

## 1.7 Metabolic symbiosis in tumor microenvironment

Recently, it has been proposed a metabolic symbiosis in the tumor microenvironment as result of the inefficient formation of blood vessels during tumor growth producing areas of normoxia and hypoxia within the tumor (Nakajima & Van Houten, 2012).

Hypoxic tumor cells depend on glucose and glycolysis to produce energy. Lactate, the end-product of glycolysis, diffuses along its concentration gradient toward blood vessels. By contrast, oxygenated tumor cells import lactate (a process mediated by MCT1 located at the cell plasma membrane) and oxidize it (instead or in addition to glucose) to produce energy, thereby sparing available glucose, which can, in turn, freely diffuses deeper into the tumor to fuel glycolysis of hypoxic tumor cells located farther away from tumor blood vessels (Sonveaux et al., 2008). The use of lactate as an energy source requires the conversion of lactate into pyruvate (and back) as well as the transport of lactate into and out of tumor cells by way of specific transporters. Consequently, LDH isoforms and MCTs family, respectively, regulate these processes (Draoui & Feron, 2011).

Moreover, it has been considered that to define a tumor as metabolically symbiotic, several criteria must be met. It is expected that metabolically distinct populations will have unique protein signatures showing different expression levels of pertinent enzymes and carbohydrate transporters (Table 1). For example, the glycolytic cell population in a tumor, whether cancer or stromal cell, would be expected in hypoxic areas of the tumor and to express high levels of HIF-1α, HK, Glut-1, MCT4, and LDHA. The cell population performing

oxidative phosphorylation, on the other hand, would have decreased expression of the aforementioned molecules and elevated expression of PDH, MCT1, and LDHB (Nakajima & Van Houten, 2012).

**Table 1 - Predicted expression levels of the most relevant enzymes and metabolite transporters to metabolic symbiosis.**
Adapted from Nakajima & Van Houten, 2012.

| Protein | Expression in hypoxic cells | Expression in oxygenated cells |
|---|---|---|
| Glucose transporter 1 (Glut-1) | High | Low |
| Hexokinase (HK) | High | Low |
| Monocarboxylate transporter 1 (MCT1) | Low | High |
| Monocarboxylate transporter 4 (MCT4) | High | Low |
| Lactate dehydrogenase subunit M (LDH-M) | High | Low |
| Lactate dehydrogenase subunit H (LDH-H) | Low | High |
| Pyruvate dehydrogenase (PDH) | Low | High |
| Pyruvate dehydrogenase kinase (PDK) | High | Low |

### 1.8 LDHs and MCTs as therapeutic targets

The current findings establish a dual role for lactate in tumors: it acts as both a metabolic fuel and a signaling molecule, positioning lactate at the intersection of key processes in cancer progression, namely tumor metabolism and angiogenesis. Therefore, although lactate shuttles are physiologically active in some types of healthy tissue, the specific characteristics of some tumors make the regulators of cellular lactate handling, namely MCTs and LDHs, potential anti-cancer targets. Indeed, the metabolic symbiosis that have been described between oxidative and glycolytic tumor cells – and also between tumor cells and stromal cells, including endothelial cells and fibroblasts – offer diverse rationales to support the development of MCT and LDH inhibitory strategies (Draoui & Feron, 2011). However, the success of these new therapeutic approaches depends firstly on the extent to which tumors are addicted to these pathways (Feron, 2010) and also on their specificity to tumor cells.

Data from *in vitro* models of uterine cervix cancer revealed that some tumors are able to produce lactate whereas others use lactate as fuel. Besides that, in some patients the tumor presents an endophytic growth, invading the endometrium, whereas in other cases the tumor grows exophytically into vaginal channel (Nguyen & Averette, 1999). In this type of tumor the composition of the vaginal flora contributes, as previously referred, to the maintenance of lactic acid rich microenvironment that can play a role in cancer cells selection and tumor progression. However, tumor cells could have plasticity to switch on and off metabolic pathways instead of being exclusively selected. Our study aims to contribute to clarify if it is a question of selection, adaptation or even both.

## 2. Objectives

The definition of the specific role of monocarboxylate transporters in uterine cervix cancer and the ability of cancer cells to produce or consume lactate will help to define therapeutic targets. Thus, the main objective of this work is to achieve the metabolic profile of two uterine cancer cells from two different histological types, adenocarcinoma (HeLa) and squamous cell carcinoma (SiHa).

The objective will be accomplished according to three specific aims: 1) to determine the relevance of LDHA, LDHB, LDHC, MCT1 and MCT4 in the metabolic switch in an *in vitro* model of uterine cervix cancer; 2) to understand the role of EGF growth factor and sodium lactate in the regulation of expression of *LDHA, LDHB, LDHC, MCT1, MCT4* and 3) to evaluate epigenetic regulation of *LDHA, LDHB* and *MCT1* promoters and also to define a possible role of c-Myc transcription factor in the regulation of *LDHA* and *MCT1* expression.

Ultimately, the development of the current project could contribute to find a link between the expression of specific monocarboxylates membrane transporters and/or glycolytic enzymes and tumor cell features in order to propose therapeutical strategies to inhibit cell proliferation, migration, angiogenic stimulation and to activate apoptosis related pathways. Finally, contribute to the identification of specific therapeutic targets in tumor cells, which could be inhibited or downregulated in order to repress vital metabolic pathways in cancer cells.

## 3. Materials and methods

### 3.1 Role of EGF growth factor in the regulation of *LDH*s (*LDHA, LDHB*, *LDHC*) and *MCT*s (*MCT1* and *MCT4*) expression in the presence and absence of Sodium Lactate (NaLac)

#### 3.1.1 Cell culture

Cell lines were obtained from American Type Culture Collection (ATCC): HeLa (CCL-2) and SiHa (HTB-35).

HeLa and SiHa cell lines were maintained at 37°C in a humidified 5% $CO_2$ environment in Dulbecco's modified essential medium (DMEM) (41965-039,Gibco) containing 4500 mg/L of glucose supplemented with 10% fetal bovine serum (FBS) (S 0615, Biochrom AG) and 1% Antibiotic-Antimycotic (15240062, Anti-Anti, Invitrogen).

Cells were grown to 75 - 100% optical confluence before they were detached by incubation with 1X 0.05% trypsin-EDTA (25300-054, Invitrogen) at Room Temperature (RT) for 5 minutes. Whenever necessary, the cell number was determined with the help of a Bürker counting chamber.

Cells in culture were exposed to 50% Sodium Lactate (NaLac) (1.06522.2500, Merck) at 10 mM and/or stimulated with EGF (PHG0311, Gibco) at 25 ng/mL. SiHa cells chronically exposed to NaLac at 10mM were grown in the presence of 50% NaLac at 10mM for 32 days. Cells grown in control conditions were maintained in the absence of NaLac and without EGF stimulation.

#### 3.1.2 Gene expression

The role of EGF in the regulation of *LDHA*, *LDHB, LDHC, MCT1* and *MCT4* gene expression in cells grown in the presence and absence of NaLac was evaluated by quantitative Real-Time PCR. Firstly, a reverse transcription-Polymerase Chain Reaction was performed.

##### 3.1.2.1 Reverse transcription–Polymerase Chain Reaction

Reverse transcription polymerase chain reaction (RT-PCR) is a variant of polymerase chain reaction (PCR) which produces DNA copies of a RNA template. In RT-PCR a RNA strand is first reverse transcribed into its complementary DNA (cDNA), using the enzyme reverse transcriptase, and the resulting cDNA is amplified by PCR (Shiao, 2003).

Total RNA was extracted using the RNeasy Mini Extraction kit (74104, Qiagen) from cultured cells, according to manufacturer's protocol. The RNA concentration was determined spectrophotometrically in a Nanodrop 2000 (Thermo Scientific).

RNA was reverse-transcribed using SuperScript III Reverse Transcriptase (18080-044, Invitrogen) from 1 µg RNA to which 0.5 µL Oligo$(dT)_{20}$ (18418-020, Invitrogen), 0.5 µL random hexamers ($p(dN)_6$) (50 $A_{260}$ units) (11034731001, Roche), 1 µL deoxynucleotides (dNTPs) Mix (10 mM) (28-4065-22V, 28-4065-02V, 28-4065-12V and 28-4065-32V, GE Healthcare) and sterile bidestilled water ($ddH_2O$) to complete a total volume of 13 µL were added. The reaction mixture was then incubated at 65ºC, for 5 minutes, in order to occur the annealing between RNA and primers. Then the reaction tubes were chilled to 4ºC and the following mixture was added: 4µL 5X First-Strand buffer (P/N Y02321, Invitrogen), 1 µL 0.1M Dithiothreitol (DTT) (P/N Y00147, Invitrogen), 1µL RNaseOUT™ Recombinant RNase Inhibitor (10777-019, Invitrogen) and 1 µL Superscript III Reverse Transcriptase (18080-044, Invitrogen) and the cDNA synthesis was performed in a T3000 thermocycler (Biometra), using the following conditions (Table 2).

**Table 2 - Program used for cDNA synthesis**

| Stage | Temperature (ºC) | Time |
|---|---|---|
| Denaturation | 65 | 5 min |
| Cooling | 4 | 10 min |
| Annealing | 25 | 5 min |
| cDNA synthesis | 50 | 50 min |
| Inactivation | 70 | 15 min |
| Cooling | 4 | ∞ |

After that, 1 µL of RT-PCR product (cDNA) was used in 25 µL PCR reaction mixture using quantitative Real-Time PCR primers (Table 13), as described in table 3, in order to assess cDNA quality and specificity of the primers.

**Table 3 - PCR program for cDNA amplification using quantitative Real Time-PCR primers**

| Stage | Temperature (ºC) | Time | Cycles |
|---|---|---|---|
| Initial denaturation | 94 | 5 min | 1 |
| Denaturation | 94 | 50 sec | 34 |
| Annealing | 60 | 30 sec | |
| Elongation | 72 | 1 min | |
| Final elongation | 72 | 7 min | 1 |
| Cooling | 15 | ∞ | |

PCR products were analyzed on a 2% (w/v) agarose gel (in 1X Tris-borate-EDTA (TBE) buffer (diluted from 10X TBE, EC-860, National diagnostics)) stained with 0.05% (v/v) ethidium bromide and under UV transillumination (BioDocAnalyse Transilluminator, Biometra).

#### 3.1.2.2 Quantitative Real-Time PCR

Quantitative Real-time PCR (qRT-PCR) is a powerful technique for gene expression studies due to its high sensitivity, specificity and broad quantification range for high throughput and accurate expression profiling of selected genes. Quantification of mRNA transcription can be either relative or absolute (Bustin, 2000). The data obtained by qRT-PCR is normalized with an endogenous control, often referred to as a housekeeping gene (Gubern et al., 2009). In relative quantification, data are secondly normalized to a reference sample.

qRT-PCR reactions were carried out for all genes of interest in each sample using LightCycler 480 SYBR Green I master (04707516001, Roche) and LightCycler 480 instrument (Roche). Each reaction mixture was performed on 25 µL containing 1µL cDNA diluted with dd$H_2O$ (1:2.5), 12.5 µL LightCycler 480 SYBR Green I master (04707516001, Roche), 10.5 µL LightCycler 480 SYBR Green II master ($H_2O$) (04707516001, Roche) and 0.5µL of each primer (10µM) or on 7 µL containing 1 µL of cDNA diluted with dd$H_2O$ (1:2.5), 3.5 µL LightCycler 480 SYBR Green I master (04707516001, Roche), 2 µL LightCycler 480 SYBR Green II master ($H_2O$) (04707516001, Roche) and 0.5 µL of both primers (5µM) (Table 13) as described in table 4. In the present thesis, relative quantification of gene expression was performed and the *Hypoxanthine phosphoribosyltransferase* (HRPT) gene (Table 13) was used as endogenous control.

**Table 4 - Quantitative Real-Time PCR program**

| Stage | Temperature (ºC) | Time | Cycles |
|---|---|---|---|
| Heat activation | 95 | 10 min 15 sec | 1 |
| PCR | | | |
| Denaturation | 95 | 15 sec | 45 |
| Annealing | 60 | 15 sec | |
| Elongation | 72 | 20 sec | |
| Melting | 60<br>95 | 14 sec | 1 |
| Cooling | 40 | 10 sec | |

All samples were run in triplicate (biological triplicates). The results of qRT-PCR were analyzed in LightCycler 480 software (Roche). Expression levels were normalized to those obtained for cells grown in control conditions (culture conditions specified in 3.1.1). Average and standard deviation of the relative gene expression values were calculated and statistical analysis was performed.

### 3.1.3 Protein levels

The role of EGF in the regulation of LDHA, LDHB, (and LDHC in SiHa cells), MCT1 and MCT4 protein levels in SiHa and HeLa cells grown in the presence and absence of NaLac was evaluated through Western blot and Immunofluorescence. The designations, LDHA and LDHB protein levels, which were used in this thesis, correspond to the detection of LDH-M subunit and LDH-H subunit, respectively.

#### 3.1.3.1 Western blot

Western blot is a widely used analytical technique used to detect specific proteins in the given sample of tissue homogenate or extract. It uses gel electrophoresis to separate native proteins by 3-D structure or denatured proteins by the length of the polypeptide. The proteins are then transferred to a membrane (typically nitrocellulose or PVDF), where they are detected using antibodies specific to the target protein (Renart et al., 1979; Towbin et al., 1979).

This method was used to assess LDHA, LDHB, MCT1 and MCT4 protein levels in cells grown in the presence of NaLac and/or after EGF stimulation (culture conditions specified in 3.1.1) and to compare them with those obtained in cells grown in control conditions (culture conditions specified in 3.1.1).

Briefly, cells were lysed in Radio-Immunoprecipitation Assay (RIPA) (Appendix I) buffer and stored at -20ºC Overnight (ON). The lysates were centrifuged at 14000 rpm for 5 minutes at 4ºC and the supernatants were collected for protein concentration determination through Spectrophotometric quantification (595 nm) based on Bradford method and using Bio-Rad Protein Assay Reagent (500-0006, Bio-Rad). After that, it was added 5X Loading buffer (Appendix I) with 10% β-mercaptoethanol (M3148, sigma) (at a final concentration ≥ 1X) to the cell lysate and incubated at 100ºC for 20 minutes. The lysates were centrifuged at 14000 rpm for 2 minutes and incubated on ice.

Equal amounts of total protein were separated by 15% Tris-glycine SDS-Polyacrylamide gel (Appendix I) electrophoresis at 150V for 1h30 in 1X Tris-Glycine-SDS (TGS) buffer (10X TGS buffer, 161-0772, Bio-Rad) in Mini-PROTEAN Tetra Electrophoresis System (Bio-Rad) and then transferred to a nitrocellulose membrane in transfer buffer (Appendix I) with a Mini Trans-Blot® Electrophoretic Transfer Cell

(Bio-Rad), at 60V for 4hours to ON. Membranes were blocked with 3% skim milk in Phosphate buffered saline (PBS) 0.1% (v/v) Tween 20 (Appendix I) for 1 hour at RT. Blots were incubated with specific antibodies anti-MCT1 (AB3538P, Millipore), anti-MCT4 (AB3316P, Millipore), anti-MCT4 (SC-50329, Santa Cruz), anti-LDHA (SAB1100050, Sigma), anti-LDH (H-subunit) (L7016, Sigma) and anti-LDHC (AV53602, Sigma) at appropriate concentrations (1:1000 in 3% (w/v) skim milk in PBS 0.1% (v/v) Tween 20 (Appendix I)) at 4ºC ON.

After rinsing 3 X 5 minutes in PBS 0.1% (v/v) Tween 20 (Appendix I), blots were then incubated for 2 hours at RT with a IgG secondary antibody-conjugated Horse raddish peroxidase (HRP) (anti-rabbit (31460, Thermo Scientific) and anti-mouse (31430, Thermo Scientific)) diluted 1:5000 in 3% (w/v) skim milk in PBS 0.1% (v/v) Tween 20 (Appendix I).

After rinsing 3 X 5 minutes in PBS 0.1% (v/v) Tween 20 (Appendix I), immunoreactive bands were detected using ECL Western blotting substrate (SuperSignal West Pico Substrate (34080, Thermo Scientific)), followed by exposure to film and photographic development with ChemiDoc XRS System (Bio-Rad). Images were analyzed using *ImageJ* software (http://rsbweb.nih.gov/ij/).

To confirm equal loading of protein lysates and in order to normalize the obtained protein levels, membranes were rinsing 3 X 5 minutes with PBS 0.1% (v/v) Tween 20 (Appendix I) and reprobed using anti-β-actin (A5441, Sigma) at 1:1000 in 3% (w/v) skim milk in PBS 0.1% (v/v) Tween 20 (Appendix I) at 4ºC ON and then processed as above.

#### 3.1.3.2 Immunofluorescence

Immunofluorescence uses the specificity of antibodies labeled with fluorochromes to target specific proteins within a cell, allowing their visualization in the sample (Robinson et al., 2009). The two main methods of immunofluorescent labeling are direct and indirect. Less frequently used is direct immunofluorescence whereby the antibody against the molecule of interest is chemically conjugated to a fluorescent dye. In indirect immunofluorescence, the antibody specific for the molecule of interest (called the primary antibody) is unlabeled, and a second anti-immunoglobulin antibody directed toward the constant portion of the primary antibody (called the secondary antibody) is labelled with the fluorescent dye (fluorophore) (Robinson et al., 2009).

In the present work, indirect immunofluorescence was performed aiming to evaluate LDHA, LDHB, LDHC, MCT1 and MCT4 protein levels in the presence and absence of NaLac and the role of EGF growth factor on its regulation.

From each cell line (HeLa and SiHa), $2x10^5$ cells/well (in 24-well plate) ($4x10^5$ cells/mL) were grown on lamellae, previously coated in 0.2% (w/v) gelatin, until they reached approximately 80% of optical confluence. EGF (PHG0311, Gibco) at 25 ng/mL and/or NaLac (1.06522.2500, Merck) at 10 mM were added to cells and incubated 37ºC 5% $CO_2$ ON. Cells were harvested and fixed in 2% (w/v) paraformaldehyde for 15 minutes at 4°C, blocked with PBS 0.2% (w/v) BSA (Appendix I) for 1hour at RT and incubated with primary antibody at 4ºC ON (anti-MCT1 (AB3538P, Millipore), anti-MCT4 (AB3316P, Millipore) and anti-MCT4 (SC-50329, Santa Cruz), diluted 1:100 in PBS 0.2% (w/v) BSA (Appendix I); (anti-LDHA (SAB1100050, Sigma), anti-LDH (H-subunit) (L7016,Sigma), anti-LDHB (WH0003945M1, Sigma) and anti-LDHC (AV53602, Sigma) diluted 1:100 in PBS 0.2% (w/v) BSA 0.1%TritonX-100 (Appendix I)).

After rinsing 3 X 5 minutes with 1X PBS (Appendix I) cells were incubated with the secondary antibodies for 2 hours, at RT. The secondary antibodies used were Alexa Fluor® 488 anti-mouse (A-11001, Invitrogen) or Alexa Fluor® 488 anti-rabbit (A-11034, Invitrogen) diluted 1:500 in PBS 0.2% (w/v) BSA (Appendix I). After that, the slides were rinsed, once again, 3 X 5 minutes with 1X PBS (Appendix I), prior to be mounted in VECTASHIELD media with 4'-6-diamidino-2-phenylindole (DAPI) (H-1200, Vector Labs) which

produces a blue fluorescence when bound to DNA, with excitation at about 360 nm and emission at 460 nm, so staining the nuclear material and consequently cell nuclei . Cells were examined by standard fluorescence microscopy using an Axio Imager.Z1 microscope (Zeiss).

The same procedures described above were performed for negative controls, with the exception of the incubation with the primary antibody.

Images were acquired with *AxioVision* software (http://microscopy.zeiss.com/microscopy/en_de /products/software/axiovision-for-biology.html) and processed with *ImageJ* software (http://rsbweb. nih.gov/ij/).

### 3.1.4 Epigenetic regulation *and LDHA, LDHB and MCT1* promoters

#### 3.1.4.1 Methylation pattern

##### 3.1.4.1.1 Bisulfite DNA conversion

The methylation status of a DNA sequence can be determined using sodium bisulfite. The bisulfite treatment introduces methylation-dependent sequence changes through selective chemical conversion of non-methylated cytosine to uracil. After treatment, all non-methylated cytosine bases are converted to uracil but all methylated cytosine bases remain cytosine. These methylation dependent C-to-T changes can subsequently be studied using conventional DNA analysis technologies, like PCR and automate sequencing of bisulfite-treated genomic DNA to determine methylation status at CpG dinucleotides (Ehrich et al., 2007).

In the context of this thesis bisulfite DNA conversion was applied to evaluate the methylation pattern of *LDHA, LDHB and MCT1* promoters in cells grown in the presence and absence of NaLac with or without EGF stimulation.

DNA was extracted from cells in culture (culture conditions described in 3.1.1) using DNA Purification Protocol for 1-2 Million Cells (Citogene) accordingly to the manufacturer's protocol.

Bisulfite treatment of genomic DNA was performed with the commercial EpiTect Bisulfite Kit (59104, Qiagen) that combines bisulfite conversion and DNA cleanup accordingly to the manufacturer's protocol. The conversion was done using 2 µg of DNA and was added 1 µL of RNaseOUT™ Recombinant RNase Inhibitor (10777-019, Invitrogen) before and after bisulfite DNA conversion.

After the bisulfite reaction the converted DNA was amplified by PCR (Tables 5 and 6) using specific primers (Methyl primers) (Table 13) and finally was performed the automate sequencing of CpG islands identified in *LDHA, LDHB* and *MCT1* promoters (Table 7), and their methylation status was evaluated.

**Table 5 - PCR program for amplification of bisulfite treated DNA**

| Stage | Temperature (ºC) | Time | Cycles |
|---|---|---|---|
| Initial denaturation | 95 | 5 min | 1 |
| Denaturation | 95 | 30 sec | 35 |
| Annealing | $T_{ann}$[1] | 30 sec | |
| Elongation | 72 | 50 sec | |
| Final elongation | 72 | 7 min | 1 |
| Cooling | 15 | ∞ | |

[1] Methyl LDHA For2Rev2 45ºC; Methyl LDHA For3Rev3 48ºC; Methyl MCT1 For2Rev2 51ºC

**Table 6 - PCR program for amplification of bisulfite treated DNA**

| Stage | Temperature (ºC) | Time | Cycles |
|---|---|---|---|
| Initial denaturation | 94 | 5 min | 1 |
| Denaturation | 94 | 50 sec | 35 |
| Annealing | $T_{ann}$[1] | 30 sec | |
| Elongation | 72 | 1 min | |
| Final elongation | 72 | 7 min | 1 |
| Cooling | 15 | ∞ | |

[1] Methyl LDHB For1Rev1 53.7ºC; Methyl LDHB For2Rev2 55.6ºC; Methyl LDHB For3Rev3 54.6ºC

PCR products were analyzed on a 2% (w/v) agarose gel (in 1X TBE buffer (10X TBE, EC-860, National diagnostics)) stained with 0.05% (v/v) ethidium bromide and under UV transillumination (BioDocAnalyse Transilluminator, Biometra). The DNA fragments were extracted from agarose and purified with Illustra™ GFX™ PCR DNA and Gel Band Purification kit (28-9034-71, GE Healthcare).

#### 3.1.4.1.2 Automate sequencing of *LDHA*, *LDHB* and *MCT1* promoters' CpG islands

DNA sequencing is the determination of the order of the nucleotides in a DNA molecule. The DNA sequence can be determined by dye-terminator (Sanger) sequencing. In this method, the double stranded DNA fragment to be analyzed is mixed with a single primer binding to a strand complementary to the strand to be sequenced, DNA polymerase and a nucleotide mixture containing ordinary dNTPs and dideoxynucleotides (ddNTPs) (nucleotides lacking a 3'-hydroxyl (-OH) group at the polymerization site, and labelled with a fluorescent molecule – a different fluorochrom specific for each nucleotide). In a reaction based on the same principle as PCR, insertion of ddNTP terminates the extension of that particular strand. The insertion of ddNTPs is random, but, after a series of cycles, the sequencing reaction contains a mixture of copies of one strand ended at each base (Shendure et al., 2004). Strands are separated by size in a capillary electrophoresis. During the electrophoresis, the dyes of strands of equal length are excited passing a laser and the specific light emission is detected, generating nucleotide sequence of the DNA fragment (Swerdlow & Gesteland, 1990). One of the sequencing reaction mixtures contained the forward primer and the other one the reverse primer, so that both strands of the DNA fragment could be sequenced.

In this particular setting, DNA sequencing was performed in order to evaluate the methylation pattern of the CpG dinucleotides of specific CpG islands identified at *LDHA*, *LDHB* and *MCT1* gene promoters.

Automate sequencing reaction mixtures of the amplified DNA fragments were performed as described as follows: 12µL of $ddH_2O$, 1µL of reverse methyl primer (at 3.33 µM) (Table 13), 2 µL of DNA and 2µL of 5X Big dye sequencing buffer and 3 µL of Big dye™ Terminator v1.1 (BigDye® Terminator v3.1 Cycle Sequencing kit, 4337456, Applied Biosystems).The automate sequencing reaction (Table 7) took place in a T3000 thermocycler (Biometra).

**Table 7 - Automate sequencing program**

| Stage | Temperature (ºC) | Time | Cycles |
|---|---|---|---|
| Initial denaturation | 96 | 5 min | 1 |
| Denaturation | 96 | 10 sec | 24 |
| Annealing | $T_{ann}$[1] | 5 sec | |
| Elongation | 60 | 4 min | |
| Cooling | 4 | ∞ | |

[1] $T_{ann}$ of Methyl LDHA Rev2 47°C; Methyl LDHA Rev3 48°C; Methyl LDHB Rev1 57.3ºC; Methyl LDHB Rev2 53.9ºC; Methyl LDHB Rev3 57.3ºC; Methyl MCT1 Rev2 51°C

Automate sequencing reaction products were then purified with Illustra AutoSeq G-50 GFX (27-5340-03, GE Healthcare) accordingly to manufacturer's and analyzed in ABI Prism 3130 Genetic Analyzer.

### 3.1.5 Activity of *LDHA*, *LDHB* and *MCT1* promoters

In order to evaluate the activity of *LDHA* and *LDHB* and *MCT1* promoters after EGF stimulation of cells grown in the presence and absence of NaLac, several deletion constructs (LDHA f1, LDHAf2 and LDHA f3; LDHB f1 and LDHB f2; MCT1 f1 and MCT1 f2) were generated using conventional molecular cloning techniques.

#### 3.1.5.1 Amplification of *LDHA*, *LDHB* and *MCT1* promoter sequences

Firstly, PCR amplification (Table 8) of genomic DNA (from HCT15 cell line) was done using specific primers with and without restriction enzyme (*MluI* and *HindIII*) sites designed for the *LDHA*, *LDHB* and *MCT1* promoter sequences (Table 13).

**Table 8 - PCR program used for amplification of *LDHA, LDHB* and *MCT1* promoter sequences**

| Stage | Temperature (ºC) | Time | Cycles |
|---|---|---|---|
| Initial denaturation | 94 | 5 min | 1 |
| Denaturation | 94 | 50 sec | 15 |
| Annealing | $T_{ann}$ [1] | 30 sec | |
| Elongation | 72 | 1 min | 20 |
| Denaturation | 94 | 50 sec | |
| Annealing | $T_{ann}$ [2] | 30 sec | |
| Elongation | 72 | 1min | |
| Final elongation | 72 | 7 min | 1 |
| Cooling | 15 | ∞ | |

[1] $T_{ann}$ of primers without restriction enzyme sites: LDHA For1Rev1 55ºC; LDHA For2Rev2 58ºC; LDHA For3Rev2 59.4ºC; LDHB For1Rev,For2Rev 55ºC; MCT1 For1Rev 59.4ºC; MCT1 For2Rev 58ºC

[2] $T_{ann}$ of primers with restriction enzyme sites: LDHA For1Rev1 65ºC; LDHA For2Rev2 67.4ºC; LDHA For3Rev2 68.1ºC; LDHB For1Rev,F2R 65ºC; MCT1 For1Rev 68.1ºC; MCT1 For2Rev 67.4ºC

PCR products were analyzed on a 2% (w/v) agarose gel (in 1X TBE buffer (diluted from 10X TBE, EC-860, National diagnostics)) stained with 0.05% (v/v) ethidium bromide and under UV transillumination (BioDocAnalyse Transilluminator, Biometra). The fragments were extracted from agarose and purified with Illustra™ GFX™ PCR DNA and Gel Band Purification kit (28-9034-71, GE Healthcare). After that DNA deletion fragments were sequenced through automate sequencing.

#### 3.1.5.2 DNA automate sequencing of *LDHA*, *LDHB* and *MCT1* promoter sequences

Each sequencing reaction mixture contained: 3 µL of Big dye™ Terminator v1.1 and 2 µL of 5X Big dye sequencing buffer (BigDye® Terminator v3.1 Cycle Sequencing kit, 4337456, Applied Biosystems), 1 µL of forward or reverse primer (at 3.33 µM) (Table 13), about 100 ng of template DNA and sterile bidestilled water up to 20 µL. Sequencing reaction was carried out in a T3000 thermocycler (Biometra), according to the program described in the table 9.

**Table 9 - Automate sequencing program**

| Stage | Temperature (ºC) | Time | Cycles |
|---|---|---|---|
| Initial denaturation | 96 | 5 min | 1 |
| Denaturation | 96 | 10 sec | 24 |
| Annealing | $T_{ann}$[1] | 5 sec | |
| Elongation | 60 | 4 min | |
| Cooling | 4 | ∞ | |

[1] $T_{ann}$ of primers without restriction enzyme sites: LDHA For1, Rev1 55.5˚C; LDHA For2, Rev2, For3 58˚C; LDHB For1, Rev, For2 55ºC; MCT1 For1, Rev1, For2, Rev2 58˚C

Sequencing reaction products were then purified with Illustra AutoSeq G-50 GFX (27-5340-03, GE Healthcare) accordingly to manufacturer's and analyzed in ABI Prism 3130 Genetic Analyzer.

### 3.1.5.3 Plasmids generation and cloning

Luciferase plasmids pGL3-Basic (Figure 4) and pGL3-Control (Figure 5) (pGL3 Luciferase Reporter Vectors, Promega) were used as negative and positive control, respectively. The pGL3-Basic vector lacks eukaryotic promoter and enhancer sequences, allowing maximum flexibility in cloning putative regulatory sequences. Expression of luciferase activity in cells transfected with this plasmid depends on insertion and proper orientation of a functional promoter upstream from *luc*+ (Figure 4). The pGL3-Control Vector contains SV40 promoter and enhancer sequences (Figure 5), resulting in strong expression of *luc*+ in many types of mammalian cells. This plasmid is useful in monitoring transfection efficiency, in general, and is a convenient internal standard for promoter and enhancer activities expressed by pGL3 recombinants (pGL3 Luciferase Reporter Vectors, Promega).

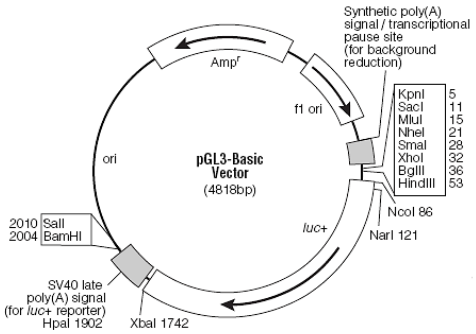


**Figure 4 - pGL3-Basic Vector.** Adapted from pGL3 Luciferase Reporter Vectors, Promega.

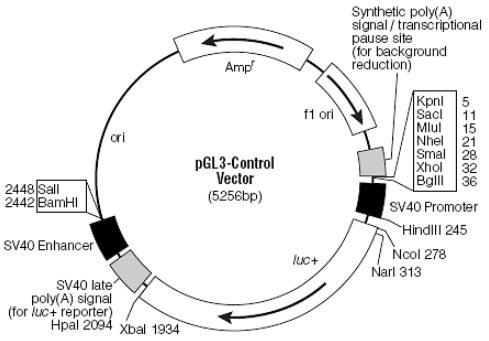


**Figure 5 - pGL3-Control Vector.** Adapted from pGL3 Luciferase Reporter Vectors, Promega**.**

DNA deletion fragments (LDHA f1, LDHA f2, LDHA f3, LDHB f1, LDHB f2, MCT1 f1 and MCT1 f2) (Table 13) and the pGL3 basic vector (Figure 4) were digested with *MluI* (ER0561, Fermentas*)* and *HindIII (*ER0501, Fermentas*)* restriction enzymes. The digestion reaction took place in a T3000 thermocycler (Biometra), at 37°C ON. The digestion products were purified with Illustra™ GFX™ PCR DNA and Gel Band Purification kit (28-9034-71, GE Healthcare). After that the deletion fragments were inserted into pGL3-basic vector that contains a modified coding region for firefly (*Photinus pyralis*) luciferase that has been optimized for monitoring transcriptional activity in transfected eukaryotic cells (Figure 3). The ligation reaction was prepared as follows: 2µL 10X T4 DNA ligase buffer (B69, Fermentas), 1µL T4 DNA ligase (EL0011, Fermentas), 1µL pGL3 basic vector previously digested and 16µL of digested DNA and was performed at 22ºC for 5 hours and 65ºC 10 minutes in a T3000 thermocycler (Biometra).

The recombinant plasmids were cloned into chemically competent *Escherichia coli* (C4040-10*,* Invitrogen) and colonies were selected by ampicillin resistance (Figure 4). Following, the recombinant plasmids were purified using Plasmid DNA Minipreps Kit (SP-PMN-250, Easy Spin, Citomed) according to manufacturer's protocol. Plasmid DNA concentration was determined spectrophotometrically in Nanodrop 2000 (Thermo Scientific). The deletion constructs were digested again with *MluI* and *HindIII* restriction enzymes in order to confirm deletion fragments insertion and a third PCR amplification was done using plasmid DNA and RVprimer3 and GLprimer2 primers (pGL3 sequencing primers – table 13) (Table 10).

**Table 10 - PCR program for plasmid constructs amplification**

| Stage | Temperature (ºC) | Time | Cycles |
|---|---|---|---|
| Initial denaturation | 94 | 5 min | 1 |
| Denaturation | 94 | 50 sec | 35 |
| Annealing | 56.9 | 30 sec | |
| Elongation | 72 | 1 min | |
| Final elongation | 72 | 7 min | 1 |
| Cooling | 15 | ∞ | |

Finally, in order to sequence the DNA inserted into pGL3 vector automate sequencing was performed using pGL3 sequencing primers (at 3.33 µM) (Table 11) to determine the exact position of generated deletion constructs. Each sequencing reaction mixture contained: 3 µL of Big dye™ Terminator v1.1 and 2 µL of 5X Big dye sequencing buffer (BigDye® Terminator v3.1 Cycle Sequencing kit, 4337456, Applied Biosystems), 1 µL

of forward or reverse pGL3 sequencing primer (at 3.33 µM) (Table 13), about 100 ng of plasmid DNA and sterile bidestilled water up to 20 µL. Sequencing reaction was carried out in a T3000 thermocycler (Biometra), according to the program described in the table 11.

**Table 11 - Automate sequencing program**

| Stage | Temperature (ºC) | Time | Cycles |
|---|---|---|---|
| Initial denaturation | 96 | 5 min | 1 |
| Denaturation | 96 | 10 sec | 24 |
| Annealing | 56.9 | 5 sec | |
| Elongation | 60 | 4 min | |
| Cooling | 4 | ∞ | |

Sequencing reaction products were then purified using Illustra AutoSeq G-50 GFX (27-5340-03, GE Healthcare) accordingly to manufacturer's and analyzed in ABI Prism 3130 Genetic Analyzer.

A second transformation of chemically competent *Escherichia coli* (C4040-10, Invitrogen) was done, in order to increase the amount of plasmid DNA. All recombinant plasmids were purified with Plasmid DNA Midipreps Kit (12143, Qiagen) according to manufacturer's protocol. Plasmid DNA concentration was determined spectrophotometrically in Nanodrop 2000 (Thermo Scientific).

#### 3.1.5.4 Transient transfection of promoters' deletion constructs into HeLa and SiHa cell lines

Transient transfection assays have been developed and broadly used to define transcriptionally regulatory elements, such as promoters, enhancers, and silencers. In a transient transfection assay, a DNA fragment of interest is placed upstream from a reporter gene and the regulatory potential of the sequence can be assessed by measuring transcription activity of the reporter gene. The firefly (*Photinus pyralis*) luciferase gene is one reporter used commonly in transient transcription assays (Yin et al., 2005).

A transient transfection assay is the delivery of the plasmid DNA into cultured cells in order to measure the activity of the reporter gene in transfected cell lysated (Yin et al., 2005). Cell type, delivery method, and properties of the vector (e.g., size, quality, and amount) might influence transfection efficiency. Bioluminescence analysis could be affected by several factors, such as cell lysis efficiency, cell viability. To correct these systematic errors, a commonly employed strategy is to introduce a control plasmid carrying a second reporter gene driven by a constitutively active promoter (Yin et al., 2005).

In the Dual Luciferase reporter system, for example, Renilla *(Renilla reniformis*) luciferase expressing plasmid is used as control. After co-transfection of two luciferase plasmids, both Firefly and Renilla luciferase activities are measured sequentially from a single aliquot of the cell lysate. The firefly luciferase activity normalized by Renilla luciferase activity represents a more accurate quantitation of transcription rates (Yin et al., 2005; Ho & Strauss, 2004).

One day before transfection cells were trypsinized with 1X 0.05% trypsin-EDTA (25300-054, Invitrogen) and seeded into 24-well plates ($2x10^5$ cells/well) ($4x10^5$ cells/mL) in DMEM supplemented with 10% FBS and 1% AA. NaLac (1.06522.2500, Merck) at 10mM was added to cells. Cells were incubated at 37ºC 5% $CO_2$ ON. Transfection was performed using Lipofectamine 2000 (11668, Invitrogen) and 0.5 µg of each deletion construct (LDHA f1, LDHA f2, LDHA f3, LDHB f1, LDHB f2, MCT1 f1 and MCT1 f2) (Table 13) per well at 3:1 ratio and 1X Opti-MEM medium (31985, Gibco).

pGL3-Control vector (that contains SV40 promoter and enhancer sequences) (Figure 5) was used as positive control and pGL3-Basic vector (the promoterless firefly plasmid) (Figure 4) as negative control. The control plasmid expressing Renilla luciferase was mixed with the Firefly luciferase deletion constructs at 1:5 ratio. The plasmids and liposome were mixed at 1:3 ratio and incubated at RT for 20 minutes. The DNAp/liposome complex was added to each well (100µL/well) followed by incubation at 37ºC 5%$CO_2$ for 4h-6h. 4h-6h after transfection 500 µL of DMEM supplemented with 10% FBS and 1% AA medium were added to the cells (DMEM supplemented with 10% FBS and 1% AA with 10 mM NaLac to the cells grown in the presence of NaLac) followed by incubation at 37ºC ON. EGF (PHG0311, Gibco) at 25 ng/mL was added to the cells 24 hours post-transfection. Cells transfected in control conditions were maintained in DMEM supplemented with 10% FBS and 1% AA in the absence of NaLac and without EGF stimulation. Cells were harvested 48h post-transfection and lysed with 1X Passive lysis buffer (5X Passive lysis buffer, E194A, Promega) and frozen at -80ºC.

#### 3.1.5.4.1 Luciferase activity of *LDHA* and *LDHB* and *MCT1* promoters' deletion constructs

In order to evaluate the luciferase activity of *LDHA* and *LDHB* and *MCT1* promoters' deletion constructs Firefly and Renilla luciferase activity were measured sequentially from a single cell lysate on Victor$^3$ 1420 Multilabel Counter Luminometer (Perkin Elmer) by using the Dual Luciferase Assay System (E1910, Promega) according to the manufacturer's protocol. The results were expressed as a ratio of Firefly luciferase activity to Renilla luciferase activity and then normalized to the pGL3-Basic vector activity. Once data were collected from three experiments (triplicates) average and standard deviation were calculated and statistics analysis was performed.

### 3.1.6 c-Myc-antibody chromatin Immunoprecipitation (ChIP)

Chromatin immunoprecipitation (ChIP) is a technique that allows the analysis of the association of specific proteins with particular genomic regions in the context of intact cells. ChIP is used to determine changes in epigenetic signatures, chromatin remodeling and transcription regulators binding (Collas, 2010; Kuo & Allis, 1999). The basic steps of this technique are cell fixation, chromatin shearing (by sonication), immunoselection, immunoprecipitation and analysis of the immunoprecipitated DNA by qRT-PCR (Das et al., 2004). Chromatin is fragmented by sonication of whole cells and nuclei, into fragments of 200–1000 base pair (bp), with an average of 500 bp (Collas, 2010).

In the present thesis ChIP was used to study c-myc transcription factor interaction with *LDHA* and *MCT1* promoters in cells grown in the presence and absence of NaLac with or without EGF stimulation.

HeLa and SiHa cells were grown in tissue culture flasks in DMEM supplemented with 10% FBS and 1% AA until they reached ~70-80% of optical confluence (100-120 million cells) and then were stimulated with EGF (PHG0311, Gibco) (25ng/mL) in the presence and absence of NaLac (1.06522.2500, Merck) (10 mM) at 37ºC 5% $CO_2$ for 12-16 hours. After that 37% formaldehyde (Merck) was added to cells to a final concentration of 1% (v/v) and incubated for 10 minutes at RT (to cross-link DNA and proteins) and then formaldehyde was quenched by addition of glycine to a final concentration of 125 mM and incubated for 5 minutes at RT. Then cells were harvested through scraping in 1X PBS (10X PBS, D1408 Sigma) centrifuged at 1200 rpm for 2 minutes and 500 µL of ChIP lysis buffer (kch-onedIP-060, Diagenode) were added to cell pellets and stored at -20ºC. Cell pellets were thawed on ice and sonication was performed (10 cycles of 30 seconds each one). In order to check chromatin fragmentation, 2 µL of chromatin were separated by a 1.2% (w/v) agarose gel

electrophoresis (in 1X TBE buffer (diluted from 10X TBE, EC-860, National diagnostics)) stained with 0.05% (v/v) ethidium bromide. Fragmented chromatin (between 500-1000 bp) was stored at -20ºC. ChIP was performed using OneDay ChIP kit (kch-onedIP-060, Diagenode) accordingly to manufacturer's protocol. c-Myc antibody (A-14) (sc-789, Santa Cruz Biotech) (target) and a rabbit non-immune IgG (kch-onedIP-060, Diagenode) were used. Amplification and analysis of Immunoprecipitated (IP'd) DNA was done through qRT-PCR, accordingly to manufacturer's protocol, in an ABI PRISM 7900HT Sequence Detection System (Applied Biosystems) (Table 12) using specific primers (Myc LDHA and Myc MCT1 primers) (Table 13). Data were analyzed in SDS 2.4.1 software (Applied Biosystems) and relative occupancy of the immunoprecipitated factor at specific loci was calculated using the following equation:

$$2\text{^}(CtNegCtl - CtTarget)$$

where CtNegCtl and CtTarget are the average threshold cycles of PCR done in triplicates on DNA samples from negative control ChIP (rabbit non-immune IgG) and targeted ChIP (using c-Myc antibody), respectively.

**Table 12 - IP'd DNA quantitative Real-Time PCR program**

| Stage | Temperature (ºC) | Time | Cycles |
|---|---|---|---|
| Activation | 50 | 2 min | 1 |
| Initial denaturation | 95 | 10 min | 1 |
| Denaturation | 95 | 15 sec | 40 |
| Annealing; Elongation | 60 | 1 min | |
| Dissociation curves | 95<br>60<br>95 | 15 sec<br>15 sec<br>15 sec | |

### 3.2 Detection of c-Myc copy number by Fluorescent in situ hybridization (FISH)

Fluorescent in situ hybridization (FISH) is a cytogenetic technique used to detect and localize the presence or absence of specific DNA sequences on chromosomes thus allowing the detection of numerical and structural abnormalities in interphase nuclei (Policht et al., 2010). FISH uses fluorescent probes that bind to those parts of the chromosome with which they show a high degree of sequence complementarity (Policht et al., 2010).

In the context of this thesis FISH was used to identify, firstly, c-Myc copy number in HeLa and SiHa cells and also to understand if c-Myc copy number variations result from genetic or chromosomal (such as aneuploidy) alterations.

Vysis LSI MYC Dual color, Break Apart Rearrangement Probe (32-191096, Abbott Molecular) was used to detect c-Myc copy number (Figure 6a). Vysis LSI IGH/MYC, CEP8 Tri-color, Dual Fusion Translocation Probe (32-191020, Abbott Molecular) (Figure 6b) was used to detect c-Myc copy number and the number of centromeres once inclusion of the SpectrumAqua™ CEP 8 serves as a control for chromosome 8 and is located at centromere.

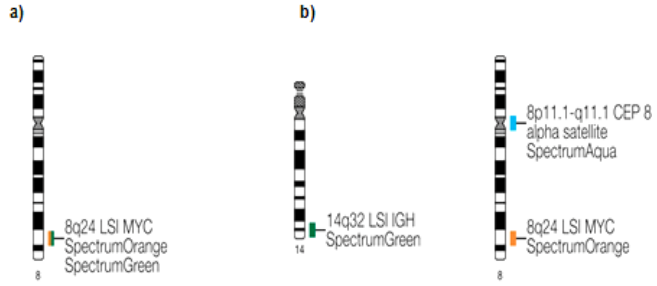


**Figure 6 - LSI MYC Dual color, Break Apart Rearrangement Probe (a) and LSI IGH/MYC, CEP8 Tri-color, Dual Fusion Translocation Probe (b) ideograms.** Adapted from Vysis product catalog, Abbott Molecular.

SiHa and HeLa cells (1x$10^6$ cells/mL) were grown on Millicell EZ slide (PEZGS0416, Millipore) previously coated with 0.2% (w/v) gelatin, in DMEM supplemented with 10% FBS and 1% AA until they reached ~70% confluence. Cells were harvested and fixed with 3:1 Methanol (106009, Merck): Glacial Acetic acid (100063, Merck) for 15 minutes at RT. Slide preparation, probe hybridization and post-hybridization washes were carried out using standard methods described in Vysis LSI (Locus Specific Identifier) DNA probes kit manual (Abbott Molecular). At least 100 nuclei were analyzed using microscopic visualization and images were acquired to verify the number of target and control signals and probe location. The frequency (in percentage) of the different number of signals of target (8q24 LSI MYC) and control probe (8p11.1-q11.1 CEP8 alpha satellite) (located at the centromere), contained in Vysis LSI IGH/MYC, CEP8 Tri-color, Dual Fusion Translocation Probe (32-191020, Abbott Molecular) (Figure 6b), were calculated. The information provided by 14q32 LSI IGH probe (Figure 5b) was not used in this context.

## 3.3 Histological analysis

### 3.3.1 Tissue microarray

Cylindrical cores are obtained from a number (up to 1000) of individual formalin-fixed, paraffin-embedded tissue blocks. These are transferred to recipient tissue microarray (TMA). Each TMA can be sectioned up to 300 times. All resulting TMA slides have the same tissues in the same coordinate positions. The individual slides can be used for a variety of analyses saving labor and reagent costs while maintaining the uniformity of assay. Typically a minimum of 3 cores for each case are used (Kumar & Rudbeck, 2009).

In the present thesis TMAs of adenocarcinoma and squamous cell carcinomas of the uterine cervix cases were performed. The total number of cases included was 44 squamous cell carcinoma cases, 14 adenocarcinoma cases and 3 cases of cervical intraepithelial neoplasia. These tissue microarrays were analyzed by immunohistochemistry and FISH.

### 3.3.2 Immunohistochemistry for MCT1

Immunohistochemistry has emerged as a powerful investigative tool that can provide additional information to the morphological assessment of tissues. The use of immunohistochemistry to study cellular markers that define specific phenotypes has provided important diagnostic, prognostic and predictive information to disease status and biology (Kumar & Rudbeck, 2009).

Tissue specimens are fixed in formalin and subsequently embedded in paraffin in the majority of the cases. While formalin fixation preserves tissue morphology, it also alters the three-dimensional structure of tissue proteins. This alteration can result in a modification of the antigen's epitopes. So, the first step of the immunohistochemistry is the demasking of antigens (Kumar & Rudbeck, 2009). In the present thesis this was performed using a water bath method in a Dako PTLink device – a module for tissue specimens for pre-treatment process of deparaffinization, rehydration and antigen retrieval – for 20 minutes at 94ºC accordingly to manufacturer's protocol. After that, a polymer-based immunohistochemistry (EnVision+System-HRP (DAB), K4011, Dako) was performed accordingly to manufacturer's protocol.

Briefly, after the antigen retrieval the tissue microarray slides were rinsed 2 X 5 minutes with 1X Tris Buffered Saline (TBS) (Appendix I) and then samples were incubated with primary antibody (anti-MCT1) (AB3538P, Millipore) diluted 1:400 in Bond Primary Antibody Diluent (AR9352, Leica bond) for 1 hour at RT. Then slides were rinsed 2 x 5 minutes with 1X TBS and incubated with Peroxidase Block (K4011, Dako) for 10 minutes at RT to block endogenous peroxidase activity. Slides were rinsed once again and incubated with Labelled Polymer-HRP anti-rabbit (K4011, Dako) for 30 minutes at RT. After that slides were rinsed and incubated with DAB+substrate buffer (K4011, Dako) plus DAB+ chromogen (K4011, Dako) (For each 1 mL of buffer one drop (20µL) of DAB+chromogen) for 8 minutes at RT. Then the slides were rinsed in warm water and specimens were immersed in Mayer's Hematoxylin for 1 minute. After that slides were rinsed again in tap water, in order to neutralize the acid and form an insoluble blue aluminium haematin complex, a procedure known as blueing. Finally specimens were immersed in alcoholic solutions with crescent percentage of ethanol and lastly in xylol to dehydrate. After that slides were mounted with Entellan (1079610500, Merck) mounting medium and examined under the optical microscope (Zeiss).

The same procedures described above were performed for negative controls, with the exception of the incubation with the primary antibody. With the information provided by immunohistochemistry analysis for MCT1 the cases in the TMA were classified as negative or positive for MCT1, and for the positive ones, a degree of MCT1 immunodetection intensity (+-, +, ++, +++) was established.

### 3.3.3 Detection of c-Myc copy number by FISH

c-Myc copy number detection in tissue microarray slides were done using FISH. Pre-treatments of the specimen target (includes digestion of tissue), slide preparation, probe hybridization and post-hybridization washes were carried out using standard methods described in Vysis LSI (Locus Specific Identifier) DNA probes kit manual (Abbott Molecular). The probe mixture used for c-Myc detection was Vysis LSI IGH/MYC, CEP8 Tri-color, Dual Fusion Translocation Probe (Abbott Molecular) (Figure 6b) that contains a target probe (8q24 LSI MYC) and a control probe (8p11.1-q11.1 CEP8 alpha satellite) located at the centromere. The information provided by 14q32 LSI IGH probe (Figure 6b) was not used in this context.

With the information provided by FISH analysis the cases in the TMA were classified as normal (disomy), aneusomy, trisomy, aneusomy and amplification for chromosome 8 and c-Myc, accordingly to the chromosome 8 and c-Myc copy number detected.

### 3.4 Role of NaLac and EGF in cell migration, cell cycle regulation and proliferation i*n vitro*

#### 3.4.1 Cell migration - *In vitro* wound healing assay

*In vitro* wound healing assay is a commonly used model to study directional cell migration *in vitro* once to a certain extent this method mimics the migration of cells during wound healing *in vivo* (Lee & Kay, 2006) .

In the present work this assay was performed to identify a possible role of NaLac by itself or in association with EGF stimulation of SiHa cells on their migration rate.

SiHa cells were plated in six-well tissue culture dishes at a concentration of $2x10^5$cells/well ($1x10^5$cells/mL) and maintained in DMEM supplemented with 10% FBS and 1% AA. When cells reached 90 to 100% of optical confluence, they were treated with 5 µg/mL Mitomycin-C (M4287, Sigma) for 3 hours at 37ºC 5% $CO_2$ in order to inhibit cell proliferation. After the incubation time a tip of a micropipette (P200 tip) was used to wound the cell layer, creating linear scrapes. After the scratch the culture medium was replaced to remove floating cellular debris and medium with NaLac (1.06522.2500, Merck) (10mM) and/or EGF (PHG0311, Gibco) (25ng/mL) was added to cells. Culture medium was replaced after approximately 16-18 hours. Wound closure, corresponding to cell migration, was photographed when the scrape wound was introduced (t=0h) and at designated times after wounding (t=8h, t=24h, t=32h). Images were analyzed with *ImageJ* software (http://rsbweb.nih.gov/ij/) in order to estimate wound closure.

Once Mitomycin-C was used in *in vitro* Wound Healing assay to inhibit cell proliferation a proliferation curve of SiHa cells grown in the presence and absence of this anti-proliferative agent was performed. SiHa cells were plated in twelve-well plate tissue culture dishes at a concentration of $2x10^5$cells/well ($2x10^5$cells/mL) and maintained in DMEM supplemented with 10% FBS and 1% AA and incubated at 37ºC 5% $CO_2$ ON. 5 µg/mL of Mitomycin-C (M4287, Sigma) was added to cells and an incubation period of 3 hours at 37ºC 5% $CO_2$ was performed. After that period of time cell number per mL was determined using a Bürker counting chamber (t=0h) and the culture medium was replaced by medium without Mitomycin-C and cells were incubated at 37ºC 5% $CO_2$ for more 8, 24 and 32 hours and cell number/mL was determined at each time point, as described before. Average and standard deviation of cell number per mL were calculated (n=4) and compared to those values obtained for cells grown in the absence of Mitomycin-C.

#### 3.4.2 Cell cycle analysis by Flow Cytometry

Flow cytometry enables the determination of the relative cellular DNA content of cells stained with propidium iodide (PI) – a fluorescent DNA intercalating dye – and also the identification of the cell distribution during the various phases of the cell cycle. Four distinct phases could be recognized in a proliferating cell population: the G1-, S- (DNA synthesis phase), G2- and M-phase (mitosis). However, G2- and M-phase, which both have identical DNA content, could not be discriminated based on their differences in DNA content (Cecchini et al., 2012; Nunez, 2001). The basic steps of this methodology are cell fixation with ethanol, staining and analysis by flow cytometry (Cecchini et al., 2012).

In the context of the present thesis cell cycle analysis was performed to identify a potential role of NaLac by itself or in association with EGF stimulation of SiHa cells in the regulation of cell cycle.

SiHa cells were plated in six-well plate tissue culture dishes at a concentration of $5x10^5$/well ($2.5x10^5$ cells/mL) and maintained in DMEM supplemented with 10% FBS and 1% AA. After ~8hours (when cells adhere) the medium was replaced by medium without FBS and incubated 37ºC 5% $CO_2$ ON. Some cells were

harvested at 0h (control) and the others were stimulated with NaLac (1.06522.2500, Merck) (10mM) and/or EGF (PHG0311, Gibco) (25ng/mL) and harvested 6 and 24 hours after stimulation and fixed in 70% ethanol and incubated at 4ºC. Then cells were stained with PI solution (Appendix I). Firstly, cells were centrifuged at 1500 rpm for 5 minutes and the cell pellet was resuspended in 500 µL of 50 µg/mL PI solution (Appendix I) and incubated at 37ºC for 40 minutes. After the incubation time it was added 3 mL of 1X PBS (Appendix I) and cells were centrifuged at 1500 rpm, 5 minutes at 4ºC. The supernatant was removed and the cells were resuspended in 500 µL PBS 0.1% (w/v) BSA (Appendix I) and analyzed through flow cytometric (FACScalibur - Becton Dickinson). Percentage of cells (death cells and cell aggregates were excluded) in each cell cycle phase was assessed. Average and standard deviation were calculated and statistical analysis was performed.

### 3.4.3 Cell proliferation *in vitro*

A proliferation curve of SiHa cells was done to evaluate a possible role of EGF in the proliferation of this cell type in the presence and absence of NaLac.

SiHa cells were plated in twelve-well plate tissue culture dishes at a concentration of $2x10^5$cells/well ($2x10^5$ cells/mL) and maintained in DMEM supplemented with 10% FBS and 1% AA at 37ºC 5% $CO_2$ for approximately 8 hours (to adhere) and then culture medium was replaced by DMEM without FBS and incubated at 37ºC 5% $CO_2$ ON (to synchronize cells). Cell number per mL was determined using a Bürker counting chamber (t=0h) and the culture medium was replaced by medium with NaLac (1.06522.2500, Merck) (10 mM) and/or EGF (PHG0311, Gibco) (25 ng/mL) and cells were incubated for 3 hours at 37ºC 5% $CO_2$. After this period of time cell concentration (cells/mL) was determined as described before. The same procedure was done after 6, 12, 24 and 30 hours of incubation at 37ºC 5% $CO_2$. The average and standard deviation of cell number per mL were calculated (n=4) and statistical analysis was performed.

**Table 13 - Primers used during the experimental work**

| Reference/Target | Primer (5'-3') | Tm (ºC) | Technique |
|---|---|---|---|
| *Mlu*pLDHA | For1:ATGACGCGTCCTTTCAACTCTCTTTTGGC | 75.6 | PCR; Automate sequencing |
| | For2:ATGACGCGTCTGGACACTGAGAAACAGG | 75.9 | |
| | For3ATGACGCGTGACTCGAGATGAGATGCCAG | 79.0 | |
| *HindIII*pLDHA | Rev1:ATGAAGCTTGACTTGGAACCAAAAGGAATC | 72.2 | |
| | Rev2:ATGAAGCTTGTGGAACAGCTATGCTGACG | 74.4 | |
| *Mlu*pLDHB | For1:ATGACGCGTCTTTTGAGACGGAATCGCTC | 78.0 | |
| | For2:ATGACGCGTCAGAGTAGAAGAATCAGTCC | 71.5 | |
| *HindIII*pLDHB | Rev :ATGAAGCTTGCACTGCAAGGAAAGAATC | 72.1 | |
| *Mlu*pMCT1 | For1:ATGACGCGTGATTGCCTAGAGCTCGTCAG | 77.7 | |
| | For2:ATGACGCGTGGACATCAAAGACACTCCATG | 78.2 | |
| *HindIII*pMCT1 | Rev :ATGAAGCTTCTGCCTCGTTTGCTTGTTCC | 75.7 | |
| | | | |
| LDHA f1 | For1: CCTTTCAACTCTCTTTTGGC | 60.4 | PCR; Automate sequencing |
| | Rev1: GACTTGGAACCAAAAGGAATC | 61.3 | |
| LDHA f2 | For2: CTGGACACTGAGAAACAGG | 58.3 | |
| | Rev2: GTGGAACAGCTATGCTGACG | 63.5 | |
| LDHA f3 | For3: GACTCGAGATGAGATGCCAG | 62.7 | |
| | Rev2: GTGGAACAGCTATGCTGACG | 63.5 | |
| LDHB f1 | For1: CTTTTGAGACGGAATCGCTC | 63.8 | |
| | Rev: GCACTGCAAGGAAAGAATC | 60.0 | |
| LDHB f2 | For2: CAGAGTAGAAGAATCAGTCC | 52.8 | |
| | Rev: GCACTGCAAGGAAAGAATC | 60.0 | |
| MCT1 f1 | For1: GATTGCCTAGAGCTCGTCAG | 61.7 | |
| | Rev: CTGCCTCGTTTGCTTGTTCC | 67.0 | |
| MCT1 f2 | For2: GGACATCAAAGACACTCCATG | 62.0 | |
| | Rev: CTGCCTCGTTTGCTTGTTCC | 67.0 | |
| | | | |
| RVprimer3 | CTAGCAAAATAGGCTGTCCC | 57.0 | PCR; Automate sequencing |
| GLprimer2 | GGAAGACGCCAAAAACATAAAG | 56.0 | PCR; Automate sequencing |
| | | | |
| Myc LDHA | For1:CTTCTGTGGTTGGAGGGCAGCA | 72.7 | qRT-PCR |
| | Rev1:GCGCAGCCAGACAACCGA | 71.4 | |
| | For2:TCGGTTGTCTGGCTGCGC | 71.4 | |
| | Rev2: GTGGAACAGCTATGCTGACG | 63.5 | |
| Myc MCT1 | For1:GCCCCACATATGCATCGTCC | 69.6 | |
| | Rev1:ATTAAAGACGAGTCGGGAAAGAAG | 64.4 | |
| | For2:GATTGCCTAGAGCTCGTCAG | 61.7 | |
| | Rev2:CCTCCACACGCTTTCAGCC | 68.3 | |
| | | | |
| LDHA | For: CTTGCTCTTGTTGATGTCATCG | 64.6 | qRT-PCR |
| | Rev: CAGCCGTGATAATGACCAGC | 65.5 | |
| LDHB | For: GAGCCTTCTCTCTCCTGTG | 59.3 | |
| | Rev: CTGATAGCACACGCCATACC | 63.1 | |
| LDHC | For: GGATCTTCAGCATGGCAGTC | 64.8 | |
| | Rev: CTATTCTGGAGTTTGCAGATACAC | 60.6 | |
| MCT1 | For: GCTGGGCAGTGGTAATTGGA | 67.1 | |
| | Rev: CAGTAATTGATTTGGGAAATGCAT | 64.4 | |
| HPRT | For: TGACACTGGCAAAACAATGCA | 67.5 | |
| | Rev: GGTCCTTTTCACCAGCAAGCT | 66.6 | |
| MCT4 | For: CACAAGTTCTCCAGTGCCATTG | 66.7 | |
| | Rev: CGCATCCAGGAGTTTGCCTC | 69.2 | |
| EGFR | For: AAGACAGCTTCTTGCAGCGATA | 65.1 | |
| | Rev: GGAGGAAGGTGTCGTCTATGCT | 65.5 | |

**Table 13 cont. Primers used during the experimental work**

| | | | |
|---|---|---|---|
| Methyl-pMCT1 | For1: GGAATTTAATATATTTTAG<br>For2: GGGTAGATTGTTTAGAGTT<br>Rev1: AACTCTAAACAATCTACCC<br>Rev2: CAACTCACCACTTTATCTAA | 42.5<br>49.6<br>49.6<br>51.7 | PCR; Automate sequencing |
| Methyl-pLDHA | For1: TTTGTGGTTGGAGGGTAGTAA<br>For2: TAGTATAGTTGTTTTATTTA<br>For3: AATTGTTTTTGGTTTTGTTG<br>Rev1: TAAATAAAACAACTATACTA<br>Rev2: CAACAAAACCAAAAACAATT<br>Rev3: CACCTTAAAACCTATCATA | 60.8<br>41.0<br>56.6<br>41.0<br>56.6<br>49.0 | |
| Methyl-pLDHB | For1:GAAATTTAAGAGGTTGTGG<br>For2:GGTAGAGGGTAGTAGTTGTG<br>For3: GAGGAGAAAGGTATTTAGATG<br>Rev1: CACAACTACTACCCTCTACC<br>Rev2: CATCTAAATACCTTTCTCCTC<br>Rev3: CCCCAAACCCTTACTACAAC | 53.6<br>52.7<br>53.7<br>52.7<br>53.7<br>59.8 | |

Tm: melting temperature
qRT-PCR: quantitative Real Time-PCR

### 3.5 Statistical analysis

Student's t test was used to evaluate the statistical significance of results, using *OriginPro8* software (OriginLab Corporation). $p<0.05$ was considered statistically significant and $p<0.001$ highly statistically significant.

# 4. Results

## 4.1 Role of EGF and NaLac in the regulation of *LDH*s (*LDHA*, *LDHB*, *LDHC*) and *MCT*s (*MCT1, MCT4*) expression

### 4.1.1 *LDHs* and *MCTs* relative gene expression and protein levels in HeLa and SiHa cell lines

The role of EGF in the regulation of *LDHA*, *LDHB, LDHC, MCT1* and *MCT4* gene expression in the presence and absence of NaLac in HeLa and SiHa cells was firstly evaluated by quantitative Real-Time PCR (Figures 7 and 10). The regulation of LDHA, LDHB, (LDHC in SiHa cells), MCT1 and MCT4 protein levels were evaluated through Western-blot (Figures 8 and 14) and Immunofluorescence (Figures 9, 10, 12 and 13) in both cell lines. The designations, LDHA and LDHB protein levels, which were used in this thesis, correspond to the detection of LDH-M subunit and LDH-H subunit, respectively (as referred in 3.1.3).

In HeLa cells it was observed a statistically significant increase in *LDHA* and *LDHB* expression after NaLac treatment comparing to cells grown in control conditions (Figure 7a). For *LDHA*, the increase obtained at mRNA levels was reflected in LDHA protein levels assessed by western-blot (Figure 8) but not in LDHA protein levels assessed by immunofluorescence (Figure 9). Concerning *LDHB*, the increase was reflected in LDHB protein levels assessed by western-blot (Figure 8) and immunofluorescence (Figure 9).

It was observed that EGF-stimulated HeLa cells exhibited higher (highly statistically significant) *LDHA* expression levels and LDHA protein levels (assessed by western-blot) comparing to unstimulated cells (Figures 7a and 8) and that this increase was even higher in stimulated cells grown in the presence of NaLac only at mRNA level (Figure 7a). In terms of *LDHB* expression levels, it was verified that EGF-stimulated cells grown in presence of NaLac exhibited decreased levels comparing to cells grown in control conditions (Figure 7a) but this decrease was not reflected in LDHB protein levels assessed by western-blot (Figure 8).

In SiHa cells grown in the presence of NaLac it was verified a statistically significant increase in *LDHA* and *LDHB* expression comparing to cells grown in control conditions (Figure 7b). This higher *LDHA* mRNA levels were not reflected in LDHA protein levels assessed through western-blot (Figure 8) and immunofluorescence (Figure 10). For *LDHB* the increase was reflected in LDHB protein levels assessed by western-blot (Figure 8) and immunofluorescence (Figure 10). In terms of *LDHC* expression, SiHa cells grown in the presence of NaLac showed decreased levels of it comparing to cells grown in control conditions (Figure 7b), however this decrease was not reflected in LDHC protein levels assessed by western-blot (Figure 8) and immunofluorescence (Figure 10).

EGF-stimulated SiHa cells exhibited higher *LDHA* expression levels comparing to unstimulated cells grown in control conditions (Figure 7b) and these higher levels were maintained in stimulated cells grown in the presence of NaLac (Figure 7b).These increases observed at mRNA level were not reflected at protein level assessed by western-blot (Figure 8) and immunofluorescence (Figure 10). *LDHB* expression levels were higher in EGF-stimulated SiHa cells (Figure 7b) comparing to unstimulated cells and this increase was reflected in LDHB protein levels assessed by western-blot (Figure 8) and immunofluorescence (Figure 10). Besides that, EGF-stimulated cells grown in the presence of NaLac exhibited higher *LDHB* expression (highly statistically significant) (Figure 7b) and LDHB protein levels

(Figure 8) comparing to cells grown in control conditions but lower *LDHB* expression levels comparing to EGF-stimulated cells (Figure 7b). However this decrease at mRNA level was not reflected in LDHB protein levels (Figures 8 and 10). EGF-stimulated SiHa cells grown in the presence and absence of NaLac exhibited lower levels of *LDHC* expression comparing to cells grown in control conditions (Figure 7b). However, LDHC protein levels were higher in EGF-stimulated cells grown either in the presence or absence of NaLac comparing to cells grown in control conditions (Figures 8 and 10).

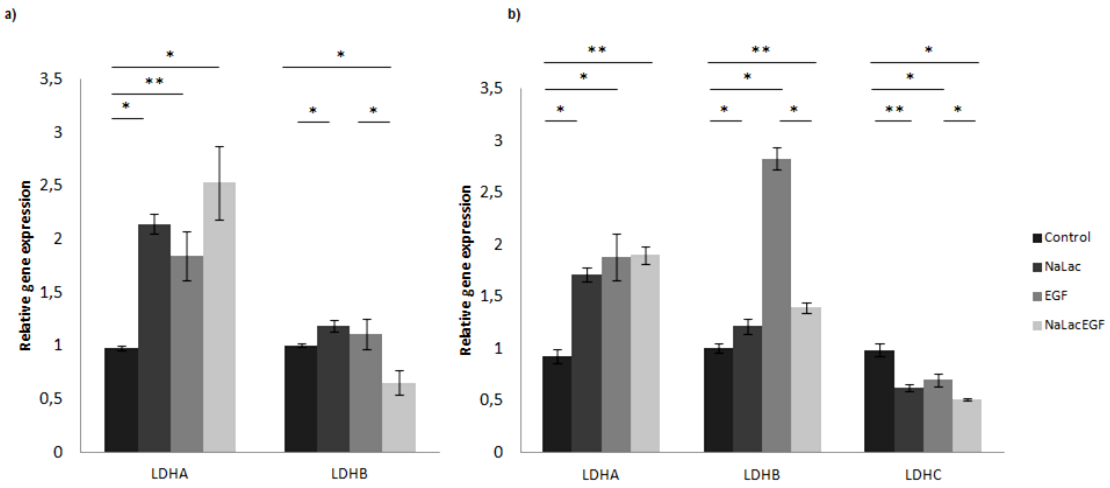


**Figure 7 - Relative gene expression of lactate dehydrogenases (LDHs) in HeLa cells (a) and SiHa cells (b).** Cells were grown in control conditions, in the presence of NaLac and with EGF stimulation in the presence and absence of NaLac**.** *Hypoxanthine phosphoribosyltransferase* gene (HPRT) was used as endogenous control. Expression levels were normalized to those obtained for cells grown in control conditions. Data are mean ± standard deviation of biological triplicates.* p< 0.05 **p<0.001

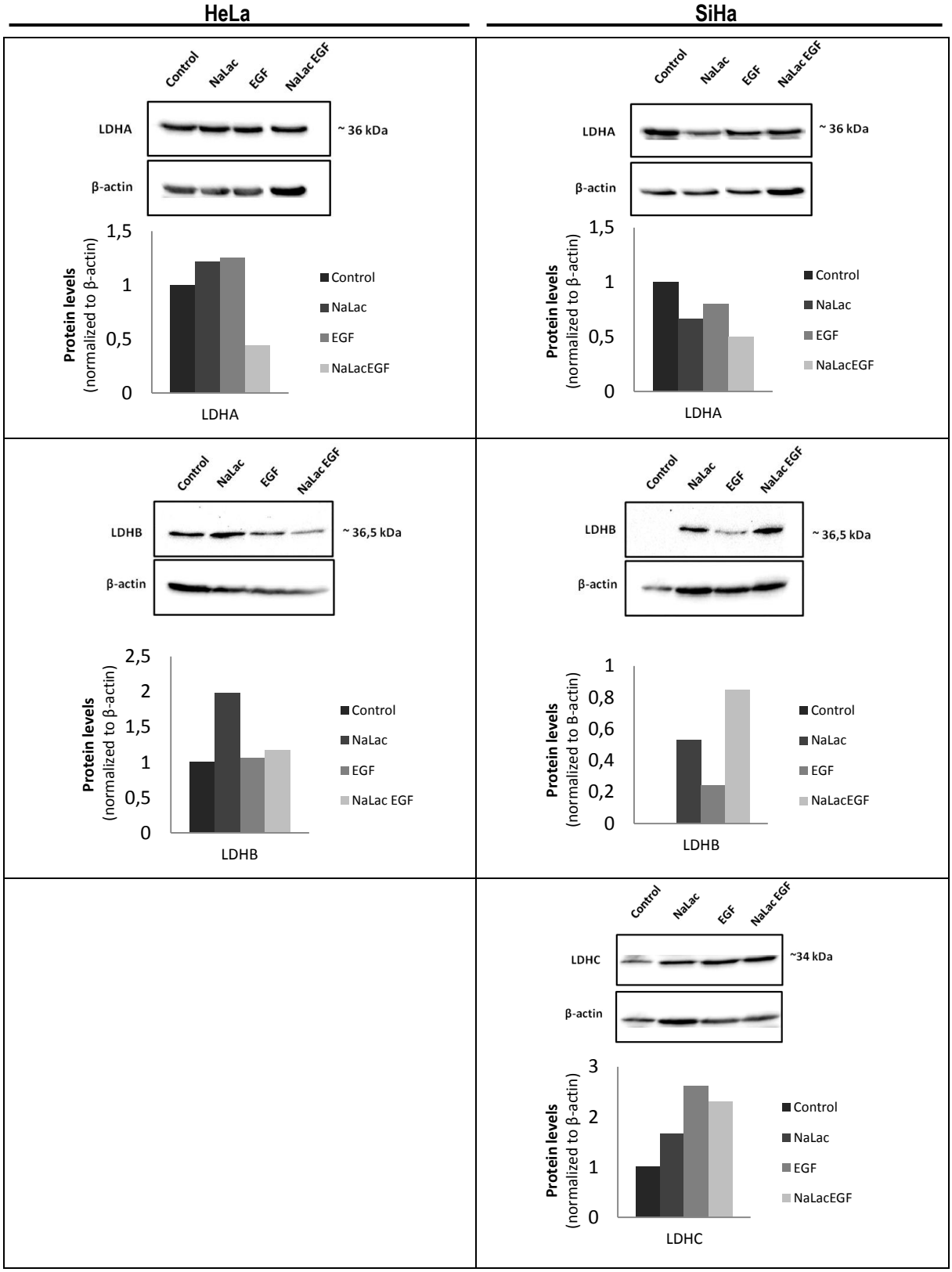


**Figure 8 - LDHs protein levels in HeLa (LDHA and LDHB) and SiHa (LDHA, LDHB and LDHC) cells assessed by western-blot.** Cells were grown in control conditions, in the presence of NaLac and with EGF stimulation in the presence and absence of NaLac. Protein levels were normalized to β-actin and are relative to those obtained for cells grown in control conditions.

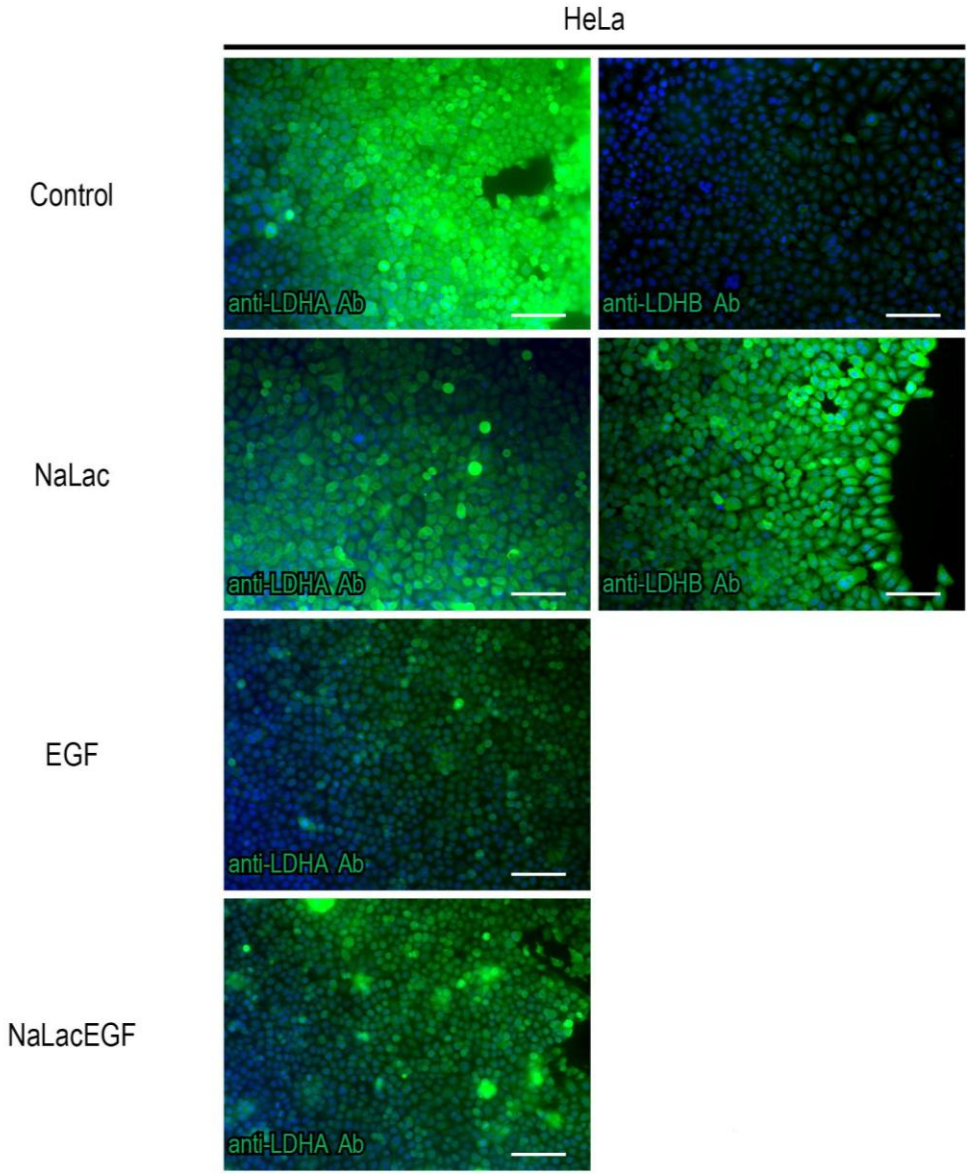


**Figure 9 - Immunofluorescence for LDHA and LDHB in HeLa cells.** Comparison between the protein levels of cells grown in control conditions, in the presence of NaLac and with EGF stimulation in the presence and absence of NaLac. Fluorescence microscopy (original magnification: 200x). Nuclei were stained with DAPI (blue). Scale bar 100 µm.

The negative controls of the immunofluorescence assay are shown in figure A1 (Appendix II).

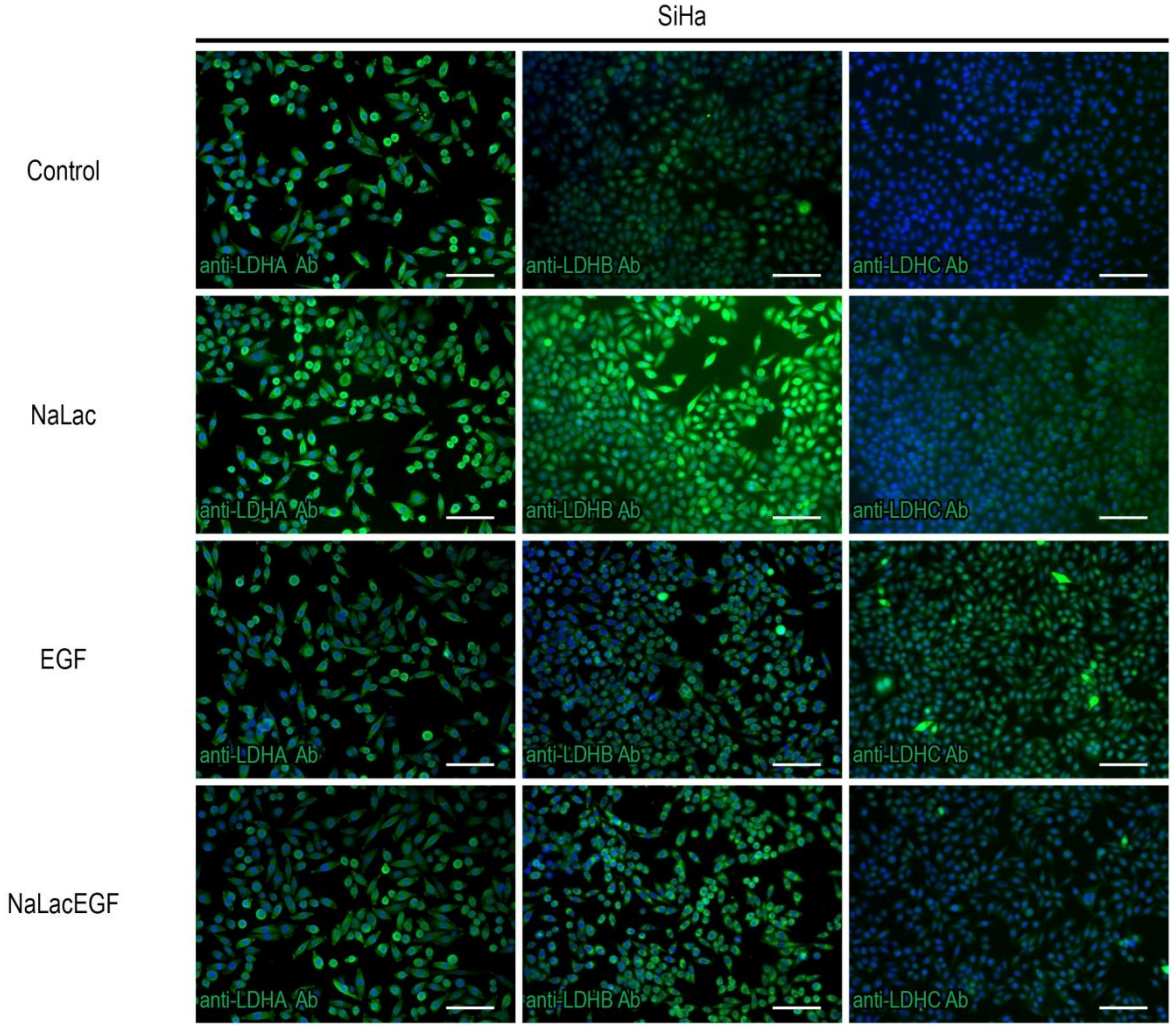


**Figure 10 - Immunofluorescence for LDHA, LDHB and LDHC in SiHa cells.** Comparison between the protein levels of cells grown in control conditions, in the presence of NaLac and with EGF stimulation in the presence and absence of NaLac. Fluorescence microscopy (original magnification: 200x). Nuclei were stained with DAPI (blue). Scale bar 100 µm.

Concerning *MCT*s expression, no differences were observed between *MCT1* expression in HeLa cells grown in the presence of NaLac comparing to those grown in its absence (Figure 11a), however it was detected a decrease in MCT1 protein levels assessed by immunofluorescence (Figure 12). Nevertheless, HeLa cells grown in the presence of NaLac exhibited higher levels of *MCT4* (Figure 11a) that was reflected in MCT4 protein levels (Figure 12).

EGF stimulation of HeLa cells seems to promote *MCT1* and *MCT4* expression (Figure 11a) and that increase was reflected also at MCT1 and MCT4 protein levels assessed through immunofluorescence (Figure 12). Concerning EGF-stimulated cells grown in the presence of NaLac, it was observed that *MCT1* expression levels were lower comparing to stimulated cells grown in its absence (Figure 11a) and that was reflected at protein levels (Figure 12).

In SiHa cells, also no significant differences were observed between *MCT1* expression in cells grown in the presence of NaLac and in its absence (Figure 11b), but an evident increase in MCT1 protein levels was detected (Figure 13). SiHa cells grown in the presence of NaLac showed increased levels of *MCT4* expression

comparing to those grown in its absence (Figure 11b) that was reflected in MCT4 protein levels (Figures 13 and 14). In this cell line EGF stimulation only had a statistically significant effect on *MCT4* expression (Figure 11b) that seems to be potentiated by NaLac exposure of these cells (Figure 11b) what was also reflected at protein levels assessed by western-blot (Figure 14).

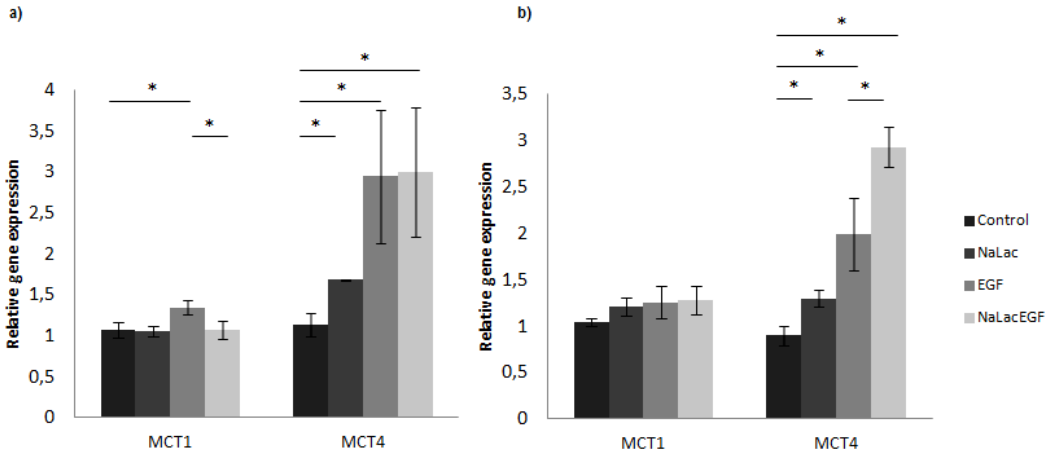


**Figure 11 - Relative gene expression of monocarboxylate transporters (MCTs) in HeLa cells (a) and SiHa cells (b).** Cells were grown in control conditions, in the presence of NaLac and with EGF stimulation in the presence and absence of NaLac**.** *Hypoxanthine phosphoribosyltransferase* gene (HPRT) was used as endogenous control. Expression levels were normalized to those obtained for cells grown in control conditions. Data are mean ± standard deviation of biological triplicates.* p< 0.05

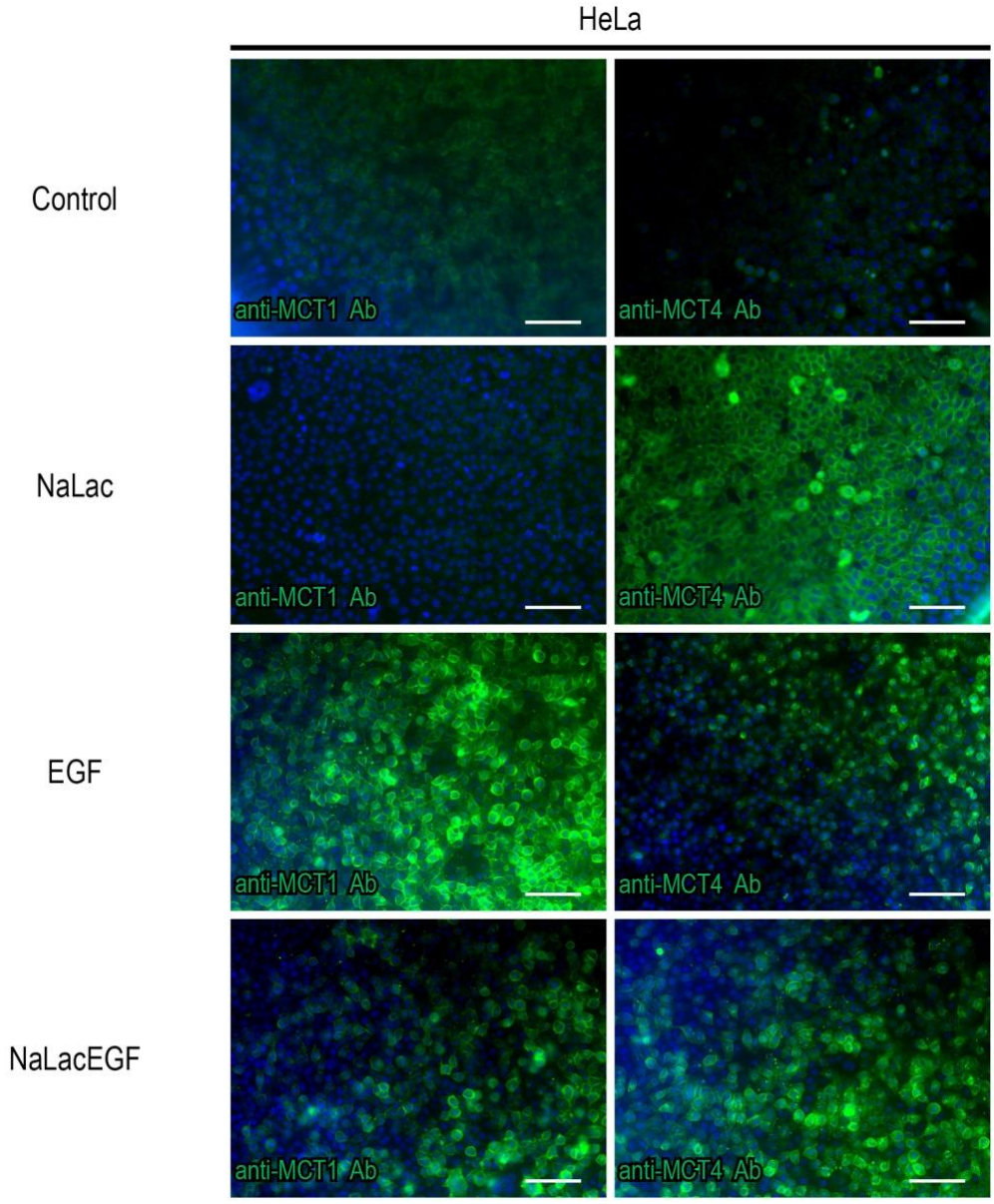


**Figure 12 - Immunofluorescence for MCT1 and MCT4 in HeLa cells.** Comparison between the protein levels of cells grown in control conditions, in the presence of NaLac and with EGF stimulation in the presence and absence of NaLac. Fluorescence microscopy (original magnification: 200x). Nuclei were stained with DAPI (blue). Scale bar 100 µm.

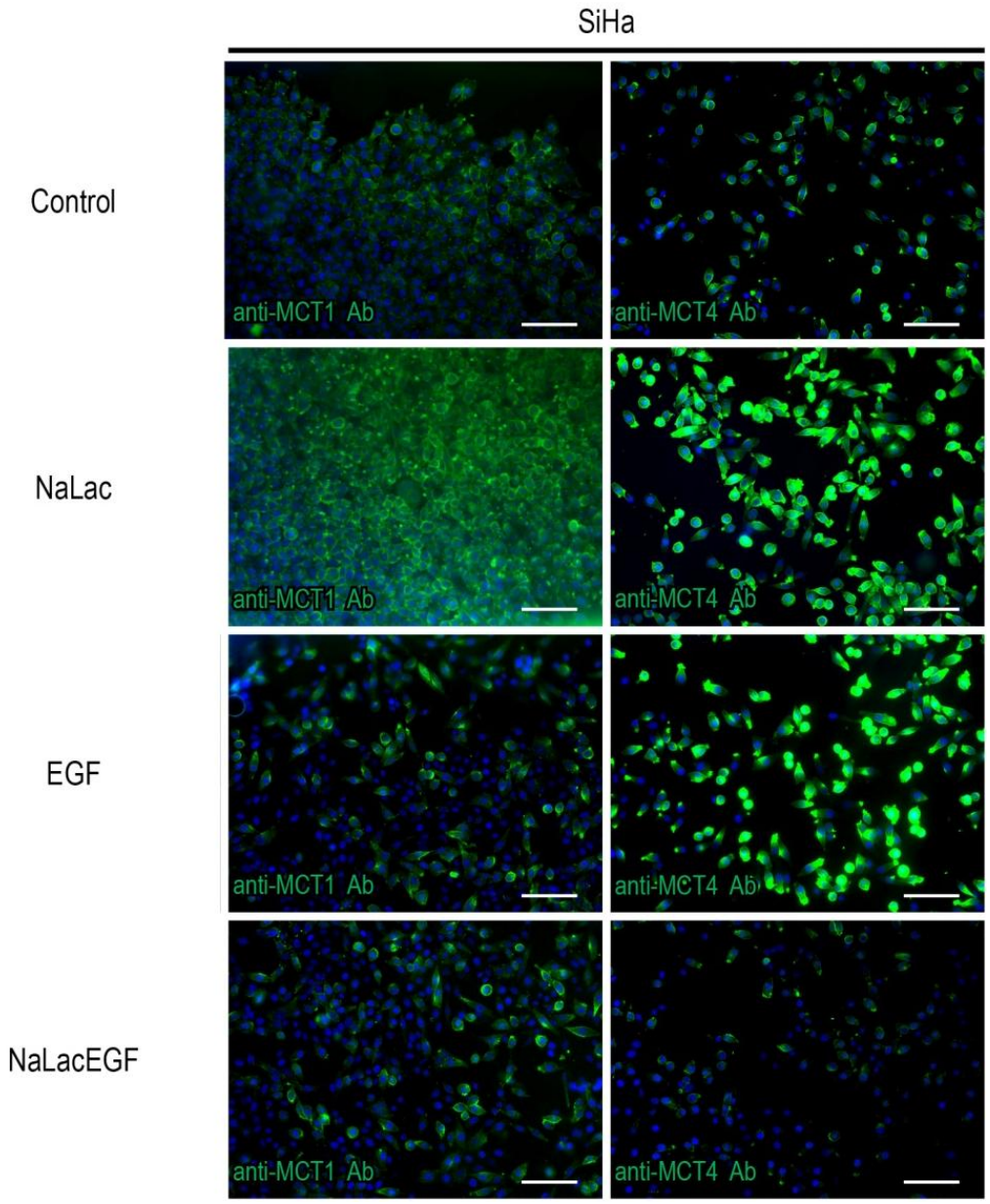


**Figure 13 - Immunofluorescence for MCT1 and MCT4 in SiHa cells.** Comparison between the protein levels of cells grown in control conditions, in the presence of NaLac and with EGF stimulation in the presence and absence of NaLac. Fluorescence microscopy (original magnification: 200x). Nuclei were stained with DAPI (blue). Scale bar 100 µm.

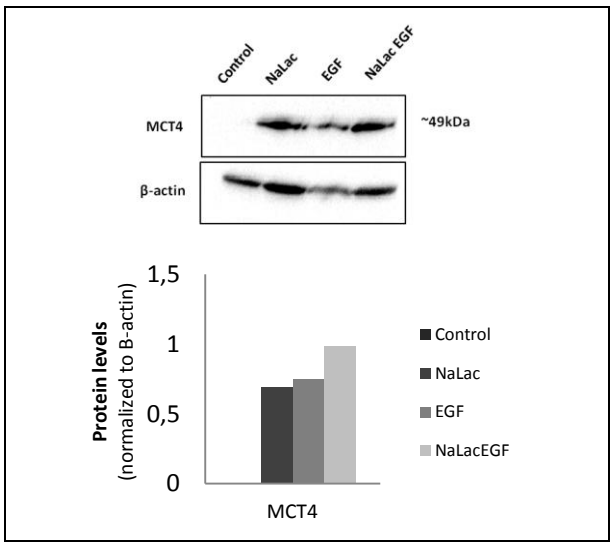


**Figure 14 - MCT4 protein levels in SiHa cells assessed by western-blot.** Cells were grown in control conditions, in the presence of NaLac and with EGF stimulation in the presence and absence of NaLac Protein levels were normalized to β-actin and are relative to those obtained for cells grown in control conditions.

MCT1 protein levels in both cell lines were not assessed through western-blot due to technical problems involving anti-MCT1 antibody.

In order to assess EGF receptor (*EGFR*) expression in HeLa and SiHa cells grown in the absence and presence of NaLac with and without EGF stimulation of these cells relative gene expression was evaluated through quantitative Real-Time PCR (Figure 15). In HeLa cells it was observed that *EGFR* expression was lower in cells grown in the presence of NaLac with or without EGF stimulation comparing to those obtained for cells grown in control conditions (Figure 15a). However, EGF-stimulated cells grown in the presence of NaLac showed higher (statistically significant) levels than those grown in its absence (Figure 15a).

EGF-stimulated SiHa cells showed a statistically significant decrease in *EGFR* expression levels comparing to cells grown in control conditions (Figure 15b). However, as verified in HeLa cells, EGF-stimulated cells grown in the presence of NaLac showed higher (statistically significant) levels than those grown in its absence (Figure 15b).

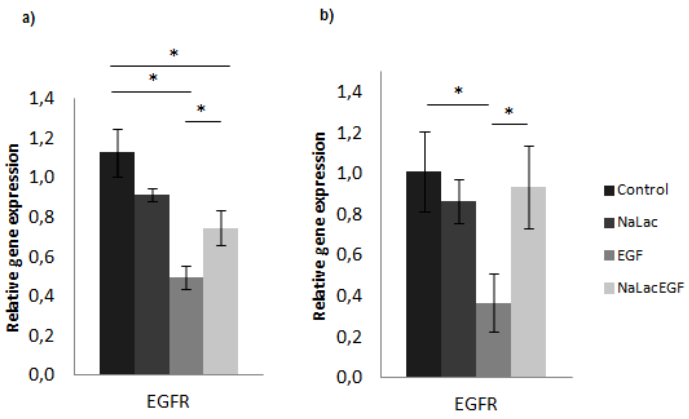


**Figure 15 - Relative gene expression of EGF receptor (*EGFR*) in HeLa cells (a) and SiHa cells (b).** Cells were grown in control conditions, in the presence of NaLac and with EGF stimulation in the presence and absence of NaLac. *Hypoxanthine phosphoribosyltransferase* gene (HPRT) was used as endogenous control. Expression levels were normalized to those obtained for cells grown in control conditions. Data are mean ± standard deviation of biological triplicates. *p<0.05

Aiming to evaluate if a chronically exposure of SiHa cells to NaLac would modify the regulation of *LDH*s and *MCT*s gene expression in this cell line, cells were chronically grown in the presence of NaLac and then relative gene expression was assessed by quantitative Real-Time PCR (Figure 16). The data revealed a statistically significant increase in *LDHA* and *LDHB* expression and a decrease (highly statistically significant) in *LDHC* levels comparing to cells grown in control conditions (Figure 16), as observed for acute exposure to NaLac (Figure 7b) . *MCT4* levels was higher (although not statistically significant) after chronic exposure to NaLac comparing to cells not exposed to it, as verified for acute exposure to NaLac (Figures 16 and 11b). So, *LDH*s and *MCT*s gene expression in SiHa cells seems do not be changed by a chronically exposure to NaLac, comparing to an acute one. A statistically significant increase in *EGFR* mRNA levels were observed in SiHa cells chronically exposed to NaLac comparing the levels of those grown in the absence of it (Figure 16) while in SiHa cells exposed to NaLac (not chronically) this difference was not evident (Figure 15b).

Regarding EGF stimulation of SiHa cells chronically exposed to NaLac, it was observed the same trend, in terms of *LDH*s and *MCT*s expression as in EGF-stimulated cells not chronically exposed to NaLac (Figures 16, 7b and 11b). However, a statistically significant increase in *EGFR* expression levels was observed in EGF-stimulated SiHa cells chronically exposed to NaLac comparing to cells grown in control conditions (Figure 16), while in EGF-stimulated SiHa cells exposed to NaLac (not chronically) this difference was not evident (Figure 15b).

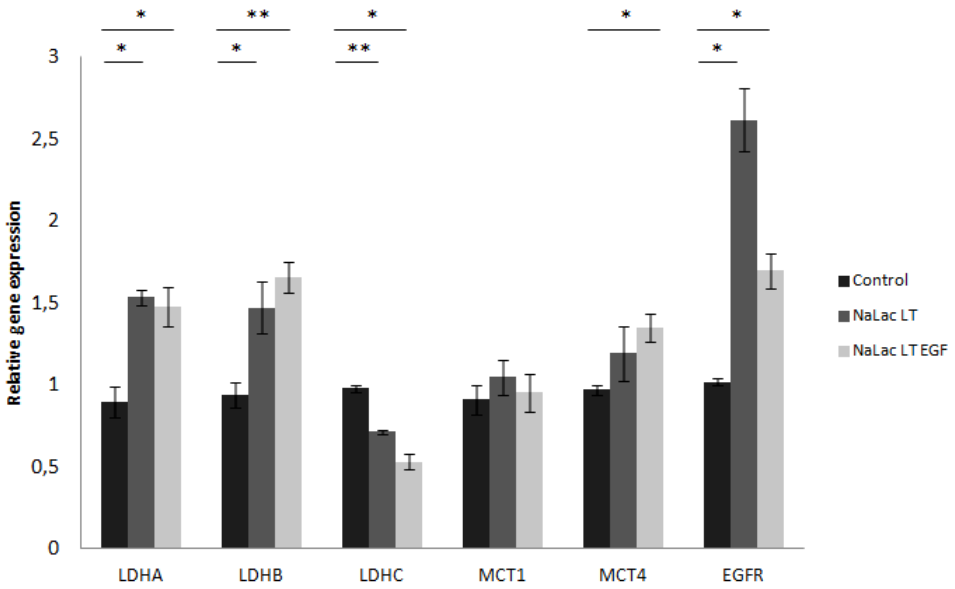


**Figure 16 - Relative gene expression in SiHa cells chronically exposed to NaLac (long term (LT) exposition) with and without EGF stimulation of these cells.** *Hypoxanthine phosphoribosyltransferase* gene (HPRT) was used as endogenous control. Expression levels were normalized to those obtained for cells grown in control conditions. Data are mean ± standard deviation of biological triplicates. * $p<0.05$ ** $p<0.001$

### 4.1.2 Epigenetic regulation of *LDHA*, *LDHB* and *MCT1* promoters

In order to evaluate the epigenetic regulation of *LDHA, LDHB* and *MCT1* promoters and to identify a potential role of NaLac by itself or in association with EGF on that regulation, the methylation pattern of specific CpG islands was determined using sodium bisulfite treatment of DNA.

#### 4.1.2.1 Methylation pattern of *LDHA, LDHB* and *MCT1* promoters

DNA was extracted from HeLa and SiHa cells in culture in the presence and absence of NaLac with and without EGF stimulation (culture conditions described at 3.1.1). Sodium bisulfite treatment of this DNA and subsequent analysis of the methylation pattern of specific CpG islands, revealed that all the CpG dinucleotides identified in the two CpG islands studied in *LDHA* promoter were unmethylated (Figure 17) in both cell lines. Besides that, all the CpG dinucleotides identified in the three CpG islands analyzed in *LDHB* promoter were unmethylated (Figure 18) in both cell lines. Finally, all the CpG dinucleotides identified in the CpG island analyzed in *MCT1* promoter were unmethylated (Figure 19) in both cell lines. Additionally, the methylation pattern of the studied CpG islands of DNA extracted from cells grown in the various culture conditions (mentioned above and described at 3.1.1) was the same.

So, in this setting, *LDHA*, *LDHB* and *MCT1* promoters are not regulated by methylation and EGF stimulation and/or NaLac treatment of cells did not affect the methylation status of these promoters in these two cell lines.

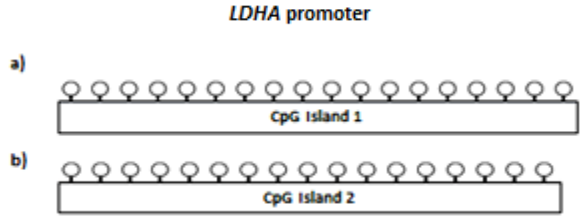


**Figure 17 - Schematic representation of the methylation pattern of two *LDHA* promoter CpG islands in HeLa and SiHa cells.** a) 18 CpG dinucleotides identified in *LDHA* promoter CpG island 1 b) 17 CpG dinucleotides identified in *LDHA* promoter CpG island 2. White circles denote unmethylated CpG sites.

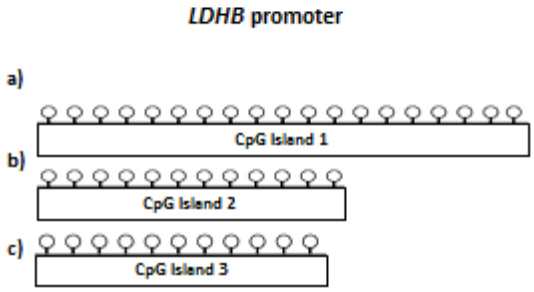


**Figure 18 - Schematic representation of the methylation pattern of three *LDHB* promoter CpG islands in HeLa and SiHa cells.** a) 19 CpG dinucleotides identified in *LDHB* promoter Island 1. b) 12 CpG dinucleotides identified in *LDHB* promoter Island 2. c) 11 CpG dinucleotides identified in *LDHB* promoter Island 3. White circles denote unmethylated CpG sites.

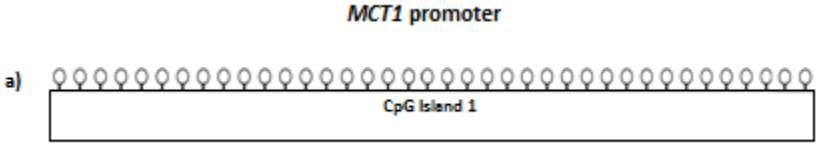


**Figure 19 - Schematic representation of the methylation pattern of one *MCT1* promoter CpG island in HeLa and SiHa cells**. a) 38 CpG dinucleotides identified in *MCT1* promoter CpG island 1. White circles denote unmethylated CpG sites.

### 4.1.3 Activity of *LDHA*, *LDHB* and *MCT1* promoters

In order to evaluate the activity of *LDHA* and *LDHB* and *MCT1* promoters after EGF stimulation of cells grown in the presence and absence of NaLac in SiHa and HeLa cell lines, different deletion constructs were generated using conventional molecular cloning techniques. After that promoter activity was detected using the Dual Luciferase Assay System.

Firstly, it was evaluated which promoter deletion construct exhibited higher luciferase activity for both cell lines. It was observed that *LDHA* f2, *LDHB* f1 and *MCT1* f2 deletion construct were those with higher luciferase activity in HeLa cells (Figures 20 and 21) while in SiHa cells *LDHA* f2, *LDHB* f1 and *MCT1* f1 exhibited the highest luciferase activity (Figures 20 and 21).

Secondly, the luciferase of the various deletion constructs was assessed in HeLa and SiHa cells transfected in control conditions, in the presence of NaLac and with EGF stimulation in the presence and absence of NaLac (as described in 3.1.5.4). The levels were then compared to those obtained for cells transfected in control conditions (as described in 3.1.5.4) for both cell lines (Figures 20 and 21).

In HeLa cells there were no statistically significant differences between the luciferase activity of *LDHA* and *LDHB* deletion constructs in cells exposed to NaLac comparing to cells grown in control conditions (Figure 20). However, in EGF-stimulated HeLa cells grown in the presence of NaLac, the luciferase activity of *LDHA* f1 deletion construct and *LDHB* f2 deletion construct was, respectively higher and lower than in those grown in control conditions (Figure 20). The luciferase activity of three *LDHA* deletion constructs and *LDHB* f1 deletion construct was higher in EGF-stimulated HeLa cells grown in the presence of NaLac than in stimulated cells grown in its absence (Figure 20).

Relating to SiHa cells, it was observed a statistically significant increase in luciferase activity of the three *LDHA* deletion constructs in cells exposed to NaLac comparing to cells grown in control conditions (Figure 20). For *LDHB* deletion constructs, it was also observed an increase, which was statistically significant for f1 construct, in their luciferase activity in cells exposed to NaLac comparing to cells grown in control conditions (Figure 20).

In EGF-stimulated SiHa cells grown either in the presence or absence of NaLac was observed a highly significant increase in luciferase activity of the three *LDHA* deletion constructs comparing to cells grown in control conditions (Figure 20). Besides that in EGF-stimulated SiHa cells the luciferase activity of the three *LDHA* deletion constructs was higher in cells grown in the presence of NaLac than in those grown in its absence (Figure 20). In EGF-stimulated SiHa cells grown either in the presence or absence of NaLac the luciferase activity of *LDHB* deletion constructs was also statistically significant higher than in those grown in control conditions (Figure 20). In addition, the luciferase activity of *LDHB* f1 deletion construct was higher in EGF-stimulated cells grown in the presence of NaLac whether the luciferase activity of *LDHB* f2 deletion construct was lower in these cells comparing to stimulated cells grown in its absence (Figure 20).

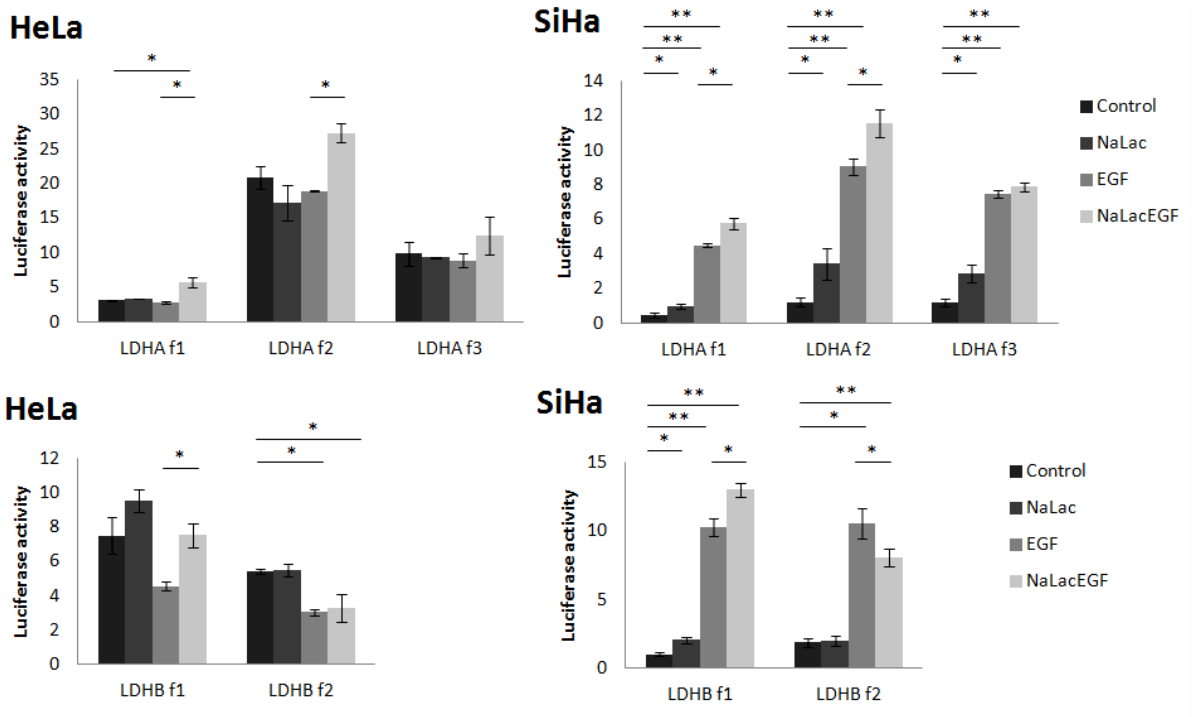


**Figure 20 - Luciferase activity of *LDHA (*f1, f2, f3) and *LDHB (*f1, f2) deletion constructs in transfected HeLa and SiHa cells.** Cells were grown in control conditions, in the presence of NaLac and with EGF stimulation in the presence and absence of NaLac. * p< 0.05 ** p<0.001

For *MCT1* f1 deletion construct, it was observed higher (statistically significant) luciferase activity in SiHa and HeLa cells transfected in the presence of NaLac comparing to cells transfected in its absence (Figure 21). In SiHa cells this increment was also verified for *MCT1* f2 deletion construct (Figure 21).

*MCT1* f1 deletion construct exhibited higher (highly statistically significant) luciferase activity in EGF-stimulated HeLa and SiHa cells transfected either in the presence of absence of NaLac comparing to those transfected in control conditions (Figure 21). In SiHa cells, this increase was also verified for *MCT1* f2 deletion construct (Figure 21). In EGF-stimulated HeLa cells transfected in the presence of NaLac both *MCT1* deletion constructs exhibited higher luciferase activity comparing to those observed in stimulated cells transfected in its absence (Figure 21). While in EGF-stimulated SiHa cells transfected in the presence of NaLac, there was no difference between luciferase activity of both *MCT1* deletion constructs comparing to those observed in stimulated cells transfected in its absence (Figure 21).

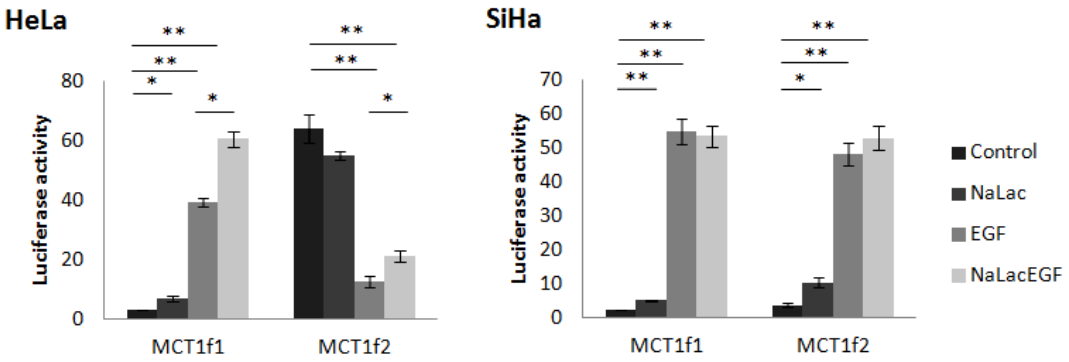


**Figure 21 - Luciferase activity of *MCT1* (f1 and f2) deletion constructs in transfected HeLa and SiHa cells.** Cells were grown in control conditions, in the presence of NaLac and with EGF stimulation in the presence and absence of NaLac.* p< 0.05 **p<0.001

Finally, TFSEARCH database (ver.1.3) (http://www.cbrc.jp/research/db/TFSEARCH.html) was consulted in order to assess which transcription factors had putative binding sites at the specific regions of the *LDHA*, *LDHB* and *MCT1* promoters that had been cloned in the generated deletion constructs. c-Myc was the elected transcription factor once *LDHA* f2, *MCT1* f1 and *MCT1* f2 deletion constructs included putative N-Myc binding sites and c-Myc has the same binding sequence of N-Myc. Besides that, this choice was based on the fact that c-Myc has an important role in the regulation of cancer cell metabolism (as referred in introduction) and it is involved in uterine cervix carcinogenesis.

### 4.1.4 Role of c-Myc transcription factor in the regulation of *LDHA* and *MCT1* expression

In order to study c-Myc transcription factor role in the regulation of *LDHA* and *MCT1* expression in the presence and absence of NaLac and/or after EGF stimulation of cells a c-Myc-antibody Chromatin Immunoprecipitation (ChIP) assay was performed for both cell lines (Figures 22 and 23).

In HeLa cells, it was observed higher occupancy of c-Myc at *MCT1* promoter in cells stimulated with EGF and grown in the absence of NaLac comparing to those grown in control conditions (Figure 22). For SiHa cells, it was detected higher occupancy of c-Myc at *MCT1* promoter for EGF-stimulated cells grown in the presence of NaLac comparing to those grown in control conditions (Figure 23). SiHa cells grown in control conditions had shown high occupancy of c-Myc at *MCT1* promoter while cells grown in the presence of NaLac and EGF-stimulated cells exhibited lower, or none, occupancy, respectively (Figure 23).

In relation to *LDHA* promoter it was observed occupancy of c-Myc at this promoter in HeLa cells grown in the presence of NaLac and also in EGF-stimulated cells grown in its presence comparing to cells grown in control conditions (Figure 22). In SiHa cells occupancy of c-Myc at *LDHA* promoter was not evident and was not influenced by NaLac or EGF stimulation of cells (Figure 23).

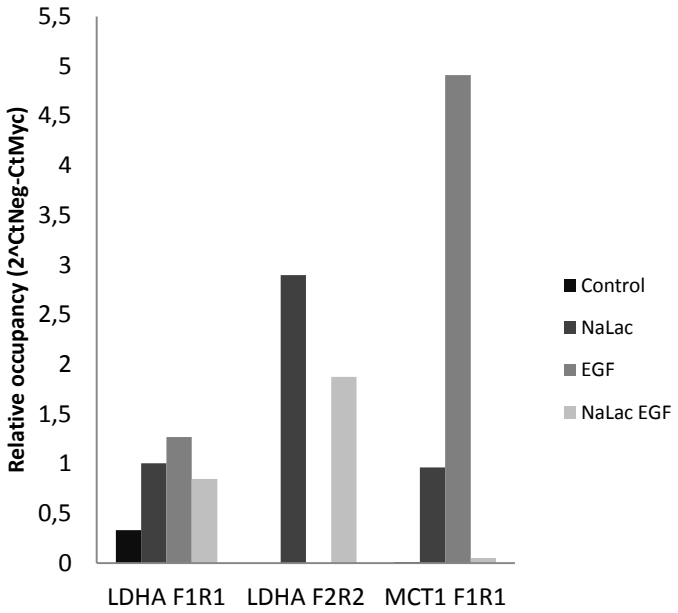


**Figure 22 - Relative occupancy of c-Myc factor at *LDHA* and *MCT1* promoters (relative to IgG) in HeLa cells.** Cells were grown in control conditions, in the presence of NaLac and with EGF stimulation in the presence and absence of NaLac.

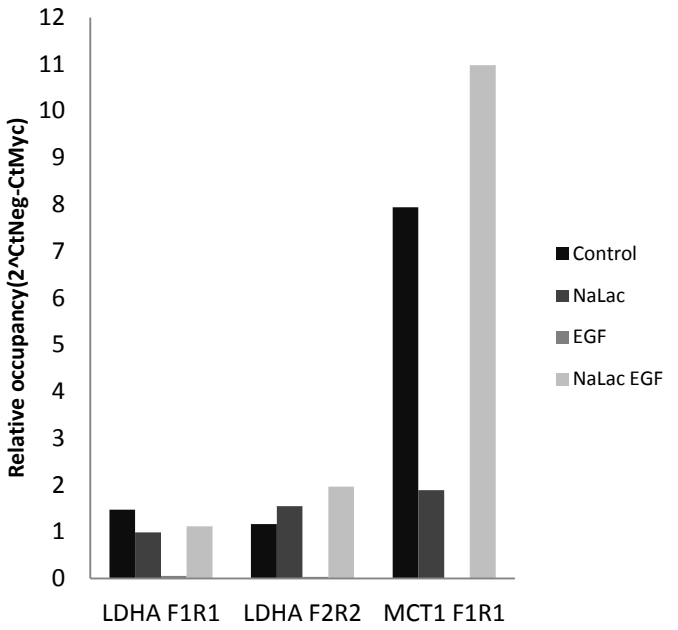


**Figure 23 - Relative occupancy of c-Myc factor at *LDHA* and *MCT1* promoters (relative to IgG) in SiHa cells.** Cells were grown in control conditions, in the presence of NaLac and with EGF stimulation in the presence and absence of NaLac.

## 4.2 Detection of c-Myc copy number by Fluorescent in situ hybridization (FISH)

Once several studies had shown amplification or increased expression of c-Myc in many tumors, including uterine cervix carcinomas, a FISH for c-Myc was performed in HeLa and SiHa cell lines to evaluate c-Myc copy number in these cells.

FISH analysis revealed that there is heterogeneity in terms of c-Myc copy number both in HeLa and SiHa cell nuclei (Table A1, Appendix II). Using 8q24 LSI MYC probe it was verified that 4 was most frequent c-Myc copy number detected in both HeLa (92.59%) and SiHa (88.46%) cells (Table A1 and Figure A2, Appendix II), suggesting c-Myc amplification in these cell lines.

Through complementary FISH analysis, using a control probe for the centromeric region at chromosome 8, it was verified that in HeLa cells nuclei 95.84% of total cell nuclei had 4 c-Myc copies (corresponding to 4 Orange (O) signals in FISH images) and 2 centromeric signals (corresponding to 2 Aqua (Aq) signals in FISH images) (Table14, Figures 24a and 24b), suggesting genetic c-Myc amplification.

For SiHa cells, 77.30% of total cell nuclei had 4 c-Myc copies (corresponding to 4 Orange (O) signals in FISH images) and 4 centromeric signals (corresponding to 4 Aqua (Aq) signals in FISH images) (Table 14, Figures 24c and 24d), suggesting that aneuploidy is in the basis of the increased number of c-Myc copies, since SiHa cells have more than two chromosome 8, where c-Myc is located.

**Table 14 - Frequency (in percentage) of c-Myc copy number detected in SiHa and HeLa cells using FISH.** c-Myc copy number and the number of centromeric signals were detected using LSI MYC SpectrumOrange (O) probe for 8q24 and SpectrumAqua (Aq) CEP8 probe (8p11.1-q11.1 CEP8 alpha satellite that serves as a control for chromosome 8), respectively, in SiHa and HeLa interphase nuclei.

| c-Myc copy number (O) + centromeric signals number (Aq) | % |
|---|---|
| | **SiHa** |
| 4O 4Aq | 77.30 |
| 5O 5Aq | 21.99 |
| 4O 5Aq | 0.71 |
| | **HeLa** |
| 4O 2Aq | 95.84 |
| 3O 2Aq | 3.33 |
| 5O 3Aq | 0.83 |

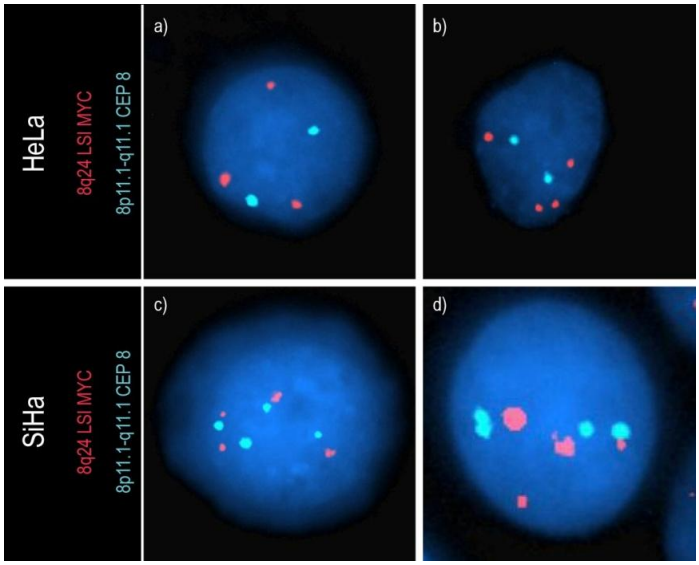


**Figure 24 - Copy number analysis of c-Myc through Fluorescent in situ hybridization (FISH).** Representative experiments of FISH analysis of c-Myc in HeLa (a,b) and SiHa (c,d) cells are shown. The probe used for c-Myc detection was the LSI IGH/MYC, CEP8 Tri-color, Dual Fusion Translocation Probe that includes the SpectrumAqua CEP8 probe (8p11.1-q11.1 CEP8 alpha satellite that serves as a control for chromosome 8) (located at the centromere), the LSI MYC SpectrumOrange probe for 8q24 and the LSI IGH SpectrumGreen probe for 14q32 whose information was not used in this context. Nuclei in interphase were counterstained with DAPI.

### 4.3 Histological analysis

Once previous studies referred MCT1 overexpression uterine cervix cancer, MCT1 immunodetection was performed in tissue microarrays of AC and SCC of the uterine cervix cases. Additionally, c-Myc amplification had also been described in this type of tumors, so, c-Myc copy number was also analyzed in these microarrays. Tissue microarrays of AC and SCC of the uterine cervix cases were analyzed by immunohistochemistry for MCT1 and FISH for Chromosome 8/c-Myc (Figures 25, 26 and 27).

Concerning AC cases, only two were positive for MCT1 (Figure 25) and were diploid (normal) for chromosome 8 and c-Myc (Figures 25). Regarding SCC cases, it seems that the increase in c-Myc copy number is associated with increase in MCT1 immunodetection despite of the detection of c-Myc diploid (normal) cases expressing MCT1 with several intensity (Figures 25 and 26).

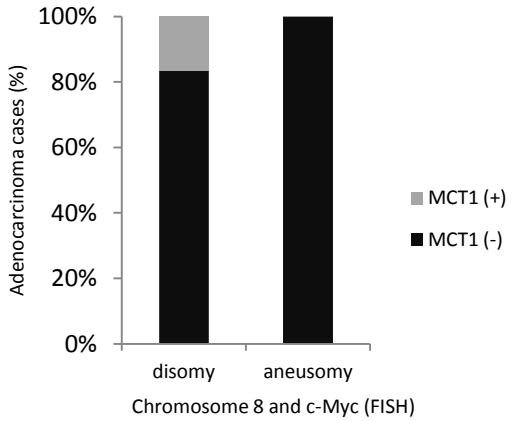


**Figure 25 - Percentage of MCT1 positive (+) and negative (-) AC cases with disomy or aneusomy for chromosome 8 and c-Myc.** AC: Adenocarcinoma

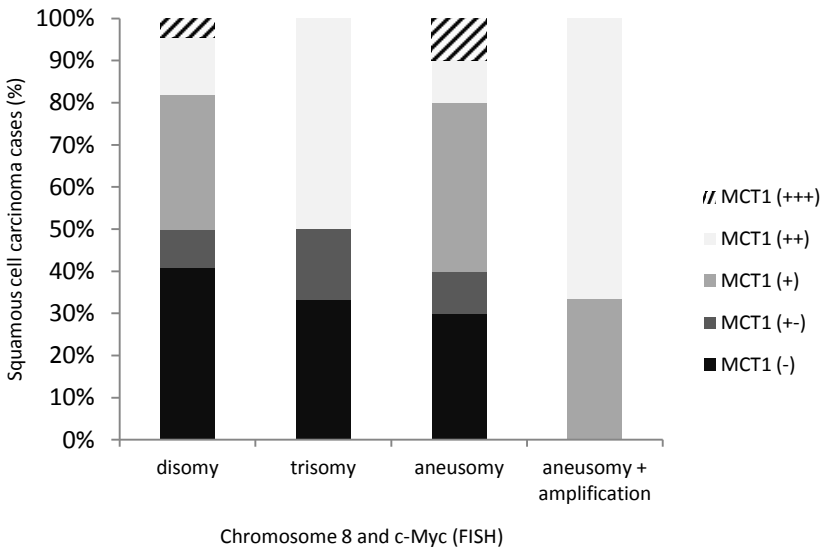


**Figure 26 - Percentage of MCT1 positive (from +/- to +++) and negative (-) SCC cases with disomy, trisomy, aneusomy or aneusomy and amplification for chromosome 8 and c-Myc.** SCC: Squamous cell carcinoma.

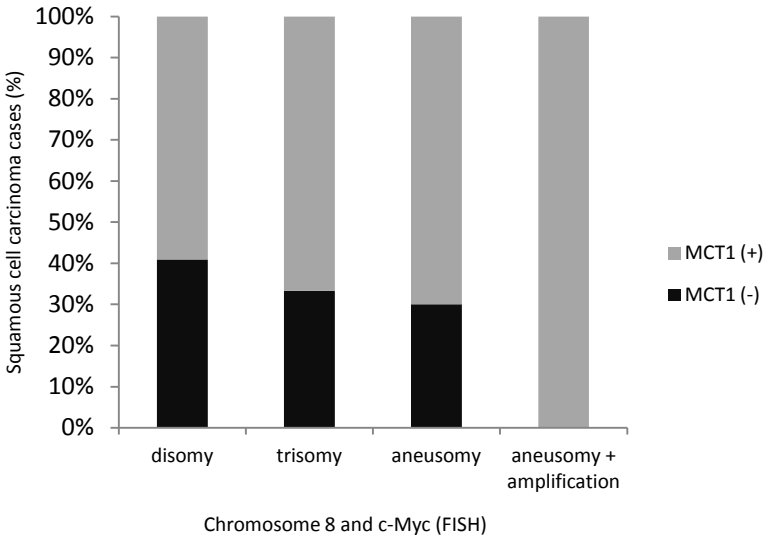


**Figure 27 - Percentage of MCT1 positive (+) and negative (-) SCC cases with disomy, trisomy, aneusomy or aneusomy and amplification for chromosome 8 and c-Myc.** SCC: Squamous cell carcinoma.

MCT1 immunohistochemistry analysis also revealed important differences between normal ectocervix (Figure 28) and normal endocervix (Figure 29), in terms of MCT1 immunodetection. It was verified that normal ectocervix samples were mainly positive for MCT1 while normal endocervix ones were mainly negative.

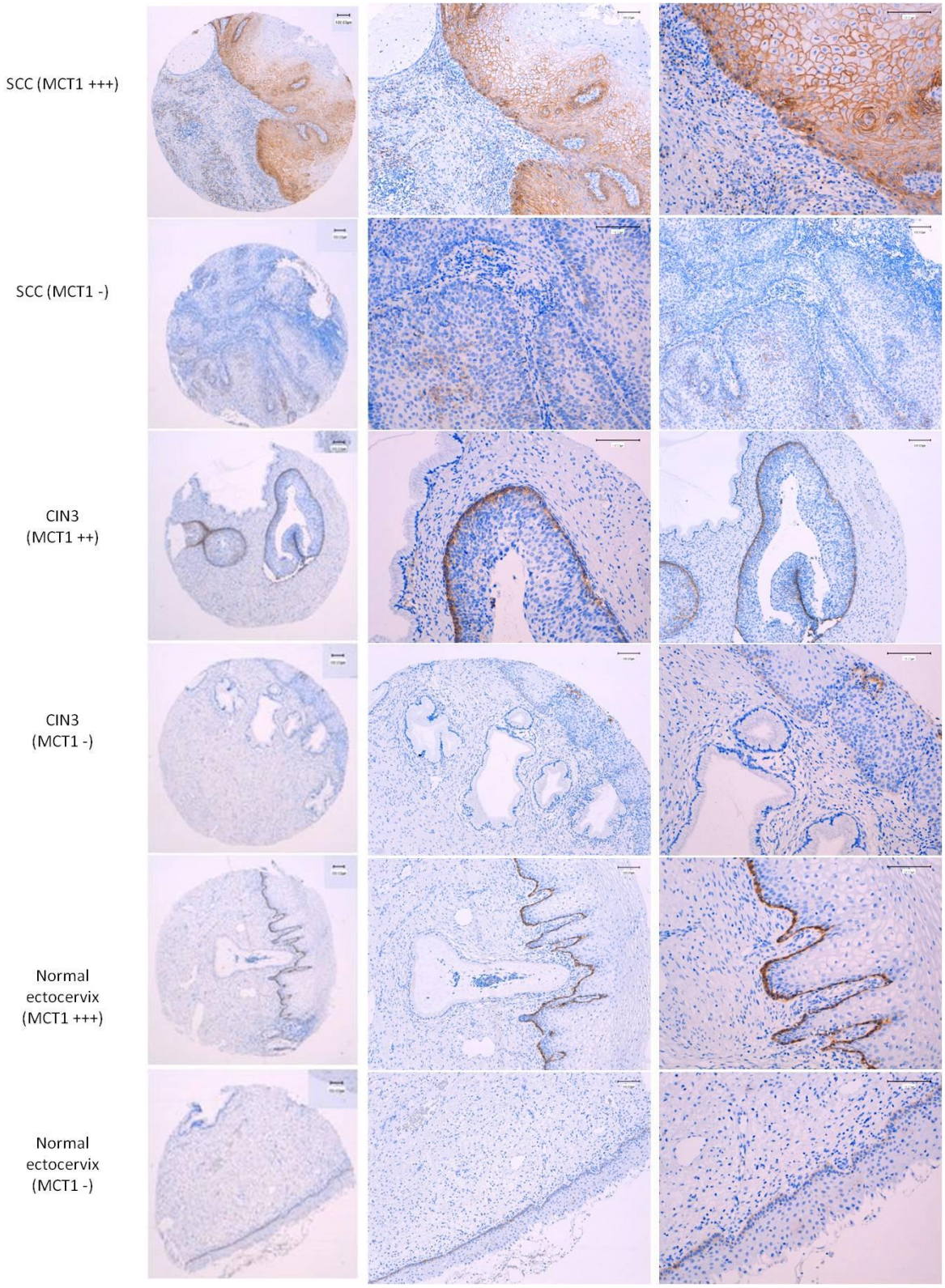


**Figure 28 - MCT1 immunodetection in SCC, CIN and normal ectocervix.** Representative images of MCT1 immunodetection in SCC, CIN cases and in normal ectocervix are shown. MCT1 negative (-) and positive (++, +++) cases are represented. SCC: squamous cell carcinoma. CIN3: cervical intraepithelial neoplasia grade 3.

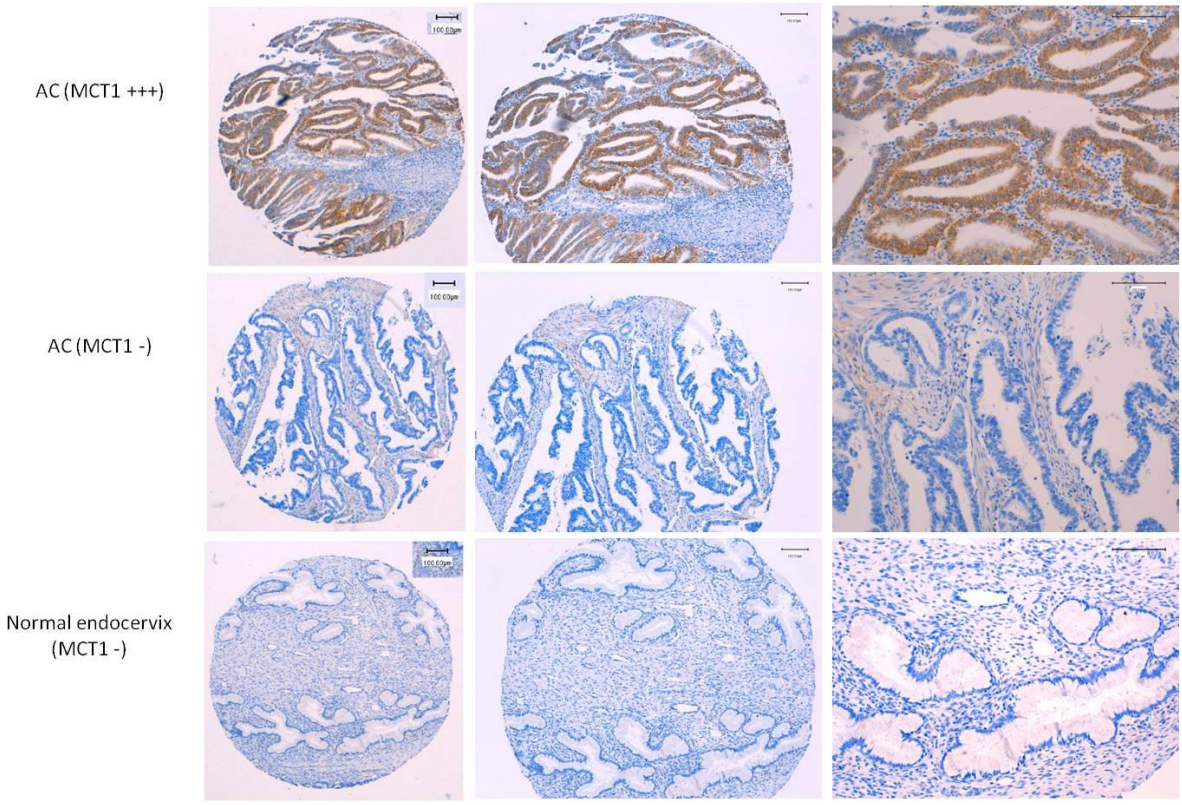


**Figure 29 - MCT1 immunodetection in AC and normal endocervix.** Representative images of MCT1 immunodetection in AC cases and in normal endocervix are shown. MCT1 negative (-) and positive (+++) cases are represented. AC: Adenocarcinoma.

### 4.4 Role of NaLac and EGF in cell migration, cell cycle regulation and proliferation i*n vitro*

#### 4.4.1 Cell migration

Since EGF has been described as an important growth factor in uterine cervix carcinogenesis *in vitro* Wound Healing assay was performed to investigate a possible role of NaLac by itself or in association with EGF stimulation of SiHa cells on their migration rate (Figure 30). The migration rate was evaluated at the following time points: 0, 8, 24 and 32 hours (Figures 30 and 31).

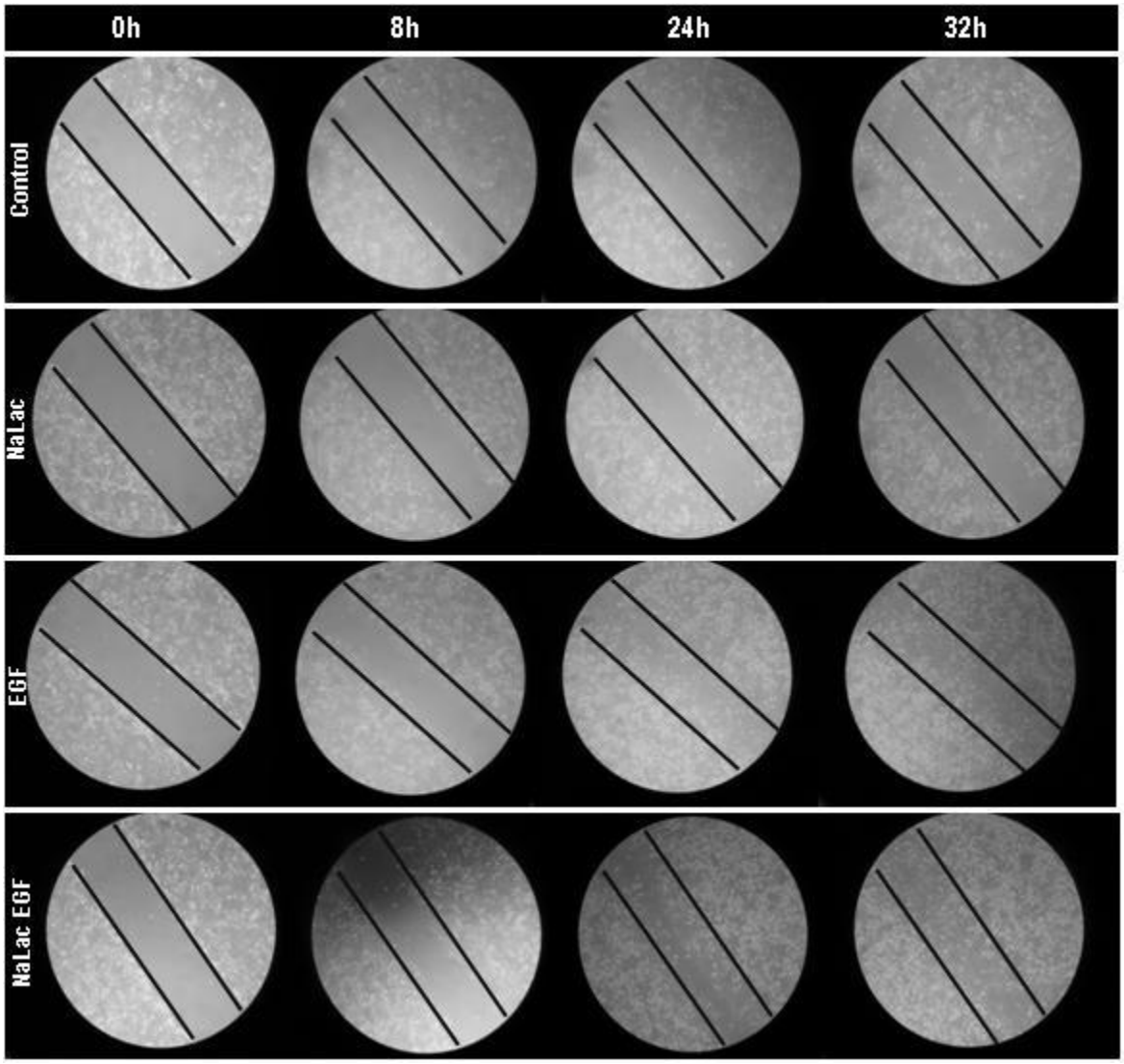


**Figure 30 - *In vitro* Wound Healing assay in SiHa cells.** Mitomycin-treated cells were grown in control conditions, in the presence of NaLac and with EGF stimulation in the presence or absence of NaLac. Wound closure was photographed when the scrape wound was introduced (t=0 hours) and at designated times after wounding (t=8hours, t=24hours, t=32hours). Phase microscopy (original magnification: 200x).

It was verified a higher cell migration rate (faster wound closure) in cells grown in the presence of NaLac comparing to cells grown in control conditions (Figures 30 and 31). EGF stimulation of cells grown in the presence of NaLac seems to promote cell migration once wound closure was faster than in cells grown only in presence of NaLac and in control conditions too (Figures 30 and 31).

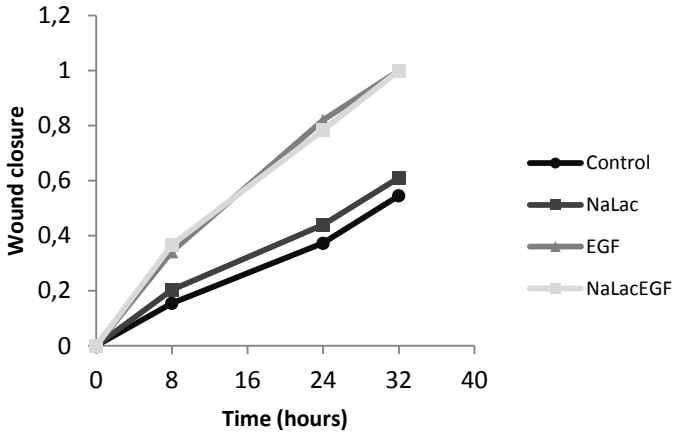


**Figure 31 - Quantification of wound closure in SiHa cells.** Mitomycin-treated cells were grown in control conditions, in the presence of NaLac and with EGF stimulation in the presence or absence of NaLac. Data were collected 0 hours, 8 hours, 24 hours and 32 hours after scratching.

Once Mitomycin was used in *in vitro* wound healing assay to inhibit cell proliferation a proliferation curve of SiHa cells grown in the presence and absence of this anti-proliferative agent was performed (Figure 32). It was observed that 5 µg/mL of Mitomycin was appropriate to inhibit SiHa cells proliferation during 32 hours (Figure 32).

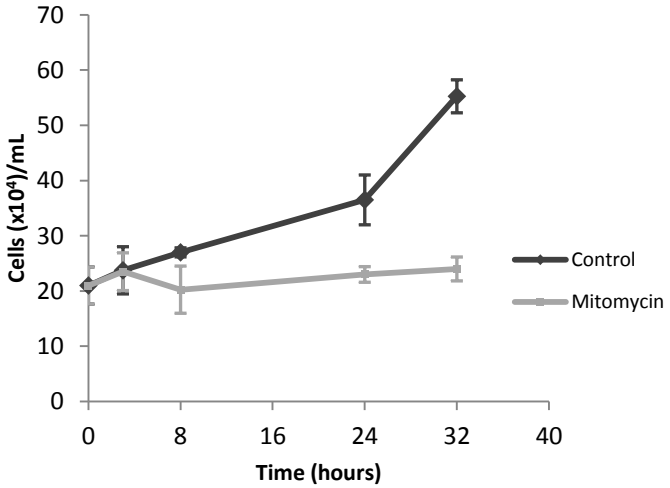


**Figure 32 - Proliferation curve of SiHa cells after treatment with anti-proliferative agent Mitomycin (5µg/mL).** Number of cells ($x10^4$)/mL was determined at 0, 8, 24 and 32 hours. Data are mean ± standard deviation.

### 4.4.2 Cell cycle regulation and proliferation *in vitro*

Once several data indicated that EGF plays an important role in the regulation of cell growth and proliferation, cell cycle analysis and a proliferation curve was performed to investigate a possible role of NaLac by itself or in association with EGF stimulation of SiHa cells on cell cycle regulation and on their proliferation *in vitro*.

#### 4.4.2.1 Cell cycle analysis

Cell cycle analysis of SiHa cells was performed by flow cytometry (Figure 33).

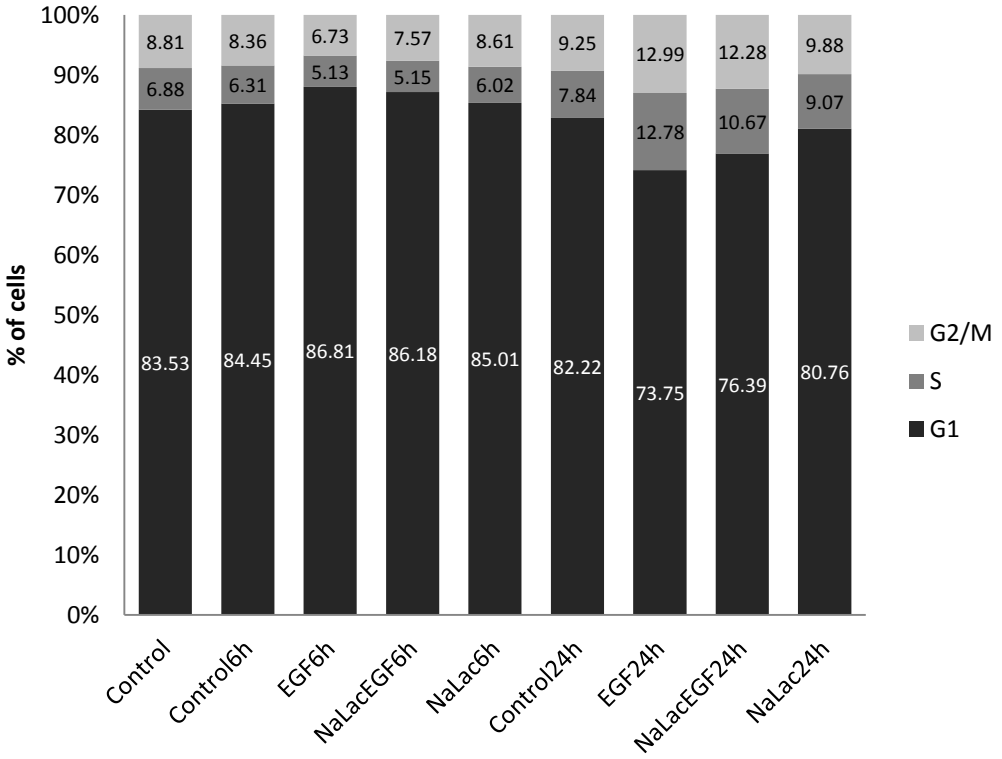


**Figure 33 - Flow cytometric analysis showing the cell cycle distribution of SiHa cells (PI staining).** Cells were grown in control conditions, in the presence of NaLac and with EGF stimulation in the presence and absence of NaLac for 6 hours and 24 hours. Data are means of triplicates.

Firstly, cell cycle analysis of SiHa cells, revealed that the majority of the cells were in G1 phase despite of culture conditions of these cells (Figure 33).

It was observed a statistically significant increase in the percentage of cells in G1 phase after 6 hours in EGF-stimulated cells (86.81%) comparing to cells grown in control conditions (84.45%) and a statistically significant decrease in the percentage of cells in S (5.13%) and G2/M phases (6.73%) comparing to cells grown in control conditions (6.31% and 8.36%, respectively) (Figure 33). The same tendency was verified in EGF-stimulated cells grown in the presence of NaLac, after 6 hours.

In EGF-stimulated cells grown in the presence of NaLac was verified a statistically significant decrease in the percentage of cells in S (5.15%) and G2/M (7.57%) phases comparing to cells grown in control conditions (6.31% and 8.36%, respectively), after 6 hours (Figure 33). It was also verified an increase, although not statistically significant, in the amount of cells in G1 phase (86.18%) for this condition (Figure 33).

In EGF-stimulated cells grown in the presence of NaLac was seen a statistically significant decrease in the percentage of cells in G1 phase (76.39%) and an increase in those in S phase (10.67%) and G2/M (12.28%) (not statistically significant) comparing to cells grown in control conditions (82.22%, 7.84% and 9.25%, respectively) (Figure 33), after 24 hours. At this time point, it was observed that EGF-stimulated cells exhibited a statistically significant higher percentage of cells in S phase (12.78%) comparing to cells grown in control conditions (7.84%) (Figure 33). In EGF-stimulated cells grown in the presence of NaLac it was observed a statistically significant decrease in the percentage of cells in S phase (10.67%) comparing to EGF-stimulated cells grown in its absence (12.78%) (Figure 33).

#### 4.4.2.2 Proliferation curve

A proliferation curve of SiHa cells was done aiming to evaluate a possible role of EGF in the *in vitro* proliferation of this cell type in the presence and absence of NaLac (Figure 34). The number of cells per mL was determined at 0,3,6,12,24 and 30 hours (Figure 34).

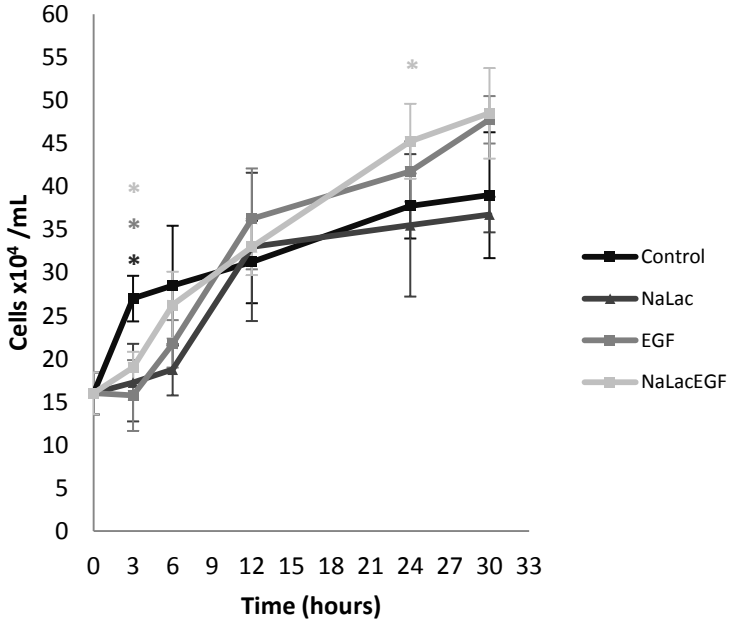


**Figure 34 - Proliferation curve for SiHa cells.** Cells were grown in control conditions, in the presence of NaLac and with EGF stimulation in the presence and absence of NaLac. Data were acquired at 0,3,6,12,24 and 30 hours after 12-16h of serum starvation and are mean ± standard deviation of four cell counts.* $p < 0.05$

After 3 hours of EGF stimulation in the presence or absence of NaLac, it was observed a statistically significant lower number of cells per mL comparing to the cell number obtained in control conditions (Figure 34). After 6 hours, the proliferation curve had the same trend but, after 12 hours, there were higher number of cells per mL in EGF-stimulated cells and also in stimulated cells grown in the presence of NaLac (Figure 34) comparing to the cell number obtained in control conditions. After 24 hours of EGF stimulation of cells in the presence of NaLac, it was seen a statistically significant higher number of cells per mL than in control conditions (Figure 34).

## 5. Discussion

Emerging evidence indicates that impaired cellular energy metabolism is the defining characteristic of nearly all cancers regardless of cellular or tissue origin (Seyfried & Shelton, 2010). Tumor cells reprogram their metabolic pathways to accomplish their higher energy demanding (Tennant et al., 2010). Recently, Porporato et al., 2011 pointed out that the shift to self-autonomous aerobic glycolysis is driven by genetic and epigenetic changes (Porporato et al., 2011). The study of metabolic alterations and adaptations of cancer cells that contribute to alter the flux along key metabolic pathways such as glycolysis and glutaminolysis must consider all the intervenients in metabolomic plateau. Several authors proposed that lactate acts as a paracrine signal in carcinogenesis by optimizing the microenvironment for tumor growth (Hussien & Brooks, 2011; Hsu & Sabatini, 2008). Additionally, lactate has been considered as a signaling molecule that could not only mirrors tumor malignancy but also enhance that (Walenta & Mueller-Klieser, 2004). As a consequence also the enzymes involved in lactate production/consumption (LDHs) and lactate transporters (MCTs) had been linked to tumor development and progression in recent reports ( Pinheiro et al., 2008; Sonveaux et al., 2008; Fang et al., 2006 Walenta & Mueller-Klieser, 2004; Lewis et al., 2000). So, the characterization of the metabolic profile of two uterine cervix cancer cell lines from two different histological types, adenocarcinoma (HeLa) and squamous cell carcinoma (SiHa), namely the role of LDHA, LDHB, LDHC, MCT1 and MCT4 in the metabolic switch verified in uterine cervix cancer was chosen as main objective of the present thesis.

In order to evaluate a potential role of EGF and NaLac in the regulation of *LDHs* and *MCTs* expression, *LDHA*, *LDHB*, (LDHC in SiHa cells), *MCT1* and *MCT4* relative gene expression were quantified for each cell line grown in the presence of NaLac with and without EGF-stimulation of cells and compared to the levels obtained for cells grown in control conditions (Figures 7 and 11).

Concerning *LDH*s expression, it was observed, for both cell lines, a statistically significant increase in *LDHA* expression levels in cells grown in the presence of NaLac and EGF-stimulated cells grown in its presence and absence comparing to cells grown in control conditions (Figures 7a and 7b). In HeLa cells grown in the presence of NaLac the observed increase at mRNA levels was reflected in LDHA protein levels assessed by western-blot (Figure 8) but not by immunofluorescence (Figure 9). EGF-stimulated HeLa cells exhibited higher *LDHA* expression and LDHA protein levels (assessed by western-blot) comparing to unstimulated cells (Figures 7a and 8) and that this increase was even higher in stimulated cells grown in the presence of NaLac only at mRNA level (Figure 7a). EGF stimulation of cells grown in the presence of NaLac seems to promote *LDHA* expression and that could be explained by c-Myc binding to *LDHA* promoter and its activation in the referred culture conditions (as discussed later).

In SiHa cells grown in the presence of NaLac and EGF-stimulated cells grown in its presence and absence the higher *LDHA* mRNA levels were not reflected in LDHA protein levels assessed through western-blot (Figure 8) and immunofluorescence (Figure 10). The absence of correlation between the level of *LDHA* mRNA and protein levels in SiHa cells could be due to diverse post-transcriptional mechanisms involved in turning mRNA into protein (as mRNA degradation) or the different *in vivo* half-lives of proteins as the result of varied protein synthesis and degradation (Greenbaum et al., 2003).

Recent data indicated that renal cell carcinoma specimens revealed a highly significant increase in the expression of *LDHA* compared to the corresponding normal kidney tissue on mRNA level (Singer et al., 2011).

The observed increase in *LDHA* expression in both HeLa and SiHa cells lines is in concordance with the analysis of the methylation pattern of *LDHA* promoter which revealed unmethylated CpG islands (Figure 17). However, previous data had revealed hypermethylation of CpG islands in the *LDHA* promoter region

leading to transcriptionally silencing of the somatic *LDHA* in R51 cells (a retinoblastoma cell line) (Maekawa et al., 2002).

Concerning *LDHB* expression, it was observed, for both cell lines, a statistically significant increase in *LDHB* expression levels in cells grown in the presence of NaLac and EGF-stimulated cells comparing to cells grown in control conditions (Figures 7a and 7b). In cells grown in the presence of NaLac, the increase was reflected in LDHB protein levels assessed by western-blot (Figure 8) and immunofluorescence (Figures 9 and 10) in both cell lines. This result is not corroborated by a previous report that demonstrated *LDHB* silencing by promoter hypermethylation in human prostate cancer (Leiblich et al., 2006). Nevertheless, the observed increase in *LDHB* expression is in concordance with the analysis of the methylation pattern of *LDHB* promoter which revealed unmethylated CpG islands (Figure 18). Other authors, however, had detected promoter methylation of *LDHB* in four gastric cancer cell lines and one pancreatic cancer cell line (Maekawa et al., 2003). Accordingly to these authors, promoter methylation of *LDHB* was observed in 3 of 20 gastric cancer tissues and in none of the corresponding healthy mucosa. Besides that, none of 25 colorectal cancer tissues and corresponding healthy mucosa had promoter methylation in *LDHB*. Therefore, the authors concluded that *LDHB* promoter was methylated in 5 of 12 cancer cell lines and in 3 of 45 cancers, suggesting that methylation of *LDHB* promoter is a relatively uncommon mechanism for the frequent increase of cathodal LDH isoenzymes in gastric and colorectal cancer patients (Maekawa et al., 2003).

However, EGF-stimulated HeLa cells grown in the presence of NaLac exhibited decreased *LDHB* expression levels comparing to cells grown in control conditions (Figure 7a) but this decrease was not reflected in LDHB protein levels assessed by western-blot (Figure 8).

Recent data revealed that *LDHA* was overexpressed in neoplastic cells and the expression of *LDHB* was downregulated (Singer et al., 2011).

In HeLa cells *LDHC* expression was not evaluated once there is data suggesting that this cell line do not express this gene (Tang & Goldberg, 2009). In SiHa cells *LDHC* expression was evaluated and it was verified that cells grown in the presence of NaLac and EGF-stimulated cells grown in its absence or presence, showed decreased levels of it comparing to cells grown in control conditions (Figure 7b), however this decrease was not reflected in LDHC protein levels assessed by and western-blot (Figure 8) and immunofluorescence (Figure 10). This absence of correlation could be due to post-translational modification of the enzyme (activation). Other authors had proposed that LDHC might be post-transcriptionally regulated by an inhibition of translation or an increase of mRNA stability through the regulation of transcript levels with non coding RNAs as microRNAs (Goldberg et al., 2010).

The expression of this human testis-specific lactate dehydrogenase has been recently reported in a broad spectrum of tumors with relatively high frequency in lung cancer, melanoma, and breast cancer, and in some prostate cancers (Tang & Goldberg, 2009; Koslowski et al., 2002). The observed decrease in *LDHC* mRNA levels could be explained by promoter hypermethylation. However, in this study, the methylation status of *LDHC* promoter was not evaluated. This hypothesis is in concordance with a previous study by Tang & Goldberg, 2009. These authors verified that *LDHC* expression in cancer cells was regulated by transcription factor Sp1 and CREB and promoter methylation (Tang & Goldberg, 2009).

Regarding *MCT*s expression, in HeLa cells was not observed a substantial difference between *MCT1* expression levels of cells grown in the presence of NaLac comparing to those grown in its absence (Figure 11a). However, it was observed a decrease in MCT1 protein levels verified by immunofluorescence analysis (Figure 12). This discrepancy between *MCT1* mRNA and protein expression is not uncommon (Kang et al., 2009). In the basis of that discrepancy could be the recognized different, and independent, mechanisms of transcriptional and translational regulation. Accordingly to Greenbaum et al., 2003 the absence of correlation

may be due to the complicated and varied post-transcriptional mechanisms involved in turning mRNA into protein and/or the fact that proteins may differ substantially in their *in vivo* stability (Greenbaum et al., 2003). Other authors had also reported little correlation between the mRNA levels and the protein expression of this monocarboxylate transporter, suggesting that post-transcriptional mechanisms may be involved in regulation of *MCT1* expression (Jackson et al., 1997).

However, EGF-stimulated HeLa cells exhibited an increase in *MCT1* expression levels (Figure 11a) comparing to cells grown in control conditions that was reflected in protein levels assessed by immunofluorescence (Figure 12). EGF-stimulated cells grown in the presence of NaLac exhibited a decrease in MCT1 expression both at mRNA (Figure 11a) and protein levels (Figure 12) comparing to those of EGF-stimulated cells.

Taking into account the lower MCT1 expression and protein levels in HeLa cells grown in the presence of NaLac and in EGF-stimulated cells grown in its presence, we proposed that NaLac regulates negatively MCT1 expression. This action could be mediated by c-Myc binding to *MCT1* promoter, with c-Myc acting, in this context, as a repressor (as described later).

SiHa cells grown in the presence of NaLac exhibited an increase in *MCT1* expression levels (Figure 11b) that was reflected in MCT1 protein levels confirmed by immunofluorescence analysis (Figure 13). Hashimoto & Brooks, 2008 had shown that lactate stimulates the overexpression of mitochondrial MCT1 (Hashimoto & Brooks, 2008). Additionally, Sonveaux et al., 2008 showed that, in SiHa cells, MCT1 is mainly responsible for lactate uptake in cells exposed to exogenous lactate (Sonveaux et al., 2008). Accordingly to these authors, SiHa cells grown in the presence of glucose and lactate switch from glucose to lactate uptake (Sonveaux et al., 2008).

Recent data reported upregulation of *MCT1* in breast cancer (Pinheiro et al., 2010) and the same observation was verified in the present thesis for SiHa cells exposed to NaLac. This result is not corroborated by a previous report pointing to a possible silencing of *MCT1* expression by gene promoter hypermethylation (Asada et al, 2003) Besides that, our analysis of the methylation pattern of this promoter had revealed that all CpG dinucleotides in the studied CpG island were unmethylated (Figure 19).

Moreover, Hussien & Brooks, 2011 had suggested that the high amount of lactate produced by cancer cells acts as a signaling molecule that increases the expression of *MCT1* and causes mitochondrial biogenesis in stroma cells surrounding tumors. This increased *MCT1* expression and oxidative capacity of stroma cells would encourage them to use lactate as their energy source and spare the glucose for the tumor cells (Hussien & Brooks, 2011). An increase of 10–15% in pyruvate and lactate uptake was seen in the cancer cell line MDA-MB-231 when transfected with plasmid containing *MCT1* gene and this uptake was accelerated at acidic pH and with an increase in lactate or pyruvate concentration in the incubation media (Garcia et al., 1994).

Also in a non tumoral context, recent data, had shown that incubation of rat muscle cell line L6 with lactate increased the expression of *MCT1* (Hussien & Brooks, 2011).

EGF stimulation of SiHa cells grown either in the presence or absence of NaLac seems do not influence *MCT1* expression both at mRNA and protein levels (Figures 11b and 13).

Concerning MCT4, it was observed that HeLa and SiHa cells grown in the presence of NaLac and EGF-stimulated cells grown in its presence and absence exhibited higher levels of *MCT4* expression comparing to cells grown in control conditions (Figures 11a and 11b) that were reflected in MCT4 protein levels assessed by western-blot, in SiHa cells, (Figure 14) and immunofluorescence analysis (Figures 12 and 13) in both cell lines. As previously referred, most cancer cells rely on high rate of aerobic glycolysis to obtain ATP in a hypoxic microenvironment (Vander Heiden et al., 2009). As a result lactate is abundantly synthesized

from pyruvate (Feron, 2009) and cancer cells increase proton efflux, in order to avoid apoptosis triggered by cellular acidosis, by upregulating, for instance, $H^+$-linked monocarboxylate transporters (Izumi et al., 2003).

Other authors had shown that MCT1, but not MCT4, was expressed at the plasma membrane of oxidative SiHa tumor cells (Sonveaux et al., 2008).

EGF plays an important role in the regulation of cell growth, proliferation and differentiation by binding to its receptor EGFR (Carpenter & Cohen, 1990). So, in the present work *EGFR* expression levels were also evaluated in both cell lines. In HeLa cells, it was observed that *EGFR* expression was lower in cells grown in the presence of NaLac with or without EGF stimulation comparing to those grown in control conditions (Figure 15a). However, EGF-stimulated cells grown in the presence of NaLac showed higher (statistically significant) levels than those grown in its absence (Figure 15a).

EGF-stimulated SiHa cells showed a statistically significant decrease in *EGFR* expression levels comparing to cells grown in control conditions (Figure 15b). However, as verified in HeLa cells, EGF-stimulated cells grown in the presence of NaLac showed higher (statistically significant) levels than those grown in its absence (Figure 15b). These results suggested that EGF stimulation of cells, by itself, do not promote *EGFR* expression. However, increased EGFR activation could result from gene amplification, protein overexpression or mutations of the EGFR (Brand et al., 2011). It has been shown that treatment of murine osteoblast cells with EGF increased the production of prostaglandin E2 (PGE2) resulting in the activation of EGFR (Narayanan et al., 2012).

Regarding chronically exposure of SiHa cells to NaLac, *LDH*s and *MCT*s gene expression seems do not be changed by a chronically exposure to NaLac comparing to an acute one (Figures 16, 7b and 11b). A statistically significant increase in *EGFR* mRNA levels were observed in SiHa cells chronically exposed to NaLac comparing the levels of those grown in the absence of it (Figure 16) while in SiHa cells exposed to NaLac (not chronically) this difference was not evident (Figure 15b).

In EGF-stimulated SiHa cells chronically exposed to NaLac, it was observed the same trend, in terms of *LDH*s and *MCT*s expression, as in EGF-stimulated cells not chronically exposed to NaLac (Figures 16, 7b and 11b). However, a statistically significant increase in *EGFR* expression levels was observed in EGF-stimulated SiHa cells chronically exposed to NaLac comparing to cells grown in control conditions (Figure 16), while in EGF-stimulated SiHa cells exposed to NaLac (not chronically) this difference was not evident (Figure 15b).

Taking into account the increase in *EGFR* mRNA levels in SiHa cells chronically exposed to NaLac and in EGF-stimulated ones grown in this conditions, and once chronically exposure to NaLac reflects better the acidic microenvironment of tumor regions, we proposed that NaLac indirectly could contribute to *EGFR* overexpression that has been reported to be frequent in uterine cervix cancer ( Shen et al., 2008; Kersemaekers et al., 1999; Hale et al., 1993), specifically in squamous cell carcinoma (Lee et al., 2004).

Once epigenetic regulation of *LDHA*, *LDHB* and *MCT1* promoters by methylation revealed that, in this setting, they are not regulated by this mechanism and EGF stimulation and/or NaLac treatment of cells did not affect the methylation status of these promoters in HeLa and SiHa cell lines, different deletion constructs were generated in order to evaluate their activity. This assay revealed that *LDHA* f2, *LDHB* f1 and *MCT1* f2 deletion construct were those with higher luciferase activity in HeLa cells (Figures 20 and 21) while in SiHa cells *LDHA* f2, *LDHB* f1 and *MCT1* f1 exhibited the highest luciferase activity (Figures 20 and 21).

Focusing on *LDHA* f2 deletion construct in HeLa cells, it was observed that its luciferase activity was higher in EGF-stimulated cells grown in the presence of NaLac than in stimulated cells grown in its absence

(Figure 20). This could be explained by the higher relative occupancy of c-Myc at this locus in cells grown in the same conditions (Figure 22). Previous data pointed out that c-Myc is able to transactivate the *LDHA* promoter and directly increase *LDHA* expression (Shim et al., 1997). So, c-Myc binding to *LDHA* promoter could explain the higher *LDHA* expression levels observed in EGF-stimulated HeLa cells grown in the presence of NaLac (Figure 7a). EGF-stimulation, by itself, of HeLa cells seems do not promote c-Myc binding to *LDHA* promoter (Figure 22), and the activity of *LDHA* f2 decrease (Figure 20), suggesting that this association is dependent of NaLac presence.

In SiHa cells occupancy of c-Myc at *LDHA* promoter was not evident and not influenced by NaLac or EGF stimulation of cells (Figure 23). However, *LDHA* f2 deletion construct exhibited higher luciferase activity in cells grown in the presence of NaLac, either EGF stimulated or not, comparing to cells grown in control conditions (Figure 20). This increment in promoter activity was reflected at *LDHA* mRNA levels (Figure 7b) but not in protein levels (as previously referred). This increase could be explained by USF binding to *LDHA* promoter region, once this construct includes USF putative binding sites. Hu et al., 2011 had shown transactivation of the LDHA gene by USFs, in oxygenated cells, implying these transcription factors as candidate drivers of aerobic glycolysis in cancer cells (Hu et al., 2011).

Regarding *MCT1* f2 deletion construct in HeLa cells, it was observed that its luciferase activity was lower in EGF-stimulated cells grown in absence of NaLac comparing to cells grown in controls conditions (Figure 21). This could be explained by the higher relative occupancy of c-Myc at this locus in cells grown in the same conditions comparing to cells grown in control conditions (Figure 22) if c-Myc acts, in this specific scenario, to decrease promoter activity. However, this decrease is not reflected at mRNA levels (Figure 11) neither at protein levels. In HeLa cells grown in the presence of NaLac this deletion construct also exhibited lower luciferase activity comparing to cells grown in control conditions (Figure 21). This could result from the higher relative occupancy of c-Myc at *MCT1* promoter locus in cells grown in the presence of NaLac comparing to cells grown in control conditions (Figure 22) if c-Myc acts, in this setting, to decrease promoter activity (act as a repressor). This decrease was reflected in MCT1 protein levels (Figure 12) (as previously referred). Previous data indicated that MCT1 protein expression appeared to be upregulated by c-Myc overexpression (Kang et al., 2009). However, Si et al., 2010 demonstrated c-Myc repression of the CCAAT/Enhancer Binding Protein δ (C/EBPδ) promoter in a Miz1 and Max-dependent manner, two c-Myc interacting proteins that are constitutively associated with C/EBPδ proximal promoter (Si et al., 2010). Other authors had shown that the activity of the minimal promoter of BRD7 (a bromodomain-containing gene identified from Nasopharyngeal carcinoma cells) was inversely related to c-Myc expression (Liu et al., 2008). Accordingly to them, c-Myc negatively regulates the promoter activity and endogenous mRNA expression of BRD7 gene (Liu et al., 2008). So, and as reviewed by McMahon, 2010, c-Myc functions not only as an activator of transcription but in some settings as a repressor (McMahon, 2010).

Regarding SiHa cells grown in control conditions, they exhibited low *MCT1* f2 deletion construct activity (Figure 21) and high relative c-Myc occupancy at this promoter (Figure 23) suggesting that, in this setting, c-Myc could act as a repressor. This observation could be validated considering the low MCT1 protein levels observed in cells grown in these conditions (Figure 13). By its turn, in the presence of NaLac, it was observed less c-Myc interaction with the MCT1 promoter region (Figure 23) which could contribute to the higher luciferase activity observed for *MCT1* f2 deletion construct in cells grown in the presence of NaLac comparing to those grown in its absence (Figure 21). This higher *MCT1* promoter activity was reflected in higher MCT1 expression and protein levels (Figures 11b and 13) comparing to those obtained in cells grown in control conditions. On the other hand, in the basis of this increased MCT1 expression could be the action of c-

Myc, in this specific setting, as an activator, as other authors had proposed (Kang et al., 2009). The elucidation of c-Myc transcriptional activator or repressive effects will result from the study of its partners.

The luciferase activity of *LDHB* deletion constructs and, consequently, *LDHB* promoter activity could not be explained by the interaction with c-Myc transcription factor since the search in TFsearch database revealed the lack of N-Myc/c-Myc putative binding sites at this promoter. In HeLa cells grown in the presence of NaLac, it was observed a slight increase in the activity of *LDHB* f1 deletion construct (Figure 20) and this was reflected at mRNA and protein levels (Figures 7a, 8 and 9). However in EGF-stimulated HeLa cells the activity of this construct was lower than in unstimulated cells (Figure 20) but their grown in the presence of NaLac promoted its increase (Figure 20). This increase was not reflected at mRNA neither at protein levels (Figures 7a and 8).

In SiHa cells grown in the presence of NaLac it was observed an increase in the activity of *LDHB* f1 deletion construct (Figure 20) that was reflected at mRNA (Figure 7b) and protein levels (Figures 8 and 10). In EGF-stimulated SiHa cells this increase was even higher (Figure 20) and was also reflected at mRNA (Figure 7b) and protein levels (Figures 8 and 10). NaLac seems to potentiate the activator effect of EGF once the activity of this promoter was even higher when EGF-stimulated cells were grown in its presence (Figure 20) and, despite of not being reflected at mRNA levels, at protein levels this was evident (Figure 8). Recent data revealed transactivation of *LDHB* gene expression by a signal transducer and activator of transcription 3 (STAT3), a key tumorigenic driver in many cancers that acts as a downstream mTOR effector in human cancer cells (Zha et al., 2011). Regarding a potential EGF-mediated activation of LDHB, previous data had shown that purified EGFR kinase phosphorylates key regulatory enzymes of the glycolytic pathway, such as phosphofructokinase and glyceraldehyde-3-phosphate dehydrogenase (GAPDH), in an EGF-dependent manner, but not LDH (Reiss et al., 1986).

Gene amplification is an important mechanism of oncogene activation and is crucial for the development and progression of cancer. The identification of frequent copy number change in certain chromosomal regions can lead to identification of functional important genes in carcinogenesis and can be used as prognostic markers (Kornegoor et al., 2012). The *c-Myc* gene has long been known to be altered by chromosomal translocations and gene amplification in human cancers (Dang et al., 2009).

In HeLa cells, it was detected genetic c-Myc amplification, being duplication the most frequently detected alteration, by FISH analysis (Figures 24a, 24b and Table 14). Four Myc gene copies would theoretically be present in nuclei in the process of DNA synthesis before mitosis, however the number of centromeric signals is reportedly unchanged throughout the cell cycle (Takahashi et al., 1998). Previous data indicated that *c-Myc* gene sequence amplification was most likely triggered by HPV 18 viral insertion at a single integration site in HeLa cells (Macville et al., 1999). Accordingly to these authors FISH localization of HPV 18 integration at the c-Myc locus in HeLa cells is common and representative for advanced stage cervical cell carcinomas (Macville et al., 1999). *c-Myc* gene amplification has been identified as one of the critical early events in the progression of uterine cervical lesion (Aoyama et al., 1998). However, other authors concluded that there was no significant difference in *c-Myc* gene amplification in samples with some type of CIN or cancer compared to those from normal cytology, only a slight gain of 12% for cancer samples when compared with samples from patients with a normal cytology result (García et al., 2011).

Considering FISH analysis it was possible to conclude that, in SiHa cells, aneuploidy is in the basis of increased number of c-Myc copies (Figures 24c, 24d and Table 14). Previous data reported that numerical abnormalities involving chromosome 8, in which c-Myc is located, have been suggested as a mechanism accounting for the increased c-Myc copy number (Takahashi et al., 1998).

Additionally, FISH results obtained for SiHa cells (Figure 24c,24d and Table14 and tableA1, Appendix II) were in concordance with previous data that showed, also through FISH, that the distribution of c-Myc copy number ranged from 3 to 5 copies in SiHa cells (Harris et al., 2003).

The c-Myc oncogene seems to be fundamental in the carcinogenesis process. Thus, the increase of the number of alleles of the proto-oncogene c-Myc is directly related to the degree of aggressiveness of the tumor, considering that the more copies of it there are, the higher level of its expression (Calcagno et al., 2005).

Given the results of c-Myc analysis by FISH and the existence of previous reports indicating an association between c-Myc amplification and malignant phenotypes (Hale et al., 1993; Pfeiffer et al., 1989) tissue microarrays of AC and SCC of the uterine cervix cases were analyzed through c-Myc/Chromosome 8 FISH. Besides that, considering the previously referred MCT1 overexpression detected in uterine cervix cancer (Pinheiro et al., 2009) and the proposed c-Myc regulation of MCT1 expression, these tissue microarrays were also analyzed by immunohistochemistry for MCT1.

MCT1 immunohistochemistry analysis revealed important differences between normal ectocervix (Figure 28) and normal endocervix (Figure 29), in terms of MCT1 immunodetection. It was verified that normal ectocervix samples were mainly positive for MCT1 while normal endocervix ones were mainly negative. These observations pointed out the crucial role of microenvironment on gene expression regulation. The squamous epithelium of the ectocervix is nearer to the lactate-enriched microenvironment and this seems to have important consequences at the regulation of MCT1 expression, increasing it. By its turn, the glandular endocervical epithelium is distant from the lactate-enriched microenvironment what could contribute to the decreased MCT1 expression.

Additionally, the analysis of tissue microarrays of AC and SCC of the uterine cervix cases revealed that, concerning AC cases, only two were positive for MCT1 and are diploid (normal) for c-Myc (Figures 25,26 and 27). Regarding SCC cases, it seems that the increase in c-Myc copy number is associated with increase in MCT1 immunodetection despite of the detection of c-Myc diploid (normal) cases expressing MCT1 with several intensity Figures 28 and 29). Accordingly to Policht et al., 2010, in SCC, c-Myc positivity rate (that is c-Myc gain) was 100% (Polichet et al., 2010). Additionally, it has been revealed that MCT1 protein expression appeared to be upregulated by c-Myc overexpression (Kang et al., 2009).

Comparing to AC cases, SCC cases revealed higher, and with different intensities, MCT1 immunodetection what is not in concordance with a previous study by Pinheiro et al., 2009. These authors had described that MCT1 was not differentially expressed among the three histological types of uterine cervix cancer studied (SCC, AC and adenosquamous carcinoma) (Pinheiro et al., 2009).

The analysis of SCC cases by FISH had shown that, in terms of c-Myc altered copy number, aneuploidy (22.7%) was the most frequently detected as shown in FISH analysis of SiHa cells. FISH analysis of AC cases revealed aneuploidy (2 cases in a total of 14 AC cases) in c-Myc copy number while the same analysis performed in HeLa cells did not revealed it.

AC and SCC microenvironment is quite different and this could explain the differences obtained, in terms of MCT1 expression, in both types of uterine cervix cancer. It has been described that high lactate concentration is one of the defining characteristics of the physiological microenvironment of locally advanced squamous cell carcinomas of the uterine cervix (Schwickert et al., 1995).

Integrating the results from MCT1 immunodetection in SCC and those obtained for MCT1 expression in SiHa cells (obtained from squamous cell carcinoma) the lactate-enriched microenvironment where SCC develops seems to contribute to the upregulation of MCT1. These observations suggest that tumor microenvironment can play a role in cancer cells selection and tumor progression. In the oxidative context

where SCC cancer cells develop, the upregulation of MCT1 confer crucial advantages to these cells, given its importance in lactate uptake. Additionally, this upregulation could be in the basis of a switch from glucose to lactate consumption in SCC tumors as described in SiHa cells (previously referred). The crucial role of tumor microenvironment had also been pointed out in a report by Sonveaux et al., 2008, where the authors revealed that microenvironmental influences can stimulate MCT1-mediated lactate consumption, which is otherwise nonexistent *in vitro* (Sonveaux et al., 2008).

In HeLa cells (obtained from adenocarcinoma) we proposed that MCT1 expression could be negatively regulated by c-Myc in cells grown in the presence of NaLac. However, considering AC cases analysis, and due to the low lactate concentration found in the microenvironment where this type of tumor develop, our observation cannot be transposed to this scenario. In AC cases, the low lactate levels, seems promote MCT1 downregulation. Or we can think in a different way: the low lactate levels presented in the microenvironment where this type of tumor develops select tumor cells expressing low MCT1 given their lower requirement of lactate uptake, comparing to SCC tumor cells.

Metastatic spread of malignant cells via migration and invasion to distant area such as pelvic lymph node is the primary cause of treatment failure and subsequent death in uterine cervix cancer patients (Chiang et al., 2008). So, in the present thesis it was also evaluated SiHa cell migration in different culture conditions.

The study of SiHa cell migration, assessed by *in vitro* Wound Healing assay (Figures 31 and 32) revealed higher cell migration rate in cells grown in the presence of NaLac comparing to cells grown in its absence (Figures 31 and 32). This is in concordance with previous data that had shown a link between lactate accumulation in tumors and enhancement of tumor cell migration (Walenta & Mueller-Klieser, 2004). Besides that, data from Bonuccelli et al., 2010 evidenced that L-lactate functioned as chemo-attractant, stimulating the migration of epithelial cancer cells, in transwell assay So, accordingly to these authors, the metabolic products of aerobic glycolysis can function as chemo-attractant for cancer cells, probably via a form of nutrient sensing (Bonuccelli et al., 2010). Additionally, Végran et al., 2011 found that lactate could enter endothelial cells through MCT1, trigger the phosphorylation/degradation of IkBα, and then stimulate an autocrine NF-kB/IL-8 (CXCL8) pathway driving cell migration and tube formation (Végran et al., 2011).

Wound healing *in vitro* assay also revealed that EGF stimulation of SiHa cells grown in the presence of NaLac seems to promote cell migration (Figures 31 and 32). This result is in concordance with previous results from Shen et al., 2006 that had shown that EGF is a potent stimulator of uterine cervix cancer cell lines (SiHa and CaSki) migration and invasiveness (Shen et al., 2006). Moreover, in a non tumoral context, Zhuang et al., 2004 had proposed that EGFR mediates RPTC migration following injury and in response to EGF (Zhuang et al., 2004).

Some mechanisms that could be in the basis of the EGF-mediated uterine cervix cancer cells migration had been proposed. Chiang et al., 2008 revealed that uterine cervical cancer cells benefit some enhanced cellular functions from $Na^+/H^+$ exchanger 1 (NHE1) abundance, such as cell volume regulation, migration, and invasion (Chiang et al., 2008). These authors had shown colocalization of NHE1 with EGF in uterine cervical cancer tissues (Chiang et al., 2008). Besides that, studies in cell culture systems indicated that EGF upregulates NHE1 abundance in a time-dependent manner by post-translational regulation (Chiang et al., 2008). So, accordingly to these authors, NHE1 activity is necessary for EGF-mediated cancer cell migration and invasiveness (Chiang et al., 2008).

Additionally, EGF plays an important role in the regulation of cell growth and proliferation (Carpenter & Cohen, 1990). It is known that EGF is a mitogen for estrogen receptor (ER). It has been recently proven that this growth factor occasionally mimics estrogen action and cross-talk with ER-α to exert its activity (Narayanan et al., 2012).

Previous data had indicated that the malignant transformation of the SCC of the uterine cervix is associated with several molecular events, including cell cycle aberration (Clarke & Chetty, 2001). So, SiHa cell cycle analysis was performed trying to establish a potential role of NaLac and/or EGF on cell cycle regulation.

Cell cycle analysis of SiHa cells revealed that the majority of the cells were in G1 phase despite of culture conditions (Figure 33) of these cells. This could be result from deficient synchronization of cells. Other authors also promote cell synchronization by serum starvation however, for a period of 48 hours (Nicolas et al., 2003). Another study suggests serum starvation for two days followed by a treatment with 5 μM aphidicolin for 16 hours for chemical synchronization of SiHa cells (Shen et al., 2000).

Besides that, it was observed a statistically significant increase in the percentage of cells in G1 phase after 6 hours in EGF-stimulated cells comparing to cells grown in control conditions and a statistically significant decrease in the percentage of cells in S and G2/M phases (Figure 33). The decrease in the percentage of cell in the S phase indicates a decrease in the rate of DNA synthesis indicating cell cycle arrest. The same tendency was verified in EGF-stimulated cells grown in the presence of NaLac, after 6 hours (Figure 33). However, after 24 hours it was seen a statistically significant decrease in the percentage of cells in G1 phase and an increase in those in S phase and G2/M (not statistically significant) in cells stimulated with EGF and grown in the presence of NaLac comparing to cells grown in control conditions (Figure 33). Besides that, at this time point, it was observed a statistically significant increase in the percentage of cells in S phase in cells stimulated with EGF comparing to cells grown in control conditions (Figure 33). This data suggests that EGF-stimulated cells undergo an increase in the rate of DNA synthesis (as indicated by the increase in the percentage of cells in the S phase) leading to cell cycle progression. This observation is in concordance with recent data in HeLa cells (Narayanan et al., 2012).

Accordingly to Narayanan et al, 2012, an exogenous EGF stimulation may enhance HPV-related uterine cervical cancer cell proliferation by activating EGFR and cyclin D1 that is independent of COX-2 levels (Narayanan et al., 2012). Previous data, in a human prostate cancer cell line, also showed that EGF induces cyclin D1, a protein required for cell cycle progression from G1 (Perry et al., 1998).

Considering cell cycle analysis data, and in order to evaluate SiHa cell proliferation in the various culture conditions, a proliferation curve was performed (Figure 34). This assay revealed that after 24 hours of EGF stimulation in the presence of NaLac it was seen a statistically significant higher number of cells per mL comparing to the cell number obtained in control conditions (Figure 34). Through this analysis it was possible to suggest that EGF promotes cellular proliferation which is in accordance with cell cycle progression previously referred.

So, in SiHa cells EGF stimulation of cells grown in the presence of NaLac seems to promote cell migration and cell cycle progression and proliferation. In SiHa cells, the identification of increased c-Myc copy number (as result of aneuploidy) and given the important role of c-Myc in, not only, the regulation of cell metabolism but also the induction of cell proliferation, this phenotype could be mediated by this crucial oncogene. Other authors proposed that c-Myc acts pleiotropically to transform cells by upregulating components of the cell cycle machinery such as CDC25A (Galaktionov et al., 1996), stimulating the production of biosynthetic enzymes such as ornithine decarboxylase (Bello-Fernandez et al., 1993) to prepare cells for S-phase entry, and activating the expression of metabolic enzymes such as LDHA to ensure an adequate supply of energy or signals for cell proliferation (Shim et al., 1997). However, we proposed that c-Myc role in inducing cell proliferation and migration could be, in this context, via MCT1. This could be supported by previous data suggesting that MCT1 have an important role in tumor progression since it was shown that inhibition of *MCT1*, either pharmacologically or using RNA interference (RNAi), results in the inhibition of xenograft tumor growth

(Tennant et al., 2010; Sonveaux et al., 2008) and also by the recent observation that high expression of both *MCT1* and *MCT4* correlates with the invasiveness of lung cancer cells (Izumi et al., 2011).

While some early reports on c-Myc targets suggested that individual genes might be critical to mediate c-Myc's ability to transform cells, our results are in concordance with more recent models assuming that it is the combinatorial effect on different c-Myc target genes and their products that control cell transformation. So, the knowledge about the potent role of c-Myc in tumorigenesis but also as a regulator of many cellular processes, including basic aspects of metabolism, cell cycle control, differentiation, and apoptosis, suggests that this oncoprotein must be precisely and decisively regulated (Lüscher, 2012).

Taking into consideration all the results obtained during this experimental work, it is important to underline the crucial role of NaLac either in association with EGF or not in the regulation of critical steps of central metabolic pathways essential to cell survival, maintenance and proliferation. Our data pointed out the necessity of consider all intervenients in the metabolomic plateau in the study of cancer metabolism and our study aim to illustrate the several metabolic alterations and adaptations of tumor cells that can contribute, ultimately to the establishment of new therapeutic targets.

## 6. Future perspectives

In order to better understand c-Myc regulation of *LDHA* and *MCT1* expression, as future perspectives, it would be important to generate mutated promoter constructs, by site mutation, abolishing c-Myc binding to this region and evaluate promoter activity. It would be also important to clarify the context of gene expression regulation by c-Myc, namely through the identification of its partners in the different conditions, given its dual role in gene expression regulation.

Besides that, the evaluation of *LDHB* expression regulation by STAT3, either in the presence and absence of NaLac and EGF stimulation, would contribute to validate the proposed role of this transcription factor on that regulation.

It would be also important to generate MCT4 deletion constructs and perform chIP analysis for c-Myc in order to assess if this transcription factor could be in the basis of MCT4 upregulation in cells grown in the presence of NaLac.

Additionally, the establishment of *in vivo* models namely to perform the inhibition of MCT1 and to evaluate the consequences for tumor growth constitutes an important future approach.

## 7. Conclusions

Emerging evidence indicates that impaired cellular energy metabolism is the defining characteristic of nearly all cancers regardless their cellular or tissue origin. Frequently, tumor cells have a remarkably different metabolism from that of the tissues from which they are derived. Although NaLac is generally considered a waste product, several studies show that it is a prominent substrate that fuels the oxidative metabolism of some oxygenated tumor cells. In uterine cervix, mainly ectocervix, the NaLac rich microenvironment may play a role in cancer cells selection due to their ability of consuming lactate as carbon and energy source. The study of the enzymes involved in lactate production (LDHA) and consumption (LDHB), as well as its transporters (MCTs), will help to define new therapeutic targets.

Our findings suggested c-Myc activation of *LDHA* expression in HeLa cells grown in the presence of NaLac and gene amplification of c-Myc in this cell line. Regarding SiHa cells it was observed LDHA upregulation, at mRNA level, by NaLac however, not c-Myc-mediated.

Additionally, our data indicated that, in both cell lines, NaLac promotes LDHB expression. In SiHa cells EGF stimulation also promotes LDHB expression, being this activator effect increased by NaLac presence. We proposed NaLac-mediated c-Myc repression of *MCT1* expression in HeLa cells. In SiHa cells we suggested that in the presence of NaLac there is a decrease in c-Myc interaction with MCT1 promoter region (as a repressor), promoting MCT1 expression, or an alternative role of c-Myc as an activator of MCT1 gene expression in this context. The elucidation of c-Myc transcriptional activator or repressive effects will result from the study of its partners.

The data from SCC and SC cases pointed out the crucial role of tumor microenvironment in tumor cells selection. In the oxidative context where SCC cancer cells develop, the upregulation of MCT1 confer crucial advantages to these cells, given its importance in lactate uptake. Additionally, this upregulation could be in the basis of a switch from glucose to lactate consumption in SCC tumors as described in SiHa cells. In AC cases, the low lactate levels, seems to promote MCT1 downregulation, or, by another hand, select tumor cells expressing low MCT1 given their lower requirement of lactate uptake, comparing to SCC tumor cells.

Finally, considering all the results obtained during this experimental work, it is important to underline the crucial role of NaLac either in association with EGF or not in the regulation of critical steps of central metabolic pathways essential to cell survival, maintenance and proliferation.

Summing up, we observed that NaLac, EGF and c-Myc regulate the expression of MCT1 in both HeLa and SiHa cells. *In vitro*, c-Myc plays a role in MCT1 expression both as activator and as repressor, depending on culture conditions and on cytogenetic alterations. In tissue arrays, we also observed in SSC a trend between the number of chromosome 8 and the expression of MCT1, in 23 cases with cytogenetic alterations, 17 (74%) are positive for MCT1. In SCC, MCT1 can be a suitable therapeutic target, since it is expressed in the majority of cases and, as we observed *in vitro*, there is a trend between the expression of MCT1 and the proliferation rate of cells.

Schematic representations of *LDHA*, *LDHB*, *MCT1* and *MCT4* gene expression regulation in HeLa and SiHa cells are presented in figure 35 and 36, respectively.

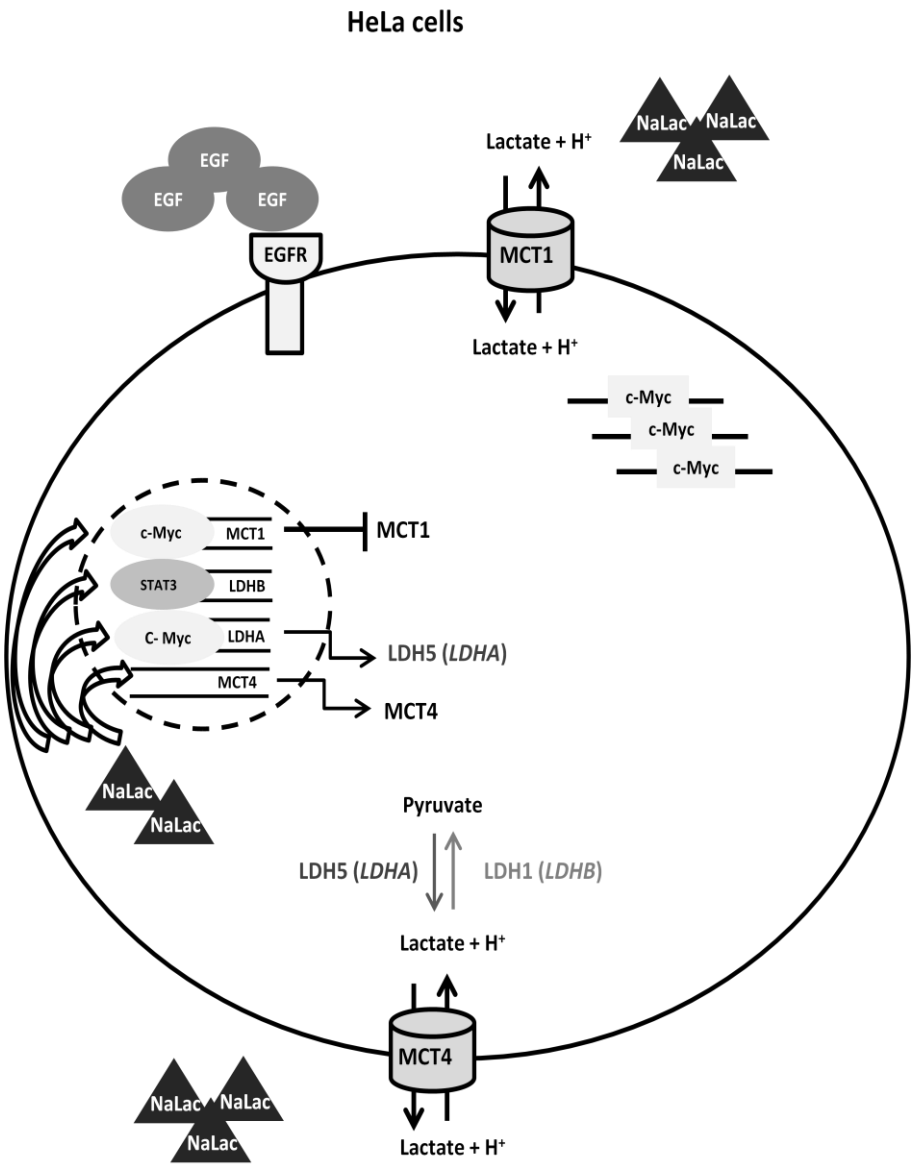


**Figure 35 - Schematic representation of *LDHA*, *LDHB*, *MCT1* and *MCT4* gene expression regulation in HeLa cells.** In HeLa cells it was detected c-Myc genetic amplification. *MCT1* expression is negatively regulated by c-Myc in cells grown in the presence of NaLac. *LDHA* expression is activated by c-Myc interaction with *LDHA* promoter in cells grown in the presence of NaLac. NaLac also promotes *MCT4* expression. Both NaLac and EGF promote *LDHB* gene expression that could be regulated by STAT3.

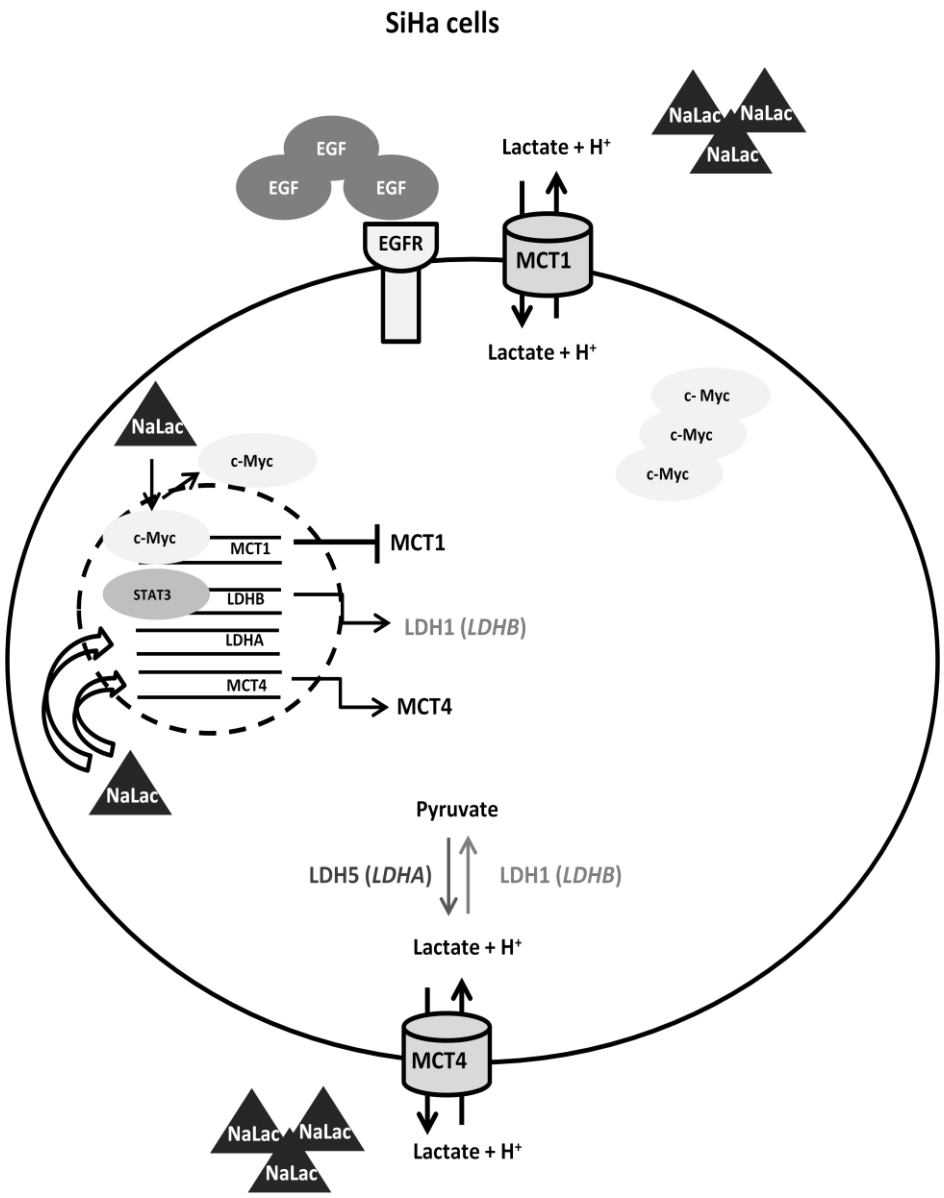


**Figure 36 - Schematic representation of *LDHA*, *LDHB*, *MCT1* and *MCT4* gene expression regulation in SiHa cells.** SiHa cells are aneusomic (more than 2 copies) for chromosome 8, where c-Myc is located. c-Myc regulates negatively *MCT1* expression in the absence of NaLac and this effect is reverted in the presence of NaLac. NaLac promotes *LDHA* upregulation, at mRNA level, in a non-c-Myc mediated manner. EGF stimulation of cells promotes *LDHB* expression, being this activator effect increased by NaLac presence, and possibly mediated by STAT3. NaLac also promotes *MCT4* expression.

## 8. Bibliographic references


Asada K, Miyamoto K, Fukutomi T, Tsuda H, Yagi Y, Wakazono K, Oishi S, Fukui H, Sugimura T& Ushijima T. 2003. Reduced expression of GNA11 and silencing of MCT1 in human breast cancers. *Oncology* 64:380-388.

Airley RE & Mobasheri A. 2007. Hypoxic regulation of glucose transport, anaerobic metabolism and angiogenesis in cancer: novel pathways and targets for anticancer therapeutics. *Chemotherapy* 53:233-256.

Anido J, Matar P, Albanell J, Guzmán M, Rojo F, Arribas J, Averbuch S & Baselga J. 2003. ZD1839 , a Specific Epidermal Growth Factor Receptor ( EGFR ) Tyrosine Kinase Inhibitor , Induces the Formation of Inactive EGFR / HER2 and EGFR / HER3 Heterodimers and Prevents Heregulin Signaling in HER2-overexpressing Breast Cancer Cells. *Clin Cancer Res* 9:1274-1283.

Aoyama C, Peters J, Senadheera S, Liu P & Shimada H. 1998. Uterine cervical dysplasia and cancer: identification of c-myc status by quantitative polymerase chain reaction. *Diagn Mol Pathol* 7:324-330.

Atsumi T, Chesney J, Metz C, Cancers H, Leng L, Donnelly S, Makita Z, Mitchell R &Bucala R. 2002. High Expression of Inducible 6-Phosphofructo-2-Kinase/Frutose-2,6-Bisphosphatase ( iPFK-2; PFKFB3 ) in Human Cancers. *Cancer Res* 62:5881-5887.

Bachman KE, Park BH, Rhee I, Rajagopalan H, Herman JG, Baylin SB, Kinzler KW & Vogelstein B. 2003. Histone modifications and silencing prior to DNA methylation of a tumor suppressor gene. *Cancer Cell* 3:89-95.

Baylin SB & Ohm JE. 2006. Epigenetic gene silencing in cancer - a mechanism for early oncogenic pathway addiction? *Nat Rev Cancer* 6:107-116.

Bello-Fernandez C, Packham G & Cleveland JL. 1993. The ornithine decarboxylase gene is a transcriptional target of c-Myc. *Proc Natl Acad Sci USA* 90:7804-7808.

Boidot R, Végran F, Meulle A, Le Breton A, Dessy C, Sonveaux P, Lizard-Nacol S & Feron O. 2012. Regulation of monocarboxylate transporter MCT1 expression by p53 mediates inward and outward lactate fluxes in tumors. *Cancer Res* 72:939-948.

Bonuccelli G, Tsirigos A, Whitaker-Menezes D, Pavlides S, Pestell RG, Chiavarina B, Frank PG, Flomenberg N, Howell A, Martinez-Outschoorn UE, Sotgia F & Lisanti MP. 2010. Ketones and lactate "fuel" tumor growth and metastasis: Evidence that epithelial cancer cells use oxidative mitochondrial metabolism. *Cell Cycle* 9:3506-3514.

Boulet GA, Horvath CA, Berghmans S & Bogers J. 2008. Human papillomavirus in cervical cancer screening: important role as biomarker. *Cancer Epidemiol, Biomarkers Prev* 17:810-817.

Bourhis J, Le MG, Barrois M, Gerbaulet A, Jeannel D, Duvillard P, Le Doussal V, Chassagne D & Riou G. 1990. Prognostic value of c-myc proto-oncogene overexpression in early invasive carcinoma of the cervix. *J Clin Oncol* 8:1789-1796.

Brand KA & Hermfisse U. 1997. Aerobic glycolysis by proliferating cells: a protective strategy against reactive oxygen species. *The FASEB j* 11:388-395.

Brand TM, Iida M & Wheeler DL. 2011. Molecular mechanisms of resistance to the EGFR monoclonal antibody cetuximab. *Cancer Biol Ther* 11:777-792.

Braun CA & Anderson CM. 2007. Pathophysiology: Functional Alterations in Human Health. Lippincott Williams & Wilkins, USA

Brezinski ME. 2006. Optical Coherence Tomography: Principles and Applications. Academic Press, USA.

Brooks GA. 2000. Intra- and extra-cellular lactate shuttles. *Med Sci Sports Exerc* 32:790-799.

Brychtová S, Brychta T, Sedláková E & Kolár Z. 2004. Proto-oncogene c-myc in uterine cervix carcinogenesis. *Neoplasma* 51:84-89.

Burghardt E & Ostör AG. 1983. Site and origin of squamous cervical cancer: a histomorphologic study. *Obstet Gynecol* 62:117-127.

Bustin SA. 2000. Absolute quantification of mRNA using real-time reverse transcription polymerase chain reaction assays. *J Mol Endocrinol* 25:169-193.

Cairns RA, Harris IS & Mak TW. 2011. Regulation of cancer cell metabolism. *Nat Rev Cancer* 11:85-95.

Calcagno DQ, Leal MF, Taken SS, Assumpção PP, Demachki S, Smith M de AC & Burbano RR. 2005. Aneuploidy of chromosome 8 and C-MYC amplification in individuals from northern Brazil with gastric adenocarcinoma. *Anticancer Res* 25:4069-4074.

Carpenter G & Cohen S. 1990. Epidermal Growth Factor. *J Biol Chem* 265:7709-7712.

Cecchini MJ, Amiri M & Dick FA. 2012. Analysis of cell cycle position in mammalian cells. *J Vis Exp* 59:1-8.

Chan PG, Sung H-Y & Sawaya GF. 2003. Changes in cervical cancer incidence after three decades of screening US women less than 30 years old. *Obstet Gynecol* 102:765-773.

Chan S-Y, Delius H, Halpern AL & Bernard H-U. 1995. Analysis of genomic sequences of 95 papillomavirus types: uniting typing, phylogeny, and taxonomy. *J Virol* 69:3074-3083.

Chen S, Yang Z, Zhang Y, Qiao Y, Cui B, Zhang Y & Kong B. 2012. Genomic amplification patterns of human telomerase RNA gene and C-MYC in liquid-based cytological specimens used for the detection of high-grade cervical intraepithelial neoplasia. *Diagn Pathol* 7:40.

Chen Y, Zhang H, Xu A, Li N, Liu J, Liu C, Lv D, Wu S, Huang L, Yang S, He D & Xiao X. 2006. Elevation of serum l-lactate dehydrogenase B correlated with the clinical stage of lung cancer. *Lung cancer* 54:95-102.

Chiang Y, Chou C-Y, Hsu K-F, Huang Y-F & Shen M-R. 2008. EGF upregulates Na+/H+ exchanger NHE1 by post-translational regulation that is important for cervical cancer cell invasiveness. *J Cell Physiol* 214:810-819.

Chiche J, Le Fur Y, Vilmen C, Frassineti F, Daniel L, Halestrap AP, Cozzone PJ, Pouysségur J & Lutz NW. 2012. In vivo pH in metabolic-defective Ras-transformed fibroblast tumors: key role of the monocarboxylate transporter, MCT4, for inducing an alkaline intracellular pH. *Int J Cancer* 130:1511-1520.

Clarke B & Chetty R. 2001. Cell cycle aberrations in the pathogenesis of squamous cell carcinoma of the uterine cervix. *Gynecol Oncol* 82:238-246.

Clifford GM, Smith JS, Plummer M, Muñoz N & Franceschi S. 2003. Human papillomavirus types in invasive cervical cancer worldwide: a meta-analysis. *Br J Cancer* 88:63-73.

Collas P. 2010. The Current State of Chromatin Immunoprecipitation. *Mol Biotechnol* 45:87-100.

Dang CV & Semenza GL. 1999. Oncogenic alterations of metabolism. *Trends Biochem Sci* 24:68-72.

Dang CV, Kim J-whan, Gao P & Yustein J. 2008. The interplay between MYC and HIF in cancer. *Nat Rev Cancer* 8:51-56.

Dang CV, Le A & Gao P. 2009. MYC-Induced Cancer Cell Energy Metabolism and Therapeutic Opportunities. *Clin Cancer Res* 15:6479-6483.

Das PM, Ramachandran K, VanWert J & Singal R. 2004. Chromatin immunoprecipitation assay. *Biotechniques* 37:961-969.

de Villiers E-M, Fauquet C, Broker TR, Bernard HU & zur Hausen H. 2004. Classification of papillomaviruses. *Virology* 324:17-27.

DeBerardinis RJ, Lum JJ, Hatzivassiliou G & Thompson CB. 2008. The biology of cancer: metabolic reprogramming fuels cell growth and proliferation. *Cell Metab* 7:11-20.

Denko NC. 2008. Hypoxia, HIF1 and glucose metabolism in the solid tumour. *Nat Rev Cancer* 8:705-713.

Dimmer KS, Friedrich B, Lang F, Deitmer JW & Bröer S. 2000. The low-affinity monocarboxylate transporter MCT4 is adapted to the export of lactate in highly glycolytic cells. *Biochem J* **350 Pt 1**:219-227.

Draoui N & Feron O. 2011. Lactate shuttles at a glance: from physiological paradigms to anti-cancer treatments. *Dis Model Mech* 4:727-732.

Duensing S & Munger K. 2004. Mechanisms of genomic instability in human cancer: insights from studies with human papillomavirus oncoproteins. *Int J Cancer* 109:157-162.

Ehrich M, Zoll S, Sur S & van den Boom D. 2007. A new method for accurate assessment of DNA quality after bisulfite treatment. *Nucleic Acids Res* 35:e29.

Fahrner JA, Eguchi S, Herman JG & Baylin SB. 2002. Dependence of Histone Modifications and Gene Expression on DNA Hypermethylation in Cancer. *Cancer Res* 62:7213-7218.

Fais S, De Milito A, You H & Qin W. 2007. Targeting vacuolar H+-ATPases as a new strategy against cancer. *Cancer Res* 67:10627-10630.

Fang J, Quinones QJ, Holman TL, Morowitz MJ, Wang Q, Zhao H, Sivo F, Maris JM & Wahl ML. 2006. The H+ -Linked Monocarboxylate Transporter ( MCT1 / SLC16A1 ): A Potential Therapeutic Target for High-Risk Neuroblastoma. *Mol Pharmacol* 70:2108-2115.

Fantin VR, St-Pierre J & Leder P. 2006. Attenuation of LDH-A expression uncovers a link between glycolysis, mitochondrial physiology, and tumor maintenance. *Cancer cell* 9:425-434.

Ferlay J, Shin H-R, Bray F, Forman D, Mathers C & Parkin DM. 2010. Estimates of worldwide burden of cancer in 2008: GLOBOCAN 2008. *Int J Cancer* 127:2893-2917.

Feron O. 2009. Pyruvate into lactate and back: from the Warburg effect to symbiotic energy fuel exchange in cancer cells. *Radiother Oncol* 92:329-333.

Feron O. 2010. Challenges in pharmacology of anti-cancer drugs - the search for addictions. *Front Pharmacol* 1:120.

Fiume L, Vettraino M, Manerba M & Di Stefano G. 2011. Inhibition of lactic dehydrogenase as a way to increase the anti-proliferative effect of multi-targeted kinase inhibitors. *Pharmacol Res* 63:328-334.

Frezza C & Gottlieb E. 2009. Mitochondria in cancer: not just innocent bystanders. *Semin Cancer Biol* 19:4-11.

Fukumura D, Xu L, Chen Y, Gohongi T, Seed B & Jain RK. 2001. Hypoxia and Acidosis Independently Up-Regulate Vascular Endothelial Growth Factor Transcription in Brain Tumors in Vivo. *Cancer Res* 61:6020-6024.

Galaktionov K, Chen X & Beach D. 1996. Cdc25 cell-cycle phosphatase as a target of c-myc. *Nature* 382:511-517.

Gambhir SS. 2002. Molecular imaging of cancer with positron emission tomography. *Nat Rev Cancer* 2:683-693.

Garcia CK, Brown MS, Pathak RK & Goldstein JL. 1995. cDNA cloning of MCT2, a Second Monocarboxylate Transporter Expressed in Different Cells than MCT1. *J Biol Chem* 270:1843-1849.

Garcia CK, Goldstein JL, Pathak RK, Anderson RG & Brown MS. 1994. Molecular characterization of a membrane transporter for lactate, pyruvate, and other monocarboxylates: implications for the Cori cycle. *Cell* 76:865-873.

García DA, Briceño I, Castillo M & Aristizábal FA. 2011. Detection of gene amplification in MYCN, C-MYC, MYCL1, ERBB2, EGFR, AKT2, and human papilloma virus in samples from cervical smear normal cytology, intraepithelial cervical neoplasia. *Colomb Med* 42:144-153.

Gatenby RA & Gillies RJ. 2004. Why do cancers have high aerobic glycolysis? *Nat Rev Cancer* 4:891-899.

Gillies RJ, Robey I & Gatenby RA. 2008. Causes and consequences of increased glucose metabolism of cancers. *J Nucl Med* 49:24S-42S.

Globocan.2008.Cancer Incidence, Mortality and Prevalence Worldwide in 2008. http://globocan.iarc.fr/ consulted in August 2012.

Goldberg E, Eddy E, Duan C & Odet F. 2010. LDHC: the ultimate testis-specific gene. *J Androl* **31**:86-94.

Grandori C, Cowley SM, James LP & Robert EN. 2000. The Myc/Max/Mad network and the transcriptional control of cell behavior. *Annu Rev Cell Dev Biol* 16:653-699.

Graves JA, Rothermund K, Wang T, Qian W, Van Houten B & Prochownik EV. 2010. Point mutations in c-Myc uncouple neoplastic transformation from multiple other phenotypes in rat fibroblasts. *PloS one* 5:e13717.

Greenbaum D, Colangelo C, Williams K & Gerstein M. 2003. Comparing protein abundance and mRNA expression levels on a genomic scale. *Genome Biol* 4:117.

Gubern C, Hurtado O, Rodríguez R, Morales JR, Romera VG, Moro MA, Lizasoain I, Serena J & Mallolas J. 2009. Validation of housekeeping genes for quantitative real-time PCR in in-vivo and in-vitro models of cerebral ischaemia. *BMC Mol Biol* 10:57.

Gupta S. 2011. A Comprehensive Textbook of Obstetrics and Gynecology. First ed. Jaypee Brothers Medical Publishers Ltd, India

Haas TD, Hasselt N, Troost D, Caron H, Popovic M, Zadravec-zaletel L, Grajkowska W, Perek M, Osterheld MC, Ellison D, Baas F, Versteeg R & Kool M. 2008. Molecular Risk Stratification of Medulloblastoma Patients Based on Immunohistochemical Analysis of MYC , LDHB , and CCNB1 Expression. *Clin Cancer Res* 14:4154-4160.

Hale RJ, Buckley CH, Gullick WJ, Fox H, Williams J & Wilcox FL. 1993. Prognostic value of epidermal growth factor receptor expression in cervical carcinoma. *J Clin Pathol* 46:149-153.

Halestrap AP & Meredith D. 2004. The SLC16 gene family-from monocarboxylate transporters (MCTs) to aromatic amino acid transporters and beyond. *Pflügers Arch* 447:619-628.

Halestrap AP & Price NT. 1999. The proton-linked monocarboxylate transporter (MCT) family: structure, function and regulation. *Biochem J* 343:281-299.

Hanahan D & Weinberg RA. 2000. The Hallmarks of Cancer. *Cell* 100:57-70.

Hanahan D & Weinberg RA. 2011. Hallmarks of Cancer: The Next Generation. *Cell* 144:646-674.

Harris CP, Lu XY, Narayan G, Singh B, Murty VVVS & Rao PH. 2003. Comprehensive molecular cytogenetic characterization of cervical cancer cell lines. *Genes, chromosomes Cancer* 36:233-241.

Hashimoto T & Brooks GA. 2008. Mitochondrial lactate oxidation complex and an adaptive role for lactate production. *Med Sci Sports Exerc* 40:486-494.

Hashimoto T, Hussien R & Brooks GA. 2006. Colocalization of MCT1, CD147, and LDH in mitochondrial inner membrane of L6 muscle cells: evidence of a mitochondrial lactate oxidation complex. *Am J Physiol Endocrinol Metab* 290:E1237-E1244.

Hashimoto T, Hussien R, Oommen S, Gohil K & Brooks GA. 2007. Lactate sensitive transcription factor network in L6 cells: activation of MCT1 and mitochondrial biogenesis. *FASEB J* 21:2602-2612.

zur Hausen H. 2002. Papillomaviruses and cancer: from basic studies to clinical application. *Nat Rev Cancer* 2:342-350.

Havens CS & Sullivan ND. 2002. Manual of Outpatient Gynecology. Fourth ed. Lippincott Williams & Wilkins, USA

Hebner CM & Laimins LA. 2006. Human papillomaviruses: basic mechanisms of pathogenesis and oncogenicity. *Rev Med Virol* 16:83-97.

Helmlinger G, Sckell A, Dellian M, Forbes NS & Jain RK. 2002. Acid Production in Glycolysis-impaired Tumors Provides New Insights into Tumor Metabolism. *Clin Cancer Res* 8:1284-1291.

Herfs M, Yamamoto Y, Laury A, Wang X, Nucci MR, McLaughlin-Drubin ME, Münger K, Feldman S, McKeon FD, Xian W & Crum CP. 2012. A discrete population of squamocolumnar junction cells implicated in the pathogenesis of cervical cancer. *Proc Natl Acad Sci USA* 109:10516-10521.

Ho CKM & Strauss JFI. 2004. Activation of the control reporter plasmids pRL-TK and pRL-SV40 by multiple GATA transcription factors can lead to aberrant normalization of transfection efficiency. *BMC Biotechnol* 4:10.

Holmes R & Goldberg E. 2009. Computational analyses of mammalian lactate dehydrogenases: human, mouse, opossum and platypus LDHs. *Comput Biol Chem* 33:379-385.

Hsu PP & Sabatini DM. 2008. Cancer Cell Metabolism: Warburg and Beyond. *Cell* 134:703-707.

Hu J, Stiehl DP, Setzer C, Wichmann D, Shinde DA, Rehrauer H, Hradecky P, Gassmann M & Gorr TA. 2011. Interaction of HIF and USF signaling pathways in human genes flanked by hypoxia-response elements and E-box palindromes. *Mol Cancer Res* 9:1520-1536.

Hussien R & Brooks G a. 2011. Mitochondrial and plasma membrane lactate transporter and lactate dehydrogenase isoform expression in breast cancer cell lines. *Physiol Genomics* 43:255-264.

Höckel M, Schlenger K, Knoop C & Vaupel P. 1991. Oxygenation of Carcinomas of the Uterine Cervix: Evaluation by Computerized O2 Tension Measurements. *Cancer Res* 51:6098-6102.

Izumi H, Takahashi M, Uramoto H, Nakayama Y, Oyama T, Wang KY, Sasaguri Y, Nishizawa S & Kohno K. 2011. Monocarboxylate transporters 1 and 4 are involved in the invasion activity of human lung cancer cells. *Cancer Sci* 102:1007-1013.

Izumi H, Torigoe T, Ishiguchi H, Uramoto H, Yoshida Y, Tanabe M, Ise T, Murakami T, Yoshida T & Nomoto M. 2003. Cellular pH regulators: potentially promising molecular targets for cancer chemotherapy. *Cancer Treat Rev* 29:541-549.

Jackson V, Price N, Carpenter L & Halestrap AP. 1997. Cloning of the monocarboxylate transporter isoform MCT2 from rat testis provides evidence that expression in tissues is species-specific and may involve post-transcriptional. *Biochem J* 324:447-453.

Jemal A, Bray F& Ferlay J. 2011. Global Cancer Statistics. *CA Cancer J Clin* 61:69-90.

Kang KW, Im YB, Go W-jung & Han H-kyung. 2009. c-Myc Amplification Altered the Gene Expression of ABC- and SLC-Transporters in Human Breast Epithelial Cells. *Mol Pharm* 6:627-633.

Kersemaekers A-marie F, Fleuren GJ, Kenter GG, Uljee SM, Hermans J & Vijver MJVD. 1999. Oncogene Alterations in Carcinomas of the Uterine Cervix: Overexpression of the Epidermal Growth Factor Receptor Is Associated with Poor Prognosis. *Clin Cancer Res* 5:577-586.

Khazaie K, Schirrmacher V & Lichtner RB. 1993. EGF receptor in neoplasia and metastasis. *Cancer Metastasis Rev* 12:255-274.

Kim JH, Kim EL, Lee YK, Park CB, Kim BW, Wang HJ, Yoon CH, Lee SJ & Yoon G. 2011. Decreased lactate dehydrogenase B expression enhances claudin 1-mediated hepatoma cell invasiveness via mitochondrial defects. *Exp Cell Res* 317:1108-1118.

Kim JW & Dang CV. 2006. Cancer's Molecular Sweet Tooth and the Warburg Effect. *Cancer Res* 66:8927-8930.

Kim JW, Tchernyshyov I, Semenza GL & Dang CV. 2006. HIF-1-mediated expression of pyruvate dehydrogenase kinase: A metabolic switch required for cellular adaptation to hypoxia. *Cell Metab* 3:177-185.

King A & Gottlieb E. 2009. Glucose metabolism and programmed cell death: an evolutionary and mechanistic perspective. *Curr Opin Cell Biol* 21:885-893.

Kinoshita T, Nohata N, Yoshino H, Hanazawa T, Kikkawa N, Fujimura L, Chiyomaru T, Kawakami K, Enokida H, Nakagawa M, Okamoto Y & Seki N. 2011. Tumor suppressive microRNA-375 regulates lactate dehydrogenase B in maxillary sinus squamous cell carcinoma. *Int J Oncol* 40:185-193.

von Knebel Doeberitz M. 2002. New markers for cervical dysplasia to visualise the genomic chaos created by aberrant oncogenic papillomavirus infections. *Eur J cancer* 38:2229-2242.

Koizume S, Tachibana K, Sekiya T, Hirohashi S & Shiraishi M. 2002. Heterogeneity in the modification and involvement of chromatin components of the CpG island of the silenced human CDH1 gene in cancer cells. *Nucleic Acids Res* 30:4770-4780

Kornegoor R, Moelans CB, Verschuur-Maes AH, Hogenes MCH, de Bruin PC, Oudejans JJ, Marchionni L & van Diest PJ. 2012. Oncogene amplification in male breast cancer: analysis by multiplex ligation-dependent probe amplification. *Breast Cancer Res Treat* 135:49-58.

Koslowski M, Türeci Ö, Bell C, Krause P, Lehr HA, Brunner J, Seitz G, Nestle FO, Huber C & Sahin U. 2002. Multiple splice variants of lactate dehydrogenase C selectively expressed in human cancer. *Cancer Res* 62:6750-6755.

Koukourakis MI, Giatromanolaki A, Sivridis E, Bougioukas G, Didilis V, Gatter KC & Harris AL. 2003. Lactate dehydrogenase-5 (LDH-5) overexpression in non-small-cell lung cancer tissues is linked to tumour hypoxia, angiogenic factor production and poor prognosis. *Br J Cancer* 89:877-885.

Koukourakis MI, Giatromanolaki A, Simopoulos C, Polychronidis A & Sivridis E. 2005. Lactate dehydrogenase 5 (LDH5) relates to up-regulated hypoxia inducible factor pathway and metastasis in colorectal cancer. *Clin Exp Metastasis* 22:25-30.

Kristensen GB, Holm R, Abeler VM & Tropé CG. 1996. Evaluation of the prognostic significance of cathepsin D, epidermal growth factor receptor, and c-erbB-2 in early cervical squamous cell carcinoma. An immunohistochemical study. *Cancer* 78:433-440.

Kumar GL & Rudbeck L eds. 2009. Education Guide - Immunohistochemical (IHC) Staining Methods. Fifth ed. Dako North America, Carpinteria, California

Kuo M-hao & Allis CD. 1999. In Vivo Cross-Linking and Immunoprecipitation for Studying Dynamic Protein: DNA Associations in a Chromatin Environment. *Methods* 19:425-433.

Lax S. 2011. Histopathology of cervical precursor lesions and cancer. *Acta dermatovenerol Alp Panonica Adriat* 20:125-133.

Lee CM, Lee RJ, Hammond E, Tsodikov A, Dodson M, Zempolich K & Gaffney DK. 2004. Expression of HER2neu (c-erbB-2) and epidermal growth factor receptor in cervical cancer: prognostic correlation with clinical characteristics, and comparison of manual and automated imaging analysis. *Gynecol Oncol* 93:209-214.

Lee CM, Shrieve DC, Zempolich KA, Lee RJ, Hammond E, Handrahan DL & Gaffney DK. 2005. Correlation between human epidermal growth factor receptor family (EGFR, HER2, HER3, HER4), phosphorylated Akt (P-Akt), and clinical outcomes after radiation therapy in carcinoma of the cervix. *Gynecol Oncol* 99:415-421.

Lee JG & Kay EP. 2006. FGF-2-induced wound healing in corneal endothelial cells requires Cdc42 activation and Rho inactivation through the phosphatidylinositol 3-kinase pathway. *Invest Ophthalmol Vis Sci* 47:1376-1386.

Leiblich A, Cross S, Catto J, Phillips J, Leung H, Hamdy F & Rehman I. 2006. Lactate dehydrogenase-B is silenced by promoter hypermethylation in human prostate cancer. *Oncogene* 25:2953-2960.

Lewis BC, Prescott JE, Campbell SE, Shim H, Orlowski RZ & Dang CV. 2000. Tumor Induction by the c-Myc Target Genes rcl and Lactate Dehydrogenase A. *Cancer Res* 60:6178-6183.

Liu H, Zhou M, Luo X, Zhang L, Niu Z, Peng C, Ma J, Peng S, Zhou H, Xiang B, Li X, Li S, He J, Li X & Li G. 2008. Transcriptional regulation of BRD7 expression by Sp1 and c-Myc. *BMC Mol Biol* 9:111.

Lu Z, Jiang G, Blume-Jensen P & Hunter T. 2001. Epidermal growth factor-induced tumor cell invasion and metastasis initiated by dephosphorylation and downregulation of focal adhesion kinase. *Mol Cell Biol* 21:4016-4031

Lynch TJ, Bell DW, Sordella R, Gurubhagavatula S, Okimoto RA, Brannigan BW, Harris PL, Haserlat SM, Supko JG, Haluska FG, Louis DN, Christiani DC, Settleman J & Haber DA. 2004. Activating Mutations in the Epidermal Growth Factor Receptor Underlying Responsiveness of Non–Small-Cell Lung Cancer to Gefitinib. *N Engl J Med* 350:2129-2139.

Lüscher B. 2012. MAD1 and its life as a MYC antagonist: an update. *Eur J Cell Biol* 91:506-514.

Macville M, Schröck E, Padilla-Nash H, Keck C, Ghadimi BM, Zimonjic D, Popescu N & Ried T. 1999. Comprehensive and definitive molecular cytogenetic characterization of HeLa cells by spectral karyotyping. *Cancer Res* 59:141-150.

Maekawa M, Inomata M, Sasaki MS, Kaneko A, Ushiama M, Sugano K, Takayama J & Kanno T. 2002. Electrophoretic variant of a lactate dehydrogenase isoenzyme and selective promoter methylation of the LDHA gene in a human retinoblastoma cell line. *Clin Chem* 48:1938-1945.

Maekawa M, Taniguchi T, Ishikawa J, Sugimura H, Sugano K & Kanno T. 2003. Promoter hypermethylation in cancer silences LDHB, eliminating lactate dehydrogenase isoenzymes 1-4. *Clin Chem* 49:1518-1520.

Markert CL, Shaklee JB & Whitt GS. 1975. Evolution of a gene. Multiple genes for LDH isozymes provide a model of the evolution of gene structure, function and regulation. *Science* 189:102-114.

McMahon SB. 2010. Emerging Concepts in the Analysis of Transcriptional Targets of the MYC Oncoprotein: Are the Targets Targetable? *Genes Cancer* 1:560-567.

Milosevic M, Fyles A, Hedley D & Hill R. 2004. The human tumor microenvironment: invasive (needle) measurement of oxygen and interstitial fluid pressure. *Semi Radiat Oncol* 14:249-258.

Moreno-Sánchez R, Rodríguez-Enríquez S, Marín-Hernández A & Saavedra E. 2007. Energy metabolism in tumor cells. *FEBS J* 274:1393-1418.

Muñoz N, Bosch FX, de Sanjosé S, Herrero R, Castellsagué X, Shah KV, Snijders PJF & Meijer CJLM. 2003. Epidemiologic classification of human papillomavirus types associated with cervical cancer. *N Engl J Med* 348:518-527.

Nagai N, Oshita T, Fujii T, Kioka H, Katsube Y & Ohama K. 2000. Prospective analysis of DNA ploidy, proliferative index and epidermal growth factor receptor as prognostic factors for pretreated uterine cancer. *Oncol Rep* 7:551-559.

Nagy VM, Buiga R, Brie I, Todor N, Tudoran O, Ordeanu C, Virág P, Tarta O, Rus M & Bălăcescu O. 2011. Expression of VEGF, VEGFR, EGFR, COX-2 and MVD in cervical carcinoma, in relation with the response to radio-chemotherapy. *Rom J Morphol Embryol* 52:53-59.

Nakajima EC & Van Houten B. 2012. Metabolic symbiosis in cancer: Refocusing the Warburg lens. *Mol Carcinog* [Epub ahead of print]

Narayanan R, Kim HN, Narayanan NK, Nargi D & Narayanan B. 2012. Epidermal growth factor-stimulated human cervical cancer cell growth is associated with EGFR and cyclin D1 activation, independent of COX-2 expression levels. *Int J Oncol* 40:13-20.

Nguyen HN & Averette HE. 1999. Biology of cervical carcinoma. *Semin Surg Oncol* 16:212-216.

Nicolas E, Roumillac C & Trouche D. 2003. Balance between Acetylation and Methylation of Histone H3 Lysine 9 on the E2F-Responsive Dihydrofolate Reductase Promoter. *Mol Cell Biol* 23:1614-1622.

Nobre RJ, Cruz E, Real O, Almeida PDL & Martins TC. 2010. Characterization of Common and Rare Human Papillomaviruses in Portuguese Women by the Polymerase Chain Reaction , Restriction Fragment Length Polymorphism and Sequencing. *J Med Virol* 82:1024-1032.

Nowak G & Schnellmann RG. 1995. Integrative effects of EGF on metabolism and proliferation in renal proximal tubular cells. *Am J Physiol* 269:C1317-C1325.

Nunez R. 2001. DNA Measurement and Cell Cycle Analysis by Flow Cytometry. *Curr issues Mol Biol* 3:67-70.

OneDay ChIP kit - The rapid Chromatin Immunoprecipitation kit Cat. No. kch-oneDIP-060 / kch-oneDIP-180. Instruction Manual Version 1 01.10. Diagenode. 2010.

Papaconstantinou J & Colowick SP. 1961. The Role of Glycolysis in the Growth of Tumor. I. Effects of oxamic acid on the metabolism of ehrlich ascites tumor cells in vitro. *J Biol Chem* 236:278-284.

Pelicano H, Xu RH, Du M, Feng L, Sasaki R, Carew JS, Hu Y, Ramdas L, Hu L, Keating MJ, Zhang W, Plunkett W & Huang P. 2006. Mitochondrial respiration defects in cancer cells cause activation of Akt survival pathway through a redox-mediated mechanism. *J Cell Biol* 175:913-923.

Perry JE, Grossmann ME & Tindall DJ. 1998. Epidermal growth factor induces cyclin D1 in a human prostate cancer cell line. *Prostate* 35:117-124.

Pfeiffer D, Stellwag B, Pfeiffer A, Borlinghaus P, Meier W & Scheidel P. 1989. Clinical implications of the epidermal growth factor receptor in the squamous cell carcinoma of the uterine cervix. *Gynecol Oncol* 33:146-150.

pGL3 Luciferase Reporter Vectors. Technical manual. Promega. 2007

Philp A, Macdonald AL & Watt PW. 2005. Lactate-a signal coordinating cell and systemic function. *J Exp Biol* 208:4561-4575.

Philp NJ, Yoon H & Lombardi L. 2001. Mouse MCT3 gene is expressed preferentially in retinal pigment and choroid plexus epithelia. *Am J Physiol Cell Physiol* 280:C1319-C1326.

Pinheiro C, Longatto-Filho A, Pereira SM, Etlinger D, Moreira MA, Jubé LF, Queiroz GS, Schmitt F & Baltazar F. 2009. Monocarboxylate transporters 1 and 4 are associated with CD147 in cervical carcinoma. *Dis Markers* 26:97-103.

Pinheiro C, Longatto-filho A, Scapulatempo C, Ferreira L, Martins S, Pellerin L, Rodrigues M, Alves VA, Schmitt F & Baltazar F. 2008. Increased expression of monocarboxylate transporters 1 , 2 , and 4 in colorectal carcinomas. *Virchows Arch* 452:139-146.

Pinheiro C, Reis RM, Ricardo S, Longatto-Filho A, Schmitt F& Baltazar F. 2010. Expression of monocarboxylate transporters 1, 2, and 4 in human tumours and their association with CD147 and CD44. *J Biomed Biotechnol* 2010:427694.

Pista A, Oliveira A, Verdasca N & Ribeiro F. 2011. Single and multiple human papillomavirus infections in cervical abnormalities in Portuguese women. *Clin Microbiol Infect* 17:941-946.

Policht FA, Song M, Sitailo S, Hare AO, Ashfaq R, Muller CY, Morrison LE, King W & Sokolova IA. 2010. Analysis of genetic copy number changes in cervical disease progression. *BMC Cancer* 10:432.

Porporato PE, Dhup S, Dadhich RK, Copetti T & Sonveaux P. 2011. Anticancer targets in the glycolytic metabolism of tumors: a comprehensive review. *Front Pharmacol* 2:49.

Price J, Wilson H & Haites N. 1996. Epidermal growth factor (EGF) Increases the in vitro invasion, motility and adhesion interactions of the primary renal carcinoma cell line, A704. *Eur J Cancer* 32A:1977-1982.

Redondo-Lopez V, Cook RL & Sobel JD. 1990. Emerging role of lactobacilli in the control and maintenance of the vaginal bacterial microflora. *Rev Infect Dis* 12:856-872.

Reiss N, Kanety H & Schlessinger J. 1986. Five enzymes of the glycolytic pathway serve as substrates for purified epidermal-growth-factor-receptor kinase. *Biochem J* 239:691-697.

Renart J, Reiser J & Stark GR. 1979. Transfer of proteins from gels to diazobenzyloxymethyl-paper and detection with antisera: A method for studying antibody specificity and antigen structure. *Proc Natl Acad Sci USA* 76:3116-3120.

Riou GF, Bourhis J & Le MG. 1990. The c-myc proto-oncogene in invasive carcinomas of the uterine cervix: clinical relevance of overexpression in early stages of the cancer. *Anticancer Res* 10:1225-1231.

Robinson JP, Sturgis J & Kumar GL. 2009. Immunofluorescence. *In:* Education guide - Immunohistochemical (IHC) Staining Methods (Kumar GL & Rudbeck L eds), Fifth ed, pp. 61-65, Dako North America, Carpinteria, California.

Roden R & Wu T-C. 2006. How will HPV vaccines affect cervical cancer? *Nat Rev Cancer* 6:753-763.

Rosen E & Goldberg I. 1989. Protein factors which regulate cell motility. *In Vitro Cell Dev Biol* 25:1079-1087.

Sarkis SA, Abdullah BH, Abdul Majeed BA & Talabani NG. 2010. Immunohistochemical expression of epidermal growth factor receptor (EGFR) in oral squamous cell carcinoma in relation to proliferation, apoptosis, angiogenesis and lymphangiogenesis. *Head Neck Oncol* 2:13.

Schwab M. 1999. Oncogene amplification in solid tumors. *Semin Cancer Biol* 9:319-325.

Schwickert G, Walenta S, Sundfør K, Schwickert G, Suiulfor K, Rofstad EK & Mueller-klieser W. 1995. Correlation of High Lactate Levels in Human Cervical Cancer with Incidence of Metastasis. *Cancer Res* 55:4757-4759.

Semenza GL. 2008. Tumor metabolism: cancer cells give and take lactate. *J Clin Invest* 118:3835-3837.

Semenza GL, Jiang B-hua, Leung SW, Passantino R, Concordet JP, Maire P & Giallongo A. 1996. Hypoxia Response Elements in the Aldolase A , Enolase 1 , and Lactate Dehydrogenase A Gene Promoters Contain Essential Binding Sites for Hypoxia-inducible Factor 1. *J Biol Chem* 271:32529-32537.

Seyfried TN & Shelton LM. 2010. Cancer as a metabolic disease. *Nutr Metab (Lond)* 7:7.

Shaw RJ. 2006. Glucose metabolism and cancer. *Curr Opin Cell Biol* 18:598-608.

Shen L, Shui Y, Wang X, Sheng L, Yang Z, Xue D & Wei Q. 2008. EGFR and HER2 expression in primary cervical cancers and corresponding lymph node metastases: implications for targeted radiotherapy. *BMC Cancer* 8:232.

Shen MR, Droogmans G, Eggermont J, Voets T, Ellory JC & Nilius B. 2000. Differential expression of volume-regulated anion channels during cell cycle progression of human cervical cancer cells. *J Physiol* 529 Pt 2:385-394.

Shen M-R, Hsu Y-M, Hsu K-F, Chen Y-F, Tang M-J & Chou C-Y. 2006. Insulin-like growth factor 1 is a potent stimulator of cervical cancer cell invasiveness and proliferation that is modulated by alphavbeta3 integrin signaling. *Carcinogenesis* 27:962-971.

Shendure J, Mitra RD, Varma C & Church GM. 2004. Advanced sequencing technologies: methods and goals. *Nat Rev Genet* 5:335-344.

Shiao Y-H. 2003. A new reverse transcription-polymerase chain reaction method for accurate quantification. *BMC Biotechnol* 3:22.

Shim H, Dolde C, Lewis BC, Wu CS, Dang G, Jungmann RA, Dalla-Favera R & Dang CV. 1997. c-Myc transactivation of LDH-A: implications for tumor metabolism and growth. *Proc Natl Acad Sci USA* 94:6658-6663.

Si J, Yu X, Zhang Y & DeWille JW. 2010. Myc interacts with Max and Miz1 to repress C/EBPdelta promoter activity and gene expression. *Mol Cancer* 9:92.

Singer K, Kastenberger M, Gottfried E, Hammerschmied CG, Büttner M, Aigner M, Seliger B, Walter B, Schlösser H, Hartmann A, Andreesen R, Mackensen A & Kreutz M. 2011. Warburg phenotype in renal cell carcinoma: high expression of glucose-transporter 1 (GLUT-1) correlates with low CD8(+) T-cell infiltration in the tumor. *Int J Cancer* 128:2085-2095.

Smith HO, Tiffany MF, Qualls CR & Key CR. 2000. The rising incidence of adenocarcinoma relative to squamous cell carcinoma of the uterine cervix in the United States-a 24-year population-based study. *Gynecol Oncol* 78:97-105.

Sonveaux P, Végran F, Schroeder T, Wergin MC, Verrax J, Rabbani ZN, Saedeleer CJD, Kennedy KM, Diepart C, Jordan BF, Kelley MJ, Gallez B, Wahl ML, Feron O & Dewhirst MW. 2008. Targeting lactate-fueled respiration selectively kills hypoxic tumor cells in mice. *J Clin Invest* 118:3930-3942.

Swerdlow H & Gesteland R. 1990. Capillary gel electrophoresis for rapid, high resolution DNA sequencing. *Nucleic Acids Res* 18:1415-1419.

Takahashi Y, Shintaku K, Ishii Y, Asai S, Ishikawa K & Fujii M. 1998. Analysis of MYC and Chromosome 8 Copy Number Changes in Gastrointestinal Cancers by Dual-Color Fluorescence In Situ Hybridization. *Cancer Genet Cytogenet* 107:61-64.

Tang H & Goldberg E. 2009. Homo sapiens Lactate Dehydrogenase c (Ldhc) Gene Expression in Cancer Cells Is Regulated by Transcription Factor Sp1, CREB, and CpG Island Methylation. *J Androl* 30:157-167.

Tennant DA, Durán RV & Gottlieb E. 2010. Targeting metabolic transformation for cancer therapy. *Nat Rev Cancer* 10:267-277.

Tennant DA, Dúran RV, Boulahbel H & Gottlieb E. 2009. Metabolic transformation in cancer. *Carcinogenesis* 30:1269-1280.

Thangaraju M, Carswell KN, Prasad PD & Ganapathy V. 2009. Colon cancer cells maintain low levels of pyruvate to avoid cell death caused by caused by inhibition of HDAC1 / HDAC3. *Biochem J* 417:379-389.

Thangaraju M, Gopal E, Martin PM, Ananth S, Smith SB, Prasad PD, Sterneck E & Ganapathy V. 2006. SLC5A8 Triggers Tumor Cell Apoptosis through Pyruvate-Dependent Inhibition of Histone Deacetylases. *Cancer Res* 66:11560-11564.

Thorn CC, Freeman TC, Scott N, Guillou PJ & Jayne DG. 2009. Laser microdissection expression profiling of marginal edges of colorectal tumours reveals evidence of increased lactate metabolism in the aggressive phenotype. *Gut* 58:404-412.

Towbin H, Staehelint T & Gordon J. 1979. Electrophoretic transfer of proteins from polyacrylamide gels to nitrocellulose sheets: Procedure and some applications. *Proc Natl Acad Sci USA* 6:4350-4354.

Ullah MS, Davies AJ & Halestrap AP. 2006. The plasma membrane lactate transporter MCT4, but not MCT1, is up-regulated by hypoxia through a HIF-1alpha-dependent mechanism. *J Biolo Chem* 281:9030-9037.

Vander Heiden MG, Cantley LC & Thompson CB. 2009. Understanding the Warburg effect: the metabolic requirements of cell proliferation. *Science* 324:1029-1033.

Végran F, Boidot R, Michiels C, Sonveaux P & Feron O. 2011. Lactate Influx through the Endothelial Cell Monocarboxylate Transporter MCT1 Supports an NF- κ B / IL-8 Pathway that Drives Tumor Angiogenesis. *Cancer Res* 71:2550-2560.

Vysis product catalog, Abbott Molecular.2004.

Walboomers J, Jacobs M, Manos MM, Bosch FX, Kummer JA, Shah KV, Snijders PJ, Peto J, Meijer CJ & Muñoz N. 1999. Human papillomavirus is a necessary cause of invasive cervical cancer worldwide. *J Pathol* 189:12-19.

Walenta S, Schroeder T & Mueller-Klieser W. 2004. Lactate in solid malignant tumors: potential basis of a metabolic classification in clinical oncology. *Curr Med Chem* 11:2195-2204.

Walenta S & Mueller-Klieser WF. 2004. Lactate: mirror and motor of tumor malignancy. *Semin Radiat Oncol* 14:267-274.

Walenta S, Wetterling M, Lehrke M, Schwickert G, Sundfør K, Rofstad EK & Mueller-klieser W. 2000. High Lactate Levels Predict Likelihood of Metastases, Tumor Recurrence, and Restricted Patient Survival in Human Cervical Cancers. *Cancer Res* 60:916-921.

Warburg O. 1956. On the Origin of Cancer Cells. *Science* 123:309-314.

Weinhouse S. 1976. The Warburg Hypothesis Fifty Years Later. Z Krebsforsch Klin Onkol *Cancer Res Clin Oncol* 87:115-126.

Witton CJ, Reeves JR, Going JJ, Cooke TG & Bartlett JMS. 2003. Expression of the HER1-4 family of receptor tyrosine kinases in breast cancer. *J Pathol* 200:290-297.

Woodburn JR. 1999. The epidermal growth factor receptor and its inhibition in cancer therapy. *Pharmacol Ther* 82:241-250.

Woodman CBJ, Collins SI & Young LS. 2007. The natural history of cervical HPV infection: unresolved issues. *Nat Rev Cancer* 7:11-22.

Yeasmin S, Nakayama K, Rahman MT, Rahman M, Ishikawa M, Katagiri A, Iida K, Nakayama N, Otuski Y, Kobayashi H, Nakayama S & Miyazaki K. 2011. Biological and clinical significance of NAC1 expression in cervical carcinomas: a comparative study between squamous cell carcinomas and adenocarcinomas/adenosquamous carcinomas. *Hum Pathol* 43:506-519.

Yeung SJ, Pan J & Lee MH. 2008. Roles of p53, MYC and HIF-1 in regulating glycolysis - the seventh hallmark of cancer. *Cell Mol Life Sci* 65:3981-3999.

Yin W, Xiang P & Li Q. 2005. Investigations of the effect of DNA size in transient transfection assay using dual luciferase system. *Anal Biochem* 346:289-294.

Yugawa T & Kiyono T. 2009. Molecular mechanisms of cervical carcinogenesis by high-risk human papillomaviruses: novel functions of E6 and E7 oncoproteins. *Rev Med Virol* 19:97-113.

Zha X, Wang F, Wang Y, He S, Jing Y, Wu X & Zhang H. 2011. Lactate dehydrogenase B is critical for hyperactive mTOR-mediated tumorigenesis. *Cancer Res* 71:13-18.

Zhuang S, Dang Y & Schnellmann RG. 2004. Requirement of the epidermal growth factor receptor in renal epithelial cell proliferation and migration. *Am J Physiol Renal Physiol* 287:F365-F372.

# Appendix I

Solutions prepared for the experimental work:

**Luria-Bertani (LB) medium (Sambrook & Russel, 2001)**
For 1L:
10g Tryptone (L42, Oxoid)
5g Yeast extract (403 687,Cultimed)
10g NaCl (106404, Merck)
dd$H_2O$ to 1L

**10X PBS (pH 7.4-7.6) (Sambrook & Russel, 2001)**
For 1L:
80g NaCl (1.37M) (106404, Merck)
2g $KH_2PO_4$ (14.7mM) (104873, Merck)
11.1g $Na_2HPO_4$ (78.1mM) (S-0876, Sigma)
2g KCl (26.8mM) (104936, Merck)
dd$H_2O$ to 1L

**10X TBS (pH 7.4-7.6)**
For 1L:
8g NaCl (106404, Merck)
0.63g Tris (15504-038, Gibco BRL)
4.4 mL hydrochloric acid (1M)
dd$H_2O$ to 1L

**5X SDS gel loading buffer (Sambrook & Russel, 2001)**
250 mM Tris HCl (pH 6.8) (0.5M 161-0799, Bio-rad)
10% SDS (V6551, Promega)
0.5% bromophenol blue
50% glycerol (1.04094.1000, Merck)

**Transfer buffer (Sambrook & Russel, 2001)**
For 5L:
75g glycine (US16407, USB)
15g Trizma-base (T-8524, Sigma)
dd$H_2O$ to 4L
1L absolute ethanol (100983, Merck)
5mL 10% SDS (V6551, Promega)

**15% resolving gel and 5% stacking gel for Tris-glycine SDS-Polyacrylamide Gel Electrophoresis prepared accordingly to Sambrook & Russel, 2001**

**PBS 0.1% (v/v) Tween 20**
For 1L:
1mL Tween 20 (20605, USB)
1X PBS to 1L

**PBS 0.2% (w/v) BSA**
0.4g BSA (A9647, Sigma)
200 mL 1X PBS

**PBS 0.2% (w/v) BSA 0.1% (v/v) Triton X-100**
For 4mL:
3.96 mL PBS 0.2% (w/v) BSA
40 µL 10% Triton X-100 diluted in $ddH_2O$ (100% Triton X-100, T8787, Sigma)

**3% (w/v) skim milk in PBS 0.1% (v/v) Tween 20**
3g skim milk (Molico, Nestlé)
100 mL PBS 0.1% (v/v) Tween 20

**RIPA buffer**
For 10 mL:
20 mM Tris-HCl pH 7.5
150 mM NaCl (106404, Merck)
5mM KCl (104936, Merck)
5mM $MgCl_2$ (M-8266, Sigma)
1% Triton X-100 (T8787, Sigma)
$ddH_2O$ to 10 mL
1 Complete, Mini, EDTA-free Protease Inhibitor Cocktail Tablet (11836170001, Roche)
1 mM Orthovanadate ($Na_3VO_4$)

**50 µg/mL Propidium Iodide (PI) solution**
For 50 mL:
1 mL of 2.5 mg/mL PI solution (P4170, Sigma) (prepared in 1X PBS)
49 mL 1X PBS
0.1 mg/mL RNase A (Easy spin kit, Citomed)
0.05% Triton X-100 (T8787, Sigma)

## Bibliographic reference

Sambrook J & Russell DW. 2001. Molecular Cloning: A Laboratory Manual, Volume 3. Third ed. Cold Spring Harbor Laboratory Press, Cold Spring Harbor, New York.

# Appendix II

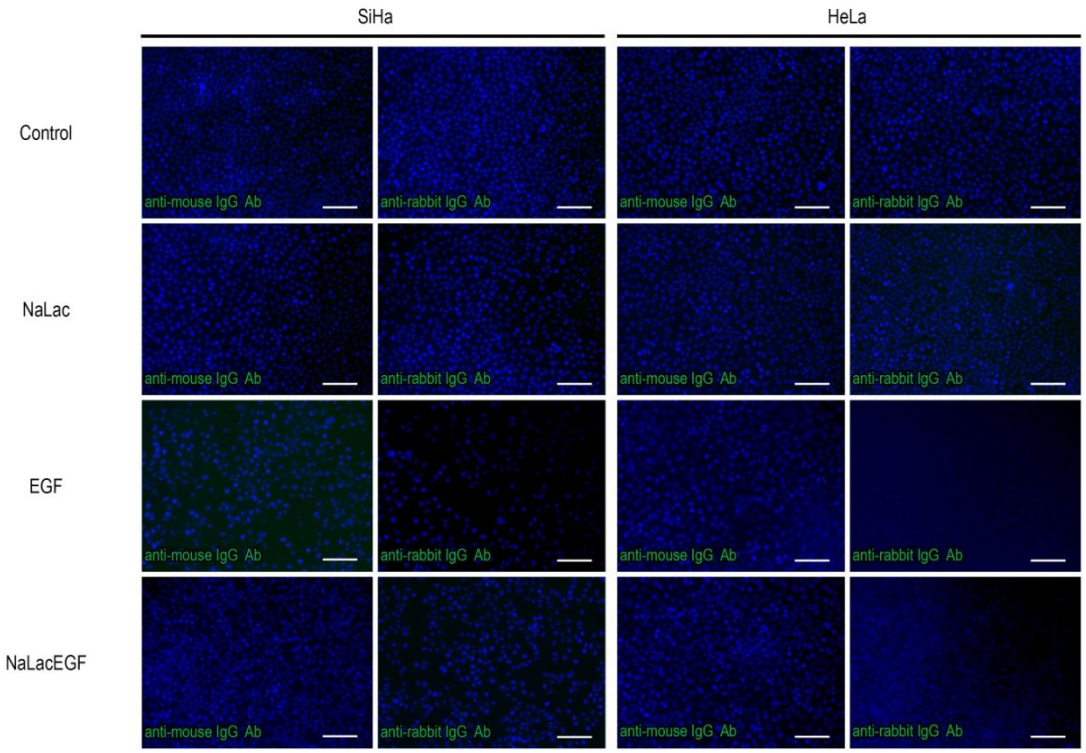


**Figure A1 - Negative controls of immunofluorescence for SiHa and HeLa cells.** Fluorescence microscopy (original magnification: 200x). Nuclei were stained with DAPI (blue). Scale bar 100 µm.

**Table A1 - Frequency (in percentage) of c-Myc copy number detected in SiHa and HeLa cells assessed by FISH, using 8q24 LSI MYC probe.**

| c-Myc copy number | % | |
|---|---|---|
| | SiHa | HeLa |
| 2 | 0.77 | - |
| 3 | 0.77 | 2.78 |
| 4 | 88.46 | 92.59 |
| 5 | 9.23 | 2.78 |
| 8 | 0.77 | 1.85 |

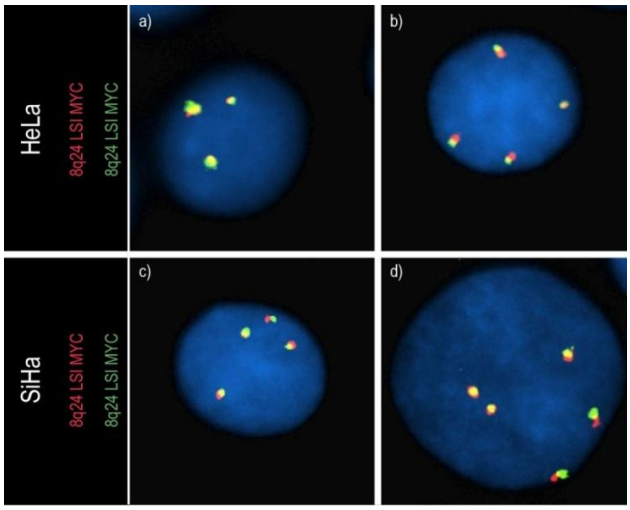


**Figure A2 - Copy number analysis of c-Myc with Fluorescent in situ hybridization (FISH**). Representative experiments of FISH analysis of c-Myc in HeLa (a,b) and SiHa (c,d) cells are shown. The probe used for c-Myc detection was the LSI MYC Dual Color, Break apart rearrangement probe that is a mixture of two probes that hybridizes to opposite sides of the region located 3' of MYC (8q24 LSI MYC SpectrumOrange, SpectrumGreen). Nuclei in interphase were counterstained with DAPI.